Distribution Agreement

In presenting this dissertation as a partial fulfillment of the requirements for an advanced degree from Emory University, I hereby grant to Emory University and its agents the non-exclusive license to archive, make accessible, and display my dissertation in whole or in part in all forms of media, now or hereafter known, including display on the world wide web. I understand that I may select some access restrictions as part of the online submission of this dissertation. I retain all ownership rights to the copyright of the dissertation. I also retain the right to use in future works (such as articles or books) all or part of this dissertation.

Signature:

_____   _____
Brandon B. Stauffer   Date

On the Modulation of CFTR Channel Function by Sphingomyelinase and VX-770

By

Brandon B. Stauffer
Doctor of Philosophy

Graduate Division of Biological and Biomedical Science
Molecular Systems Pharmacology

_____
Nael A. McCarty, Ph.D.
Advisor

_____
Edward Balog, Ph.D.
Committee Member

_____
Randy A. Hall, Ph.D.
Committee Member

_____
H. Criss Hartzell, Ph.D.
Committee Member

_____
Andrew Jenkins, Ph.D.
Committee Member

Accepted:

_____
Lisa A. Tedesco, Ph.D.
Dean of the James T. Laney School of Graduate Studies

_____
Date

On the Modulation of CFTR Channel Function by Sphingomyelinase and VX-770

By

Brandon B. Stauffer
B.S., University of the Sciences in Philadelphia, 2008

Advisor: Nael A. McCarty, Ph.D.

An abstract of
A dissertation submitted to the Faculty of the
James T. Laney School of Graduate Studies of Emory University
in partial fulfillment of the requirements for the degree of
Doctor of Philosophy
in Molecular Systems Pharmacology
2017

Abstract

On the Modulation of CFTR Channel Function by Sphingomyelinase and VX-770
By Brandon B. Stauffer

Cystic Fibrosis (CF) is a debilitating disease that results from loss-of-function mutations in the Cystic Fibrosis Transmembrane Conductance Regulator chloride channel (CFTR). CF is associated with widespread exocrine dysfunction and patients most often succumb to pulmonary failure following the accumulation of mucus, inflammatory cells, and bacteria in the small airways. The discovery of small molecules that directly improve CFTR function, for example the potentiator VX-770, has ushered is a new era of CF therapeutics in which the goal is to directly improve protein ion channel function. The advent of CFTR pharmacotherapy provokes new questions about what kind of cellular and biophysical factors influence the efficacy of these novel potentiators. Sphingolipids are of particular interest because their metabolism is disrupted in CF and the breakdown of plasma membrane sphingomyelin by sphingomyelinase (SMase) has been shown to directly inhibit CFTR channel function. Despite potentially acting as a hurdle to successful treatment, the full extent of this interaction remains unknown. The Background section will provide an overview of CF pathophysiology, abnormalities in sphingolipid metabolism that have been associated with CF, and briefly discuss evidence suggesting that these two pathways interact. The first Results section will discuss experiments performed to characterize the functional interaction of sphingomyelin metabolism on CFTR channel function. Results herein provide evidence that SMase is a state-dependent gating modifier of CFTR. The second Results section will focus on our efforts to characterize the effect of VX-770 on CFTR channel function. Given that these CFTR potentiators are relatively new, much has yet to be determined about their mechanism of action and ideal screening parameters. Our data provide evidence that current small molecule screening approaches have likely underestimated the value of these drugs, and we provide rationale for how to improve screening approaches for CFTR potentiators. Finally, the Discussion will provide a broader context for our results regarding these two CFTR modulators and pose new questions for future studies.

On the Modulation of CFTR Channel Function by Sphingomyelinase and VX-770

By

Brandon B. Stauffer
B.S., University of The Sciences in Philadelphia, 2008

Advisor: Nael A McCarty, Ph.D.

A dissertation submitted to the Faculty of the
James T. Laney School of Graduate Studies of Emory University
in partial fulfillment of the requirements for the degree of
Doctor of Philosophy
in Molecular Systems Pharmacology
2017

Acknowledgments

This dissertation would not have been possible without the support of many individuals. First and foremost, I would like to thank my mentor, Dr. Nael McCarty. In addition to providing professional and financial support, he continually encouraged me to explore my scientific curiosity and enabled me to initiate a project that was outside of the laboratory's area of expertise – for that courage and vision I am immensely thankful. Next, I would like to thank the members of my committee for donating their valuable time and consistently providing insightful feedback. I would also like to thank the members of the McCarty lab, past and present, who enabled the success of this project by donating time, brainpower, and technical assistance. Most notably Dr. Guiying Cui who contributed valuable data to this dissertation. Barry Imhoff and Kerry McGill provided lab support and comic relief, making the McCarty lab a truly wonderful environment in which to work everyday. Thanks to the Emory community, particularly the faculty and staff of the MSP program for the opportunity to train here at Emory, for the financial support via the training grant, and for their helpful feedback. Thanks to the CF-AIR research group for so many useful discussions and critiques. Thanks to Drs. Joanna Goldberg, Alfred Merrill, Michael Koval, Samuel Molina and Raymond Dingledine for their technical assistance. Last but certainly not least, I would like to thank my family and friends for their unconditional support through this sometimes-turbulent journey. In particular, many thanks to Beth Helfman for keeping me focused and grounded when things got difficult. This journey has been truly enlightening and I am happy to consider you all friends and honored to have you as colleagues.

Table of Contents

7.2. *Junctional Abnormalities In Human Airway Epithelial Cells Expressing F508del CFTR.* Molina SA, Stauffer BB, Moriarty HK, Kim AH, McCarty NA, Koval M. AJP: Lung Cellular and Molecular Physiology 2015 Sep.;309(5):L475-L487.

7.3. *Inflammation and ER stress downregulate BDH2 expression and dysregulate intracellular iron in macrophages.* Zughaier SM, Stauffer BB, McCarty NA. J Immunol Res. 2014;2014(11):1-16.

List of Abbreviations:

ABC transporter – ATP-Binding Cassette Transporter

ASL – Airway Surface Liquid

aSMase – acid sphingomyelinase

β2AR –type 2 beta adrenergic receptor

cAMP – cyclic adenosine monophosphate

CaCC – calcium-activated chloride channel

CDase – ceramidase

CerS – ceramide synthase

CFHBE – CF human bronchial epithelial cell

CERT – ceramide transfer protein

CF – Cystic Fibrosis

CFTR – Cystic Fibrosis Transmembrane conductance Regulator

COPD – chronic obstructive pulmonary disease

Cryo-EM – cryo-electron microscopy

DAG - diacylglycerol

DPC - diphenylamine-2-carboxylate

DRMs – detergent resistant membranes

ECL – Extracellular loop

ER – Endoplasmic Reticulum

FRT – Fisher Rat Thyroid

FSK - Forskolin

GalCer-synthase – Galactosylceramide synthase

GlcCer-synthase – glucosylceramide synthase

GI – Gastrointestinal

GSL - glycosphingolipids

ICL – Intracellular Loop

INH_{172} – CFTR inhibitor 172

IP_3 - inositol trisphosphate

KO – knockout

mAchR – muscarinic acetylcholine receptor

mRNA – messenger RNA

MTS - Methane Thiosulfonate

NBC – Na^+-bicarbonate cotransporter

NBD – Nucleotide Binding Domain

NE – Neutrophil Elastase

NHBE – normal human bronchial epithelial cell

NPD – Nasal Potential Difference

NPPB - 5-nitro-2-(3-phenylpropylamino) benzoic acid

nSMase – neutral sphingomyelinase

PATP – N^6-(2phenylethyl)-ATP

PC - phosphatidylcholine

PE – phosphatidylethanolamine

PI - phosphatidylinositol

PIP_2 - phosphatidylinositol 4,5-bisphophate

PKA – protein kinase A

P_o – open probability

pS – picosiemens

PS - phosphatidyserine

R-domain – Regulatory Domain

S-1-P – sphingosine-1-phosphate

SDS PAGE – Sodium Dodecyl Sulfate Polyacrylamide Gel Electrophoresis

SM – sphingomyelin

SMase – Sphingomyelinase C

SMS - sphingomyelin synthase

SPT - serine palmitoyl transferase

TEVC – Two electrode voltage clamp

TMD – Transmembrane Domain

TRP channel - Transient receptor potential channel

WT – Wild type

List of Figures:

1) Introduction

The Cystic Fibrosis Transmembrane Conductance Regulator chloride channel (CFTR) has important roles in epithelial homeostasis. Loss-of-function mutations in CFTR lead to the life-shortening disease Cystic Fibrosis (CF). The recent discovery of the small molecule potentiator VX-770, commercially known as Kalydeco®, has ushered in a new era of CF therapy wherein the goal is to utilize small molecules to correct the underlying cause of channel dysfunction. The advent of CF pharmacotherapy provokes the question, what cellular and biophysical factors influence the efficacy of VX-770?

This dissertation will begin to explore this question by approaching the problem from two directions. The first Results section focuses on the possibility that sphingomyelinase, a sphingolipid metabolizing enzyme that can directly inhibit CFTR channel activity, may act as a hurdle to successful treatment. The second Results section explores how the efficacy of VX-770 depends on the initial activity of CFTR channels and has significant implications for drug screening. Our findings lay the groundwork for future studies regarding the modulation of CFTR channel function using small molecule therapeutics for the treatment of CF.

1.1) Cystic Fibrosis: CFTR Dysfunction, Inflammation, and Bacterial Infection

The goal of Section 1.1 is to introduce CF and the protein associated with the disease, CFTR. The first part will cover the epidemiology of disease along with some historical perspective on how CF was clinically characterized. It will also discuss the role of CFTR in secretory epithelial tissues and how loss of functional CFTR might lead to the pathologies observed in CF patients. In some organs this relationship is clear while it is still debated in regard to others. Finally, this section will discuss the structure of the CFTR

protein, how its structure translates into the ATP-powered anion channel activity for which it is best known, and how different types of mutations lead to CF disease.

Cystic Fibrosis

Cystic Fibrosis is a genetic, progressive, and typically fatal disease that results from loss-of-function mutations in the gene encoding the CFTR anion channel. It is estimated to afflict 70,000 people worldwide with 30,000 of those patients living in the United States. The highest prevalence of CF is seen in Caucasians with genetic links to northern Europe. In this group the incidence is estimated at 1:2,500 live births (CFF.org). Cases of CF have been reported in individuals with Middle Eastern, African, and Asian descent, though the prevalence is considerably less (1:17,000 live births in African Americans and 1:31,000 live births for Asian Americans). Inheritance follows a Mendelian autosomal recessive pattern and it is estimated that 4% of non-Hispanic Caucasians worldwide are carriers for the disease. The recent inclusion of CF in newborn screening panels has led to diagnosis of most CF patients by the age of 2. This early diagnosis enables physicians to implement treatments early in life and is one reason that the median expected life expectancy of CF patients has increased dramatically, from approximately 6 months when the disease was first formally described in 1938 to approximately 40 years of age today (1; 2).

Cystic Fibrosis is a multi-organ disease that primarily affects exocrine epithelial tissues such as the pancreas, sweat glands, intestines, and lungs. In these tissues, CFTR-mediated chloride and bicarbonate flux are crucial to normal secretory physiology (3) (4). In the pancreas, CFTR is expressed in the ductal cells where it regulates hydration and pH of pancreatic secretions (5; 6). Loss of CFTR function in the pancreas leads to viscous secretions that block pancreatic ducts and lead to inflammation and fibrosis of the interstitial

space. The name Cystic Fibrosis is derived from early observations of these pancreatic

pathologies. CF patients also suffer from an abnormally high incidence of early-onset

diabetes that is distinct from both types 1 and 2 (1). How loss of CFTR activity affects the

endocrine pancreas remains unknown.   A secondary consequence of failed pancreatic

secretion is a decreased amount of digestive enzymes that are secreted into the intestines.

The resulting decrease leads to poor digestion and, consequently, an inability to absorb

nutrients. This nutritional insufficiency is compounded by loss of CFTR in the intestinal

epithelia where it regulates hydration of food boluses. In severe cases, the resulting intestinal

dehydration and decrease in intestinal motility in infants leads to meconium ileus, a

condition characterized by a complete bowel obstruction that requires surgery (1). Adult CF

patients can suffer from similar obstructions, a condition known as distal intestinal

obstructive syndrome. In the early 20th century, CF patients succumbed most often to

malnutrition in early childhood as a result of these GI complications; however, the use of

orally administered pancreatic enzyme replacement therapy and high calorie diets has

drastically improved their nutritional status. These improvements in GI-focused treatment

and the resulting increase in life expectancy over the last five decades have transformed CF

from a disease of malnutrition to one of progressive lung disease (7).

Airway obstruction is the classic pulmonary pathology associated with CF and results

form the accumulation of mucus plugs containing inflammatory cells and bacteria (8-10).

Mucus accumulation is thought to occur as a result of two abnormalities that arise with loss

of CFTR function. First, the loss of CFTR-mediated Cl⁻ transport in the apical membrane

of pulmonary epithelial cells leads to a reduction in the height of the airway surface liquid

(ASL). In healthy lungs, ASL lifts mucus off the surface of epithelial cells and enables

movement by providing a low-viscosity medium in which the epithelial cilia can oscillate

(11). CFTR drives the formation of ASL by conducting chloride ions into the apical space and generating a transepithelial electrochemical gradient (discussed in detail later) that draws Na^+ and water into the luminal space. The primary evidence for this problem stems from a direct comparison of ASL depth in CF epithelial cell lines as compared to control lines expressing WT CFTR (12).

Recent evidence suggests that a loss of CFTR-mediated bicarbonate secretion leads to a second anomaly in mucus dynamics, a loss of mucus detachment from the submucosal gland. In a CF pig model it was observed that mucus remained attached to submucosal glands, an effect the authors named "mucus tethering," and the mucus could be released by submerging the tissue in bicarbonate buffer. Consistent with a requisite role of bicarbonate in mucus detachment, the CF phenomenon could be replicated in WT pig trachea by submerging them in bicarbonate-free buffer (13). Thus, the additive effects of reduced ASL depth and tethered mucus reduce ciliary motility and lead to the mucocilliary abnormalities observed in CF patients (14; 15). Over the long term, mucus accumulation leads to progressive blockade of the airway, air trapping, a reduction in vital capacity, and ultimately a decline in pulmonary function (10). Until the recent development of specific small molecule therapeutics targeted at restoring CFTR channel function, the obstructions were treated with a combination of mechanical clearance techniques, inhaled enzymes to degrade extracellular DNA, and inhaled hypertonic saline (7). While effective, these therapeutic approaches are incomplete and novel approaches to lung clearance are still being developed.

In addition to airway blockages, the CF lung environment is highly inflamed. Some of this inflammation seems to be due to an inherent defect in CF cells because abnormally high levels of the inflammatory mediator IL-8 and neutrophil infiltration can be seen in environments that are not overtly infected, such as the lungs of CF-infants and human fetal

xenografts (16; 17) (18). The contribution of this inherent defect is still controversial, but the clinical condition is made worse by the observation that CF epithelia also secrete higher levels of proinflammatory cytokines in response to bacterial exposure. This hypersensitivity leads to a positive feedback loop upon exposure to microbes wherein increased release of inflammatory mediators and recruitment of activated neutrophils. This is noteworthy because neutrophil derived proteases like Neutrophil Elastase (NE) have been implicated in catalyzing much of the damage observed in patients. Recent studies have shown that levels of NE in the airways of school aged-children correlate negatively to long-term lung function and bronchiectasis (9). The subsequent inflammation-driven remodeling further disrupts airway dynamics and pulmonary physiology, and ultimately significantly contributes to pulmonary failure.

In addition to the inherent defect, pulmonary inflammation is also driven by the frequent presence of microbial pathogens from an early age (19). The presence of "mucopurulent material" was one of the original observations of Dorothy Anderson who found that the most common pathogen present was *Staphylococcus aureus* (20). This observation led to the early implementation of anti-staphylococcal therapies such as sulfonamides and penicillin and resulted in significant clinical improvement. The early detection of *S. aureus* is still common today and epidemiological data suggest that it is often the first colonizing pathogen (CFF.org). With time, and possibly catalyzed by the use of antistaphylococcal therapeutics early in life, patients become colonized with other pathogens. *Pseudomonas aeruginosa* is now widely considered to be the most important pathogen in CF because it has been associated with worse lung function outcomes, greater respiratory inflammation, and a higher risk of mortality (9). *Pseudomonas* is also the most prevalent pathogen in the CF lung; however, with the advent of modern sequencing-based

microbiology approaches, it is now widely accepted that the CF lung is polymicrobial and includes numerous bacterial strains that cannot be easily cultured in clinical microbiology labs (21; 22). A current goal of CF microbiologists is to understand the observed polymicrobial diversity and their ecological relationships with the goal of understanding how bacteria facilitate pulmonary decline.

The link between loss of CFTR and increased bacterial infection is multifaceted and the clearest deficit stems from the absence of normal mucocilliary clearance (23). In primary airway epithelial cultures, loss of CFTR reduces the depth of ASL and decreases ciliary beat frequency (12). If this deficit occurs *in vivo*, it would be expected to cause a buildup of inhaled bacteria in the airway. The increased residence time might also allow for adaptations that increase survival and lead to more persistent infections. Airway pH has also been shown to influence bacterial killing. The pulmonary surface of CF pigs is slightly acidic with a pH of ~6.8 versus 7.2 in healthy pigs, presumably due to a loss of bicarbonate transport by CFTR (24). This change in pH is thought to impede bacterial killing by decreased efficacy of pH-sensitive antibacterial peptides in the airway (24; 25). A third and more controversial hypothesis is that loss of CFTR leads to dysfunction in immune cells. While some groups have shown reduced bacterial killing by neutrophils and macrophages (26), other groups have not observed a difference (27-29). Interestingly some groups have shown that CF airway fluid can alter the metabolism and activation state of neutrophils suggesting that perhaps there is a defect facilitated by the CF lung environment (30). This hypothesis is supported by the clinical observation that CF patients do not have an increased susceptibility to systemic infection and sepsis despite having a high pulmonary bacterial load. A fourth and final observation related to bacterial clearance was first reported by Pier and colleagues in 1996 when they showed that epithelial cells expressing mutant CFTR were unable to

internalize *P. aeruginosa* as efficiently as cells transfected with WT CFTR DNA (31). Other groups have repeated this observation in additional cell models (32; 33). Ultimately, this defect in innate epithelial immunity may contribute to the inability to clear pathogens from the airway. Taken together, it seems that disruptions in CFTR expression and function have multiple effects on airway immune responses which likely compound to produce the hypersusceptibility observed in the clinic.

1.2) CFTR: an overview of structure and function

1.2.1) CFTR function in epithelia

It was clear from clinical evidence that Cystic Fibrosis led to abnormal epithelial function but the primary defect was not discovered until the mid-1980s. Initially it was suggested that the primary defect may lie in mucus production itself based on the observation that CF patients had abnormally think epithelial secretions; however, the discovery of high concentrations of Na^+ and Cl^- in the sweat of CF patients as well as abnormal chloride conductance in the sweat ducts suggested that CF instead arose from an inability to properly regulate electrolyte movement across epithelia (34). This was confirmed in 1986 when Frizzell and colleagues showed that pulmonary epithelial cells from CF patients lacked a beta-adrenergic stimulated chloride channel in the apical membrane (4). This section will discuss how this CFTR-mediated anion conduction contributes to normal epithelial physiology in four tissues: the airway, the intestine, the pancreatic duct, and the sweat gland.

All epithelia that secrete water use the vectoral transport of electrolytes to generate an initial osmotic gradient. The polarized nature of epithelia enables vectoral electrolyte movement by asymmetrically distributing pumps and ion channels across the apical and

basolateral sides of the cell monolayer. The apical side faces the tissue lumen and contains

the anion channels that determine the rate of secretion and absorption. The basolateral side

faces the interstitium and contains transporters that create the electrochemical gradients that

drive anion flux. In addition to the active processes discussed, there is also a passive

component of epithelial secretion in which sodium ions and water flow between cells, a

pathway known as "paracellular flux." Each tissue discussed below utilizes a unique protein

expression profile and spatial distribution of CFTR to achieve their respective goals of

secretion and/or absorption.

The Airway and Intestine

Airway and intestinal epithelia can achieve both secretion and absorption depending

on the level of sympathetic input (3). These tissues are grouped together in this section

because they use a similar mechanism to regulate water movement. A schematic diagram of

airway epithelial ells is shown in Figure 1.1. As with all ion-dependent processes in human

cells, the Na^+/K^+ ATPase provides the initial energy by hydrolyzing ATP and catalyzing the

extracellular transport of 3 Na^+ ions and the intracellular transport of 2 K^+ ions. In secretory

epithelia, the Na^+/K^+ ATPase is located on the basolateral membrane. The resulting

gradient drives efflux of potassium ions through constitutively active potassium channels to

create a cytosol-negative resting membrane potential. The Na^+ gradient created by Na^+/K^+

ATPase activity is utilized by the $Na^+/K^+/2Cl^-$ symporter (NKCC) to move 2 Cl^- ions, one

K^+, and one Na^+ ion into the cell. This combination of high intracellular chloride and a

negative membrane potential is the driving force for the outward flux of chloride through

apical CFTR channels following stimulation. Secretion is stimulated by PKA–mediated

phosphorylation of the CFTR regulatory (R) domain following sympathetic activation of

Figure 1.1) Fluid transport in healthy and CF epithelia: *Left* - A schematic shows the classical model of epithelial secretion in which cells utilize vectoral ion transport to move NaCl and H_2O. Activity of the coupled basolateral Na/K ATPase and NKCC transporters generate high intracellular chloride and potassium concentrations that enable the generation of a cytosol-negative resting potential. Upon activation by PKA-mediated phosphorylation of the R-domain, apical CFTR facilitates the extracellular flux of chloride and bicarbonate ions. Voltage gated potassium channels, for example KCNQ1, are also activated to maintain the cytosol-negative potential that enables continuous chloride flux. A high concentration of chloride in the apical space then draw sodium ions and water through the paracellular pathway via electrochemical and osmotic forces, respectively. The movement of electrolytes and water to the apical surface enable the functioning of cilia and the movement of mucous. *Right* - In CF, mutations in CFTR disrupt chloride movement and prevent secretion. CF-associated loss-of-function mutations in the CFTR chloride channel prevent the movement of chloride out of the cell and lead to net absorption of electrolytes and water.

Figure 1.1) Fluid Transport in healthy and CF epithelia
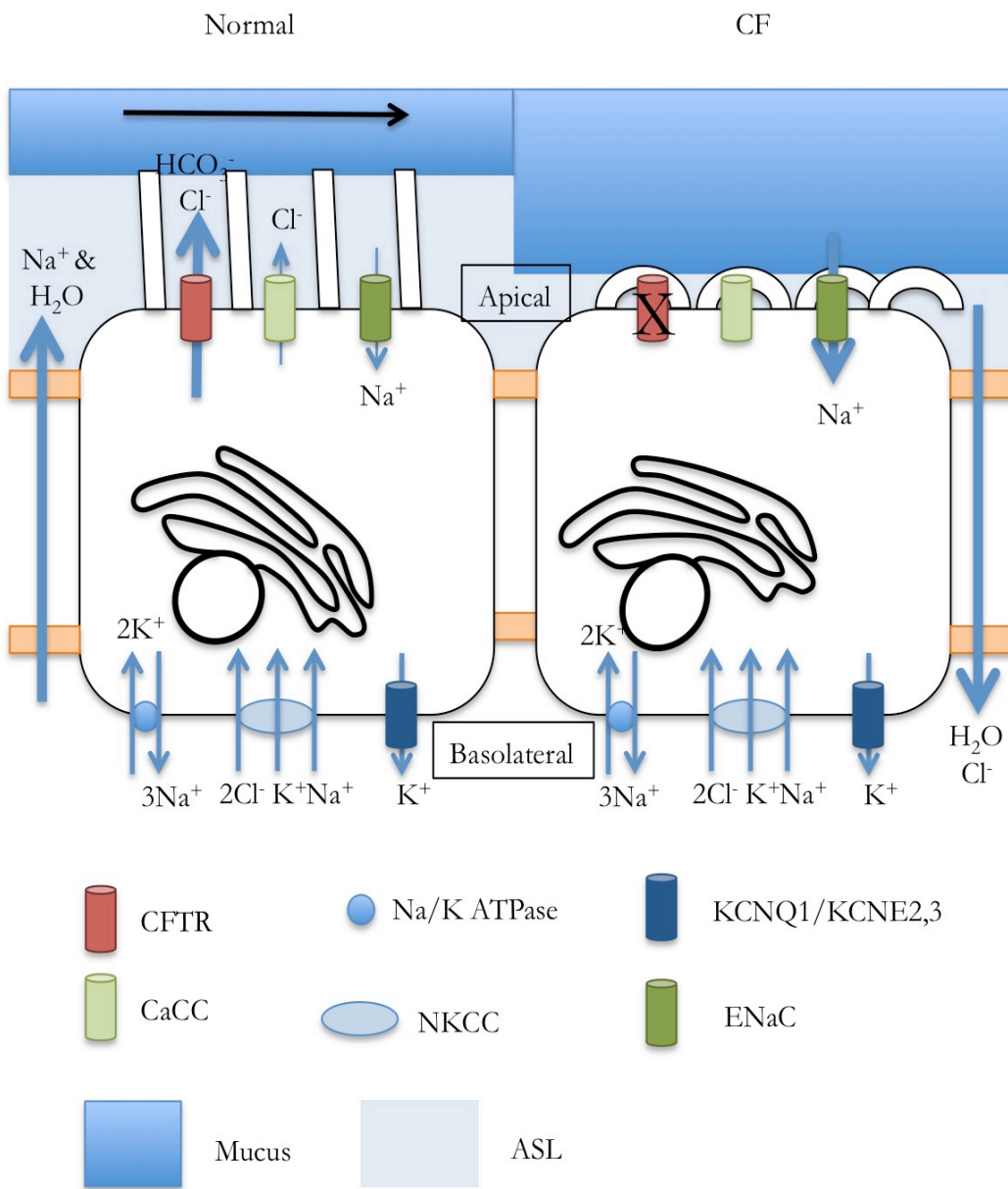
β2AR. The intracellular chloride ions then move down their electrochemical gradient through CFTR and into the lumen, which creates a lumen-negative transepithelial potential. This potential draws sodium ions from the interstitial space though paracellular junctions and the resulting high luminal electrolyte concentration draws water into the luminal space, also primarily via the paracellular route. To enable continuous secretion, PKA simultaneously increases the activity of the voltage-gated K^+ channels (KCNQ1/KCNE2,3) and WNK kinase signaling increases the activity of the NKCC transporter (3).

In patients with CF, loss-of-function mutations in CFTR prevent normal chloride flux into the lumen. The loss of secretory capability means that the absorptive function of exocrine tissues dominates. Absorption is primarily driven by apical sodium channels, specifically the epithelial sodium channel ENaC. As sodium flows down its electrochemical gradient and into the cell the Na^+/K^+ ATPase moves it into the interstitial space. This net basolateral movement of sodium keeps interstitial osmotic forces high in the absence of apical chloride secretion and prevents water from moving into the lumen. There is some evidence that ENaC activity is enhanced in CF cells due to a loss of CFTR-mediated inhibition of ENaC, but this conclusion is still actively debated (35). As discussed previously, the reduction in water movement into the airway decreases ASL depth and prevents normal function of the apical cilia. In the intestine, reduced secretion can lead to potentially fatal blockages such as meconium ileus in infants or distal intestinal obstruction syndrome in adults. This intestinal function of CFTR is highly conserved and has been seen in all CFTR-KO organisms created to date (36-38).

The CFTR-mediated secretion system can also be over-activated with potentially deadly consequences. The most notable example of this is the pathology associated with cholera toxicity, a condition resulting from the ingestion of *Vibrio cholera*. When *V. cholera* is

consumed in drinking water, it secretes cholera toxin that enters the epithelial cells of the intestine and irreversibly activates $G\alpha_s$ proteins by catalyzing a ribosylation reaction (39). The resulting increase in cAMP activates PKA and leads to supraphysiological levels of CFTR phosphorylation and hypersecretion. Consistnet with this mechanism, intestinal tissue from CFTR KO mice is resistant to the effects of cholera toxin (40). Cholera toxin-mediated intestinal hypersecretion leads to potentially fatal dehydration and electrolyte loss and is still a significant public health issue in developing nations (41). Residents in most countries with well-established sewage systems do not often suffer from cholera outbreaks because the microbe is spread via feces; however, citizens of third world countries are afflicted rather often. In 2015, the World Health Organization reported 172,454 cases of cholera that led to 1,304 deaths (WHO.int). This global health issue has motivated the development of specific CFTR inhibitors for use in the treatment of cholera and examples of some of these drugs will be discussed later.

The sweat gland

As mentioned, abnormalities in sweat gland function were integral to the realization that CF results from a fundamental abnormality in electrolyte handling and still serve as an early diagnostic marker in children. The link between sweat electrolyte composition and CF disease was originally described by Paul di Sant'Agnese in 1953 after reading a report by Kessler and Anderson (1951) reporting an increased incidence of heat prostration in CF patients during a heatwave in the summer of 1948 (8).

Unlike the other epithelial tissues discussed, the sweat gland utilizes CFTR-mediated chloride flux to facilitate NaCl reabsorption (3; 11). As shown in Figure 1.2, the sweat gland divides absorption and secretion into two separate areas along the lumen. Secretion occurs

Figure 1.2) CFTR-mediated secretion in the sweat gland and pancreas: *Top* - In the sweat duct, the secretory coil epithelium secretes electrolytes and H_2O in a manner similar to the pulmonary epithelium discussed in Figure 1. Unlike the airway, however, apical CaCCs enable movement of Cl^- in to the lumen of the secretory duct. The secretions move into the reabsorptive duct which has epithelial cells that express high levels of CFTR at both the apical and basolateral membranes. Sodium and chloride are then reabsorbed while H_2O remains in the lumen due to the presence of tight junctions between cells. Thus, the salinity of the ductal solution is reduced and hypotonic sweat is created. *Bottom* - While pancreatic epithelial cells have much of the same machinery as the other epithelia discussed, they rely mostly on the secretion of bicarbonate instead of chloride. To accomplish bicarbonate flux, they express large amounts of the basolateral sodium/bicarbonate cotransporter (NBC) and apical bicarbonate/chloride exchangers (SLC26A3/A6). In this context, CFTR chloride channel contributes to the bicarbonate flux directly while its chloride channel activity creates the chloride gradient that is used by the SLC transporters to power bicarbonate secretion.

Figure 1.2) CFTR mediated secretion in the sweat gland and pancreas

Sweat duct:

CaCC

CFTR

Cl⁻

Na⁺

H_2O

Reabsorptive Duct
Epithelium

Secretory Coil Epithelium

Pancreatic duct:

CFTR   SLC26A3/A6   NBC

Cl^- & HCO_3^-

Na^+ & H_2O

Cl^- HCO_3^-

$2K^+$
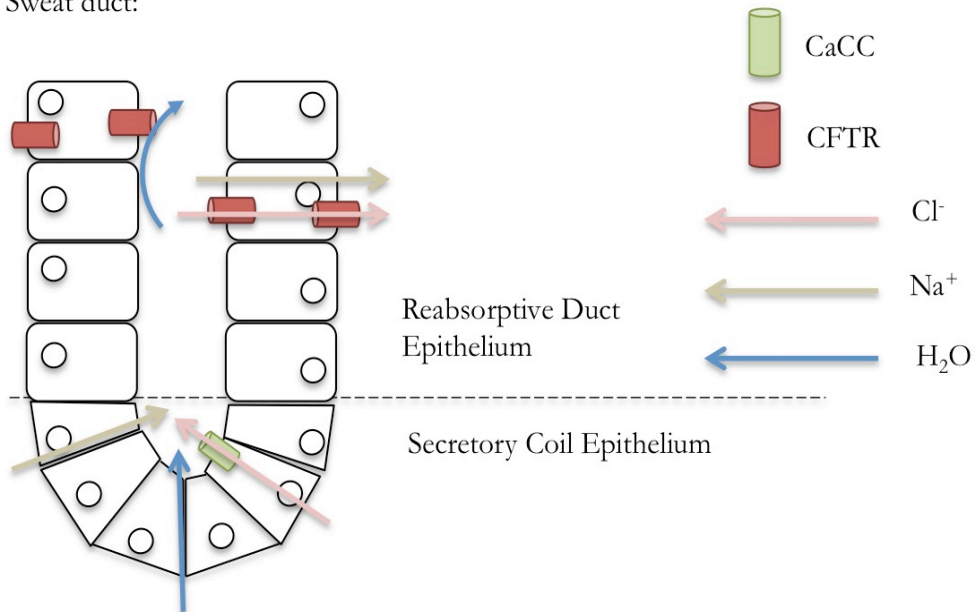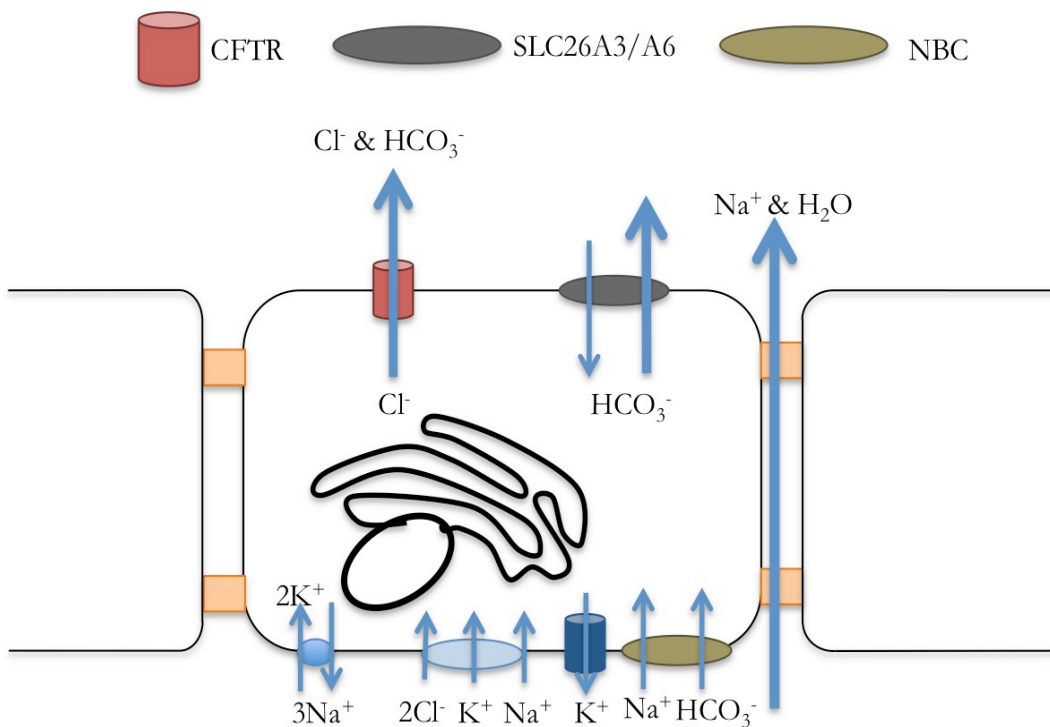
$3Na^+$ $2Cl^-$ K^+ Na^+ K^+ Na^+ HCO_3^-

deeper in the tissue in an area known as the secretory duct epithelium. Like in the airway, apical chloride flux drives secretion with subsequent paracellular flux of sodium and water into the luminal space. Unlike the airway, however, secretion is driven by activation of muscarinic acetylcholine receptors (AchRs) that activate calcium-activated chloride channels (CaCCs) and CFTR is not involved in this process. This area uses the same combination of the Na^+/K^+ ATPase, NKCC, and potassium channels to create an outward driving force for chloride. This generates the primary sweat, which is isotonic to blood as it leaves the secretory coil. Long-term secretion of isotonic sweat would lead to excessive electrolyte loss so sodium and chloride are reabsorbed in a superficial section of the sweat gland known as the reabsorptive duct. The reabsorptive duct epithelial cells in this section lack the basolateral NKCC transporter, so when coupled with Na^+/K^+ ATPase activity, intracellular concentrations of sodium and chloride remain low. Constitutive activity of both ENaC and CFTR facilitate the movement of these ions back into the cell through the apical membrane. These reabsorptive cells are also unique in that they express CFTR on both the apical and basolateral membrane, which enables the return of Cl^- back into the interstitial space from the cytosol. Despite the resulting strong osmotic force, impermeable tight junction proteins linking the epithelial cells together limit water reabsorption through the paracellular pathway resulting in the formation of hypotonic sweat.

The pancreatic duct

Fibrosis of the pancreas was one of the early clinical descriptions of CF and the high prevalence of pancreatic dysfunction associated with the disease highlights the integral role of CFTR in pancreatic physiology (5; 6). The exocrine pancreas secretes a bicarbonate-rich, isotonic solution containing digestive enzymes into the GI tract where it mixes with the food

bolus to facilitate digestion and neutralize the duodenal pH. Pancreatic duct cells express many of the same transporters and channels discussed previously that create sodium and potassium gradients and set the negative membrane potential. In addition, these cells express high levels of the Na^+-bicarbonate cotransporter (NBC) on the basolateral membrane that moves bicarbonate into the cell. CFTR channel activity contributes both directly and indirectly to the outward flux of bicarbonate across the apical membrane. As discussed previously, CFTR can conduct both bicarbonate and chloride in response to PKA-mediated signaling, and due to the high levels of bicarbonate in pancreatic duct cells, it constitutes a significant fraction of CFTR-mediated anion flux in these cells. Bicarbonate is also moved into the lumen by the Cl^-/HCO_3^- antiporter (SLC26A3 or SLC26A6), which utilizes apical chloride to export bicarbonate (3; 11).

1.2.2) CFTR Structure and Gating

Cystic fibrosis was linked to mutations in the CFTR gene in 1989 (42-44). Sequence and hydropathy analysis suggested that CFTR shares many characteristics with the ATP-binding cassette transporter (ABC Transporter) family of proteins; however, it is the only member known to function as an ion channel. The basic "functional unit" of all ABC transporters consists of four domains - two transmembrane domains (TMDs) that interact to form the channel pore or substrate binding pocket and two cytosolic Nucleotide Binding Domains (NBDs) that bind two ATP molecules, dimerize, and drive conformational change in the TMDs. In the case of CFTR, NBD dimerization leads to the opening of an anion-permeation pathway. Closure of the pore is driven by ATP catalysis in the NBDs and subsequent NBD dedimerization. Unlike most other ABC transporters, CFTR contains only one functional ATP hydrolysis site that dictates channel closure. The CFTR gene encodes

all four of these domains and, thus, functions as a single peptide. CFTR also contains a

cytosolic regulatory domain (R-domain) that must be phosphorylated before ATP can elicit

anion channel activity. This process of channel opening and closing (also known as gating)

involves coordinated events across the entirety of the peptide and will be discussed further

below. Figure 1.3 provides visual representations of the domains that will be discussed in

the following sections along with a simplified gating diagram.

Figure 1.3) CFTR is an anion channel evolved from the ABC transporter family of proteins: (a) A two dimensional representation of CFTR topology shows that it consists of two transmembrane domains (TMDs, orange and blue) that are made up of six transmembrane helices each and are integrated into the membrane. The two nucleotide binding domains (NBDs, green and cyan) follow their respective TMDs, and the regulatory (R) domain sits cytoplasmically in between NBD1 and TMD2. (b) A homology model based on the crystal structure of the bacterial ABC transporter Sav1866 shows how the TMDs might interact in the membrane and how each TMD has contacts with both NBDs. The Sav1866 crystal structure was obtained in the presence of ADP and shows dimerized NBDs, thus modeling an open conformation of CFTR. The view shown would be that expected when looking at the protein parallel to the membrane. Lipids are shown in grey and have been removed from the viewed side of CFTR for clarity. (c) A crystal structure of isolated, dimerized NBD1 peptides from human CFTR with nucleotide binding motifs highlighted (PDB: 2pze). The vantage point is looking in the direction of the membrane from cytosolic side of the protein. ATP molecules are shown as sticks adjacent to magnesium ions (grey spheres) and are colored according to atom. One ATP can be seen at the interface of the NBD in the top half of this picture while a second can be seen in the bottom half. The signature sequence is adjacent to the magnesium ion and is shown in red. The Walker A motif is adjacent to the ATP and is shown in blue. The Walker B motif is shown in orange and the terminal aspartic acid residue on the beta sheet side interacts with the magnesium ion. The adenosine ring interacts with a tryptophan residue (W401) upstream of the Walker A motif. (d) A simplified gating scheme for CFTR shows that after phosphorylation of the R-domain (not shown) NBD dimerization occurs after binding of two ATP molecules. Dimerization leads to conformational changes in the TMDs associated with opening of the anion-permeant pore, a process known as "pore gating." Hydrolysis of the ATP at nucleotide binding site 2 leads to closure of the pore. Diffusion of ADP and P_i from the NBDs enables binding of a new ATP to reopen the pore.

Figure 1.3) CFTR is an inion channel evolved from the ABC transporter family

a)

Extrcellular side

Cytoplasmic side

b)

c)

d)
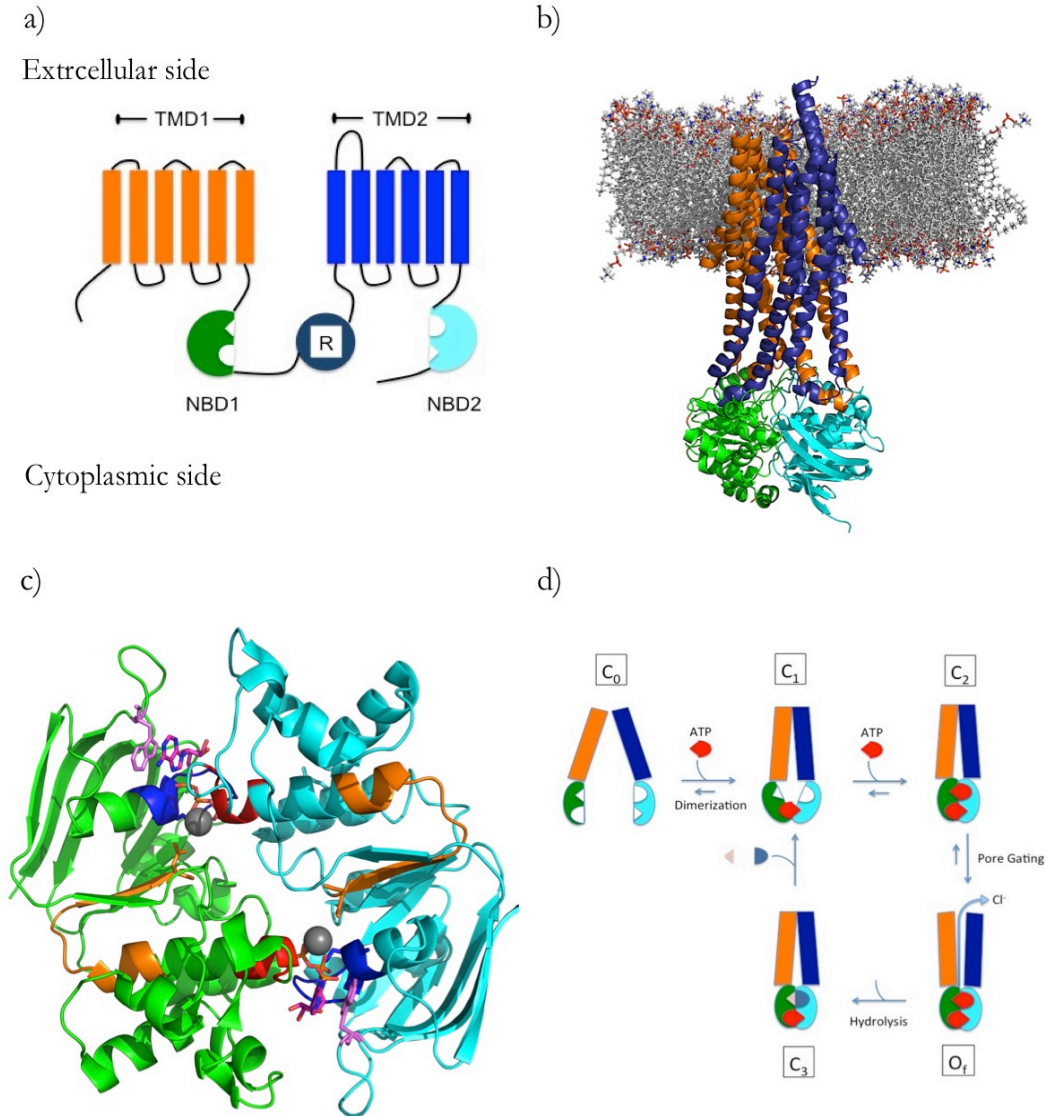
The R-domain:

As mentioned previously, the first step in CFTR channel activation is phosphorylation of the cytosolic R-domain. In terms of the primary sequence, the R-domain lies between NBD1 and TMD2 and is schematized in purple in Figure 1.3a. The predominant kinase that is thought to mediate R-domain phosphorylation is PKA. CFTR channel activity can be monitored in epithelial cell monolayers using the Ussing chamber recording technique by activating $G\alpha_s$-mediated signals with agonists as isoproterenol, acetylcholine, vasoactive intestine peptide (VIP), and adenosine (45) (46). Additionally, cAMP analogues known to directly bind and activate PKA can also be used to activate channel activity in this system (47). There are 18 potential phosphorylation sites with 12 serines thought to be the predominant regulatory sites. Their contributions to CFTR gating are not equal, with loss of sites such as S700, S795, and S813 leading to a decrease in maximal channel activity while loss of S737 and S768 leads to an increase in channel activity (48). Phosphorylation leads to an increase in the number of opening events and does not significantly affect the open duration or the single channel amplitude (49; 50). How phosphorylation at specific residues leads to channel activity is not well understood but some evidence suggests that at least a portion of the R-domain serves as an inhibitor of channel opening in the absence of phosphorylation. This is supported by the observation that a CFTR construct lacking the R-domain, split-ΔR-CFTR, retains anion channel function and shows basal activity in the absence of PKA activation (51). However, it has also been observed that perfusion of a phosphorylated R-domain onto patches containing split-ΔR-CFTR channels can increase channel activity suggesting that the R-domain may facilitate some level of channel opening (52). The complexity of R-domain interactions was reaffirmed by Bozoky and colleagues who showed NMR evidence of phosphorylation-

dependent R-domain interactions across multiple domains of CFTR including NBD1, NBD2, and the C-terminus (53). Additionally, the recent unpublished Cryo-EM structure of human CFTR seems to contain part of the R-domain in the intracellular vestibule between the TMDs. Interestingly, the cumulative affect of phosphorylation at the numerous sites discussed leads to varying levels of channel activity and ultimately the R-domain enables tuning of CFTR channel activity in a graded fashion.

The nucleotide binding domains:

After phosphorylation, CFTR channel gating is initiated by binding of ATP to the Nucleotide Binding Domains and their subsequent dimerization. Evidence for NBD dimerization in the presence of ATP includes increased NBD crosslinking efficiency following phosphorylation of the R-domain (54) and energetic coupling between residues located on opposing NBDs (R555K and T1246N) (55). The NBDs interact in a "head-to-tail" configuration with the N-terminal side of NBD1 interacting with the C-terminal side of NBD2 and visa versa (55) (54) (56). The ATPs are "sandwiched" between the NDBs with each domain contributing part of each ATP binding site. Figure 1.3c shows a crystal structure of a murine CFTR-NBD1 homodimer in complex with ATP. The interaction between ATP and the NBDs relies on highly conserved sequences that are characteristic of ABC transporters. Conserved regions include the Walker A motif (shown in blue), the Walker B motif (shown in orange), and the signature sequence (shown in red). A conserved lysine in the Walker A sequence (G-X-X-G-X-G-K-S/T) interacts with the γ-phosphate of ATP and is essential for ATP hydrolysis. A terminal aspartic acid in the Walker B sequence (R-X$_7$-h-h-h-h-D) interacts with the Mg^{2+} ion that is coordinated by ATP and is required for effective hydrolysis (57; 58). The signature sequence (also called the LSGGQ motif) is

highly conserved amongst ABC transporters and is present in NBD1; however the NBD2 of

CFTR has an atypical signature sequence that prevents effective catalysis at this site

(LSHGH). The serine hydroxyl side chain and glycine main-chain nitrogens interact with the

γ-phosphate of ATP via hydrogen bonding (59-61).   Mutations in the signature sequence

have deleterious effects on CFTR channel function and many are associated with CF disease.

Finally, an aromatic side chain upstream of the Walker A motif interacts with the adenosine

ring of the ATP via π-electron stacking (62).

The ATP binding sites span the NBD interface such that each ATP is stabilized by

the Walker A and B motifs from one NBD and the signature sequence in the other NBD.

Nucleotide Binding Site 1 (NBS1) is made up of the Walker A and B motifs from NBD1

and the atypical signature sequence of NBD2. Because the signature sequence is involved in

ATP catalysis, loss of the glutamine residue (G → H) in the signature sequence of NBD2

renders this site noncatalytic (63; 64). Conversely, the catalytic NBS2 site is made up of the

Walker A and B motifs from NBD2 and the signature sequence of NBD1. The differential

ATPase activity in the Nucleotide Binding Sites means that the kinetics of NBS2 drive

CFTR channel gating in the presence of ATP. The difference in catalytic activity at each site

is also thought to lead to dramatically different ATP residence times. ATP is thought to

reside in the noncatalytic site (NBS1) for tens of seconds, a conclusion supported by

increased labeling with the photolabile ATP analogue N_3ATP (65) and a biphasic change in

channel gating behavior after a rapid switch to N^6-(2phenylethyl)-ATP (PATP), an ATP

analogue that elicits more current upon binding to CFTR (66). The importance of ATP

catalysis at NBS2 in the gating cycle can be seen experimentally by introducing NBS2

mutations that abolish catalysis or the incubation with nonhydrolyzable ATP analogues.

Specifically, channels harboring the K1250A mutation lose hydrolytic capacity (64) and

remain in the open state for extended periods of time (mean burst duration is on the order of tens of seconds instead of the normal 300 ms seen in WT channels). WT channels incubated with nonhydrolyzable ATP analogues, for example AMP-PNP, show similar a gating behavior with extended burst durations (67). How far the NBDs separate following catalysis at NBS2 has yet to be clearly defined. While past evidence using mutant cycle analysis and ligand exchange protocols suggest little separation at the noncatalytic site (66; 68), Gadsby and colleagues recently found that cysteines engineered into NBS1 become accessible to cys-reactive MTS reagents equally as often as cysteines engineered into NBS2 suggesting that full dedimerization occurs quickly during normal channel gating (69).

In addition to binding ATP and driving the transition to the open state, NBD2 contains a C-terminal PDZ binding domain that is integral to normal CFTR function in epithelia. The class 1 PDZ ligand in CFTR has the sequence D-T-R-L and links it to the cytoskeleton though the PDZ-domain proteins NHERF1 and NHERF2 (70-72). This interaction localizes CFTR into a complex with proteins that can activate its ion channel function, for example the β2AR, and has been shown to be essential for proper trafficking of the channel to the plasma membrane and evidence suggests that it is also crucial for protein stability in the membrane (73; 74). Once in the membrane, the PDZ-mediated interactions immobilize the protein and limit diffusion as measured by single particle tracking (75; 76). Recent evidence from Hanrahan's group implicates a role for cholesterol in this process as well, though the mechanism that links cholesterol content to cytoskeletal tethering of CFTR has not remains unknown (77).

The transmembrane domains and pore:

How NBD dimerization leads to a conformational change in the TMDs that opens

the pore has yet to be clearly defined. The interaction between the TMDs and the NBDs in ABC transporters is rather complex and occurs mostly through the intracellular loops (ICLs) of the TMDs. CFTR contains four ICLs and the interaction is not strictly vertical. Instead, each TMD has contacts with both NBD1 and NBD2 (Fig. 1.3b) (78). This was recently confirmed in the cryo-EM structure of the zebrafish homologue of CFTR in the dedimerized (closed) conformation (79). Biochemical crosslinking studies have shown relatively close proximities for ICL residues and the top of the NBDs (80). The functional role of these contacts in CFTR gating is complex with interactions changing during the course of gating. In general, He and colleagues found that crosslinking of domain-swapping contacts (i.e. ICLs from TMD1 contacting NBD2) led to a reduction in the ability of CFTR to gate properly, while crosslinking of the interdomain contacts on the same half of the protein had a lesser impact (80). These data suggest that while cross-protein residues interact in the closed conformation of CFTR, they change during the transition to the open conformation. The most discussed ICL/NBD interaction involves the phenylalanine at position 508 (F508) because deletion of this residue (F508del) is the most common allele associated with CF. F508 is located in NBD1 and is thought to intercalate into a hydrophobic pocket created by aromatic residues in ICL4 and TM11, specifically F1068 and F1074 (79; 81). In addition to the dramatic deleterious effects on channel trafficking and maturation that will be discussed later, loss of F508 upon mutation to cysteine leads to a decrease in channel activity, with introduction of a charge via reaction with the positively charged, cys-reactive reagent MTSET effectively silences the channel (81; 82).

Input from NBD dimerization leads to changes in the orientation of multiple residues lining the pore. This dynamic nature of the pore is commonly refered to as "pore gating" and is integral to the characteristic gating behavior of WT-CFTR channels. Despite

being evolutionarily and structurally distinct from other channels, the pore of CFTR shares some common functional characteristics with other ion channels. First it selectively conducts anions over cations with an anion permeability sequence as follows (83):

$$SCN^- > NO_3^- > Br^- > Cl^- > I^-$$
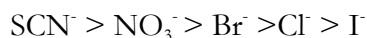
The CFTR conductance sequence is as follows:

$$Cl^- > NO3^- > Br^- > acetate > I^- > SCN^-$$
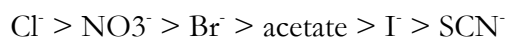
Like most anion channels, the CFTR pore is less selective than the commonly studied cation channels, for example voltage-gated sodium and potassium channels (84).

A great deal of work has focused on elucidating the pore structure of CFTR, and much of this work was recently validated by the cryo-EM structure of zebrafish CFTR. For example, functional cysteine scanning experiments based on residue reactivity to methane thiosulfonate (MTS) reagents enabled multiple groups to determine pore lining residues along TM 4 and 6 (85-88). Additionally, the narrowest part of the pore, which acts as a gate to block Cl⁻ conduction when the channel is in the closed conformation, is located near the extracellular boundary of the membrane, formed by the close proximity of residues near the extracellular ends of TM 6 and 12 (83; 88-90). During gating, the formation of interhelix salt bridges stabilize the open conformation of the pore. Specifically, ionic interactions between residues R347 and D924 and between R352 and D993 (91) enable the stable burst behavior of CFTR. Loss of any of these residues leads to unstable channel openings and decreased macroscopic current despite normal phosphorylation and ATP-dependence. In fact, mutations in R347 diminish activity to the extent that they cause CF (85).

1.2.3) – CFTR inhibitors

CFTR channel activity is sensitive to multiple classes of compounds through a

variety of mechanisms. As with all ion channels, CFTR chloride conductance can be blocked by compounds that bind in and occlude the flow of ions through the pore. These compounds are referred to as "pore blockers" and are often large organic anions that interact with the pore lining residues of CFTR via electrostatic interactions. Classic examples of pore blockers include diphenylamine-2-carboxylate (DPC), 5-nitro-2-(3-phenylpropylamino) benzoic acid (NPPB), niflumic acid, glibenclamide, and the glycine hydrazide GlyH-101 (92-95). Pore blocker efficacy is voltage dependent and sensitive to the local chloride concentration. Electrophysiologically, these compounds appear to introduce brief closures in single channel recordings (89; 96-98). While experimentally useful, these inhibitors are generally nonspecific due to their mechanism of action.

The second approach to blocking CFTR channel activity is to block the normal gating cycle. These molecules are known as "gating modifiers" and the best example of this class is the thiazolidinone CFTR inhibitor 172 (INH_{172}) (99) (94). INH_{172} reduces total current by decreasing the frequency with which the channel opens (100). While its exact mechanism and binding site is not known, it is likely that INH_{172} works by interacting with and stabilizing a closed conformation of the channel. Like other gating modifiers, the efficacy of INH_{172} is voltage independent (100). This drug was discovered via high throughput screening with the hope of being utilized as a therapy for cholera. While its potency was not adequate, the increased specificity of INH_{172} for CFTR over other chloride channels has proven beneficial to basic research. There is no doubt that the variety of CFTR inhibitors will continue to increase as the hunt for a useful cholera therapeutic continues.

1.3) CF-associated mutations and therapeutics:

Disease associated mutations occur throughout the CFTR gene. In total, over 2000

mutations have been associated with CFTR and >200 have been associated with CF disease. Mutations have traditionally been categorized into six classes based on their biochemical and biophysical consequences. The six classes are:

- Class 1 - Mutations that disrupt protein synthesis

- Class 2 - Mutations result in defective protein processing and maturation

- Class 3 - Mutations that prevent normal activation

- Class 4 - Mutations that prevent normal ion conductance

- Class 5 - Mutations that lead to a reduction in mRNA synthesis

- Class 6 – Mutations that decrease the stability of CFTR protein in the plasma membrane

While generally helpful, continued research has suggested that this classification scheme is not complete and that some mutations cause multiple defects (101). For clarity, this section will be organized according to the traditional classification scheme. The goals are to review the functional consequences of each mutation class, provide common examples, and review the current, targeted therapeutic approaches for each; however, some discussion of secondary consequences will be included where appropriate.

Class 1 – These mutations are relatively rare among the CF population. In patients with Class 1 mutations, the CFTR sequence contains a premature stop codon, a splice site mutation, or a frame shift mutation that prevents synthesis of the full-length protein. In these patients, mRNA levels are greatly reduced and any truncated proteins are quickly degraded via nonsense-mediated decay (102; 103). These patients do not have any functional CFTR at the cell membrane and present with a very severe disease phenotype. The most common Class 1 mutation is the G542X in which translation of the nascent

peptide stops at residue 542 (a full 938 residues early) and comprises 2.4% of CF-associated alleles. Other examples of Class 1 mutations are W1282X and R553X.

Treating Class 1 mutations is difficult and the only therapeutic progress seen in this class of mutation is in the treatment of premature stop codons. Treating these mutations relies on compounds known as "read-through agents," which cause the ribosome to disregard the premature stop codon and insert a random amino acid in its place. Numerous read-though agents have shown positive results in the lab and have moved into clinical trials (104). One complication of this approach is that point mutations often lead to dysfunctional CFTR channels so the insertion of random amino acids at the premature stop positions may not result in a fully functional protein product. Alternatively, it may lead to a misfolded protein product that fails to traffic properly. While this remains to be seen, these complications might necessitate the use of other therapeutics, for example the correctors and potentiators discussed in the treatment of Class 2 and 3 mutants, to successfully treat patients with Class 1 mutations.

Class 2 - The most common mutation in the U.S. CF population belongs to Class 2 and is the in-frame deletion of the phenylalanine at position 508 (F508del) that was discussed previously. According to the CFTR2 database, which is freely available and curated by Johns Hopkins University (www.cftr2.org), 69.9% of CF patients carry at least one F508del allele. Deletion of the F508 residue prevents proper protein folding by destabilizing the interaction between NBD1 and TMD2 (81). The defect in protein folding and trafficking that results from F508del has been known since shortly after cloning CFTR due to its distinct electrophoretic characteristics (63). CFTR folding is a complex process that involves a series of glycosylation steps: the first glycosylation step occurs in the

endoplasmic reticulum (ER) and appears to occur regardless of the structural integrity of the nascent protein; the second occurs in the Golgi where, after the protein is folded correctly, a second set of modifications is added to the fourth extracellular loop (ECL4). The misfolded protein fails to leave the ER when a mutation like F508del is recognized by the cellular chaperones and the second glycosylation step does not occur (105). These two distinctly glycosylated forms of CFTR can be separated by SDS-PAGE with WT CFTR appearing as two bands (one representing the immature form and one representing the mature form) while F508del appears as a single band (only immature). This simple SDS-PAGE assay is the gold standard for the detection of Class 2 mutations as well as for determining the efficacy of therapeutics that improve F508del trafficking.

As discussed previously, mutations at the F508 position also lead to gating defects. This dual effect is also seen in other traditionally Class 2 mutations, for example P67L. Given the dual nature of the defect, treating patients with Class 2 mutations requires a two-pronged approach: one drug to address the folding problem and another to solve the gating problem. Drugs used to solve the gating problem are also used to treat patients with Class 3 mutations and will be discussed in the next section. To solve the folding problem, drug development has focused on the discovery of compounds known as correctors. These drugs enable the F508del-CFTR to undergo complete glycosylation and traffic through the Golgi to the plasma membrane (106). In theory, this class of drugs can work through multiple different mechanisms: by directly binding to and stabilizing CFTR into a conformation that is compatible with maturation, by modulating the function of a chaperone protein that is involved in folding or checking folded CFTR, or by altering the proteostasis network to slow degradation and allow increased maturation (107). There is currently one clinically prescribed corrector on the market, VX-809, which is found in the combination therapeutic

Orkambi, and it is currently unclear which mechanism VX-809 uses to facilitate F508del-CFTR maturation. Orkambi has proven less effective in patients than in cell-based assays *in vitro* and has significant side effects (108). Given the prevalence of Class 2 patients, the development of correctors is a top priority for both researchers and pharmaceutical companies and there are multiple corrector compounds currently being tested in clinical trials, for example VX-661, FDL-169, and VX-152 (cff.org/Trials/Pipeline).

Class 3 – Patients with Class 3 mutations are the second most common group seen in the clinic. These mutations alter some aspect of CFTR gating and are observed over a wide swath of the protein, perhaps not surprising given the complex dynamics that enable transition of the pore from the closed to the open state. The most common Class 3 mutation seen in the clinic is G551D, which represents 2.1% of patient alleles. The glycine at position 551 lies in the signature sequence of NBD1 (NBS2) and the presence of a negatively charged aspartic acid in the ATP binding site decreases the affinity of the NBS2 site for ATP (109). The decrease in ATP binding leads to a decrease in channel activity despite normal phosphorylation of the R-domain.

Class 3 mutations have seen the most progress in therapeutic development, specifically through the development of VX-770 (Kalydeco, Ivacaftor) and its FDA approval in 2012. Kalydeco has proven to be a very efficacious potentiator of Class 3 mutants (and WT-CFTR) *in vitro* and *in vivo*. Homozygous G551D-CFTR patients enrolled in the clinical trial exhibited a rapid increase in lung function as well as improvement in their BMI and weight gain (110; 111). How VX-770 overcomes the defect introduced by the G551D mutation is not clear; however, it effectively potentiates purified CFTR that has been incorporated into planar lipid bilayers (112) suggesting that it works by interacting directly

with the ion channel. While the exact binding site is not known, the ability of VX-770 to potentiate the next class of mutations suggests that it might work by stabilizing the TMDs into an open conformation. The second section of the Discussion will more thoroughly highlight what is known about the mechanism of VX-770.

Class 4 – Class 4 mutations alter the structure of the CFTR pore such that the TMDs fail to open an adequate conduction pathway for chloride ions following dimerization of the NBDs. One example of a Class 4 mutation is R347H. The R347 residue lies in TM6 near the intracellular vestibule (intracellular side of the pore) where it forms a salt bridge with the aspartic acid residue at position 924, across the pore in TM8. The interaction stabilizes the open conformation of the pore and, when lost, the channel is unable to stably maintain a pore architecture that conducts chloride at the WT level of 8 pS (85; 91). The R347H mutation leads to a 90% decrease in total current as compared to WT-CFTR expressed in FRT epithelial monolayers (113). Other examples of Class 4 mutations occur all along the TMDs and have varying levels of dysfunction. Other examples of Class 4 mutations include R347P (intracellular vestibule), R334W (extracellular vestibule), and R117H (extracellular loop) (114).

The ideal treatment of Class 4 mutations would involve restoring the pore architecture, but an alternative approach is to simply increase channel activity to compensate for the reduced single channel conductance. In this regard, the small molecule potentiator VX-770 is promising because it has shown the ability to rescue chloride channel function in some Class 4 mutants. For example, treatment with VX-770 increases the macroscopic current in FRT cells expressing R347H-CFTR to near 100% of the current level of FRT cells expressing WT-CFTR (113). This is likely due to the fact that the R → H mutation is

relatively mild, with histidine maintaining some positive polarity and being slightly smaller in size than arginine. The ability to correct the conductance defect seems to depend on how biochemically different the mutant residue is compared to the WT residue as a similar efficacy can be seen with the R117H mutant. However, other more biochemically disparate changes have proven less responsive to Kalydeco treatment. For example, Kalydeco has proven less effective against the R334W mutant, with maximal rescue of ~ 5% of normal function, and is unable to elicit any current from cells expressing R347P CFTR (113). While the clinically available potentiator may be useful for some patients with Class 4 mutations, treatment of many will rely on the development of new drugs that overcome the specific structural abnormality introduced by each type of mutation.

Class 5 – These mutations reduce the level of CFTR mRNA in the cell leading to a reduction in the level of CFTR protein. The most common Class 5 mutation is located in the promoter and is called "3849 + 10kB C→ T". While these patients have a normal, WT CFTR coding sequence, disease arises from inadequate levels of protein at the epithelial cell surface (115).

Treatment of Class 5 mutations relies on increasing the level of CFTR messenger RNA in the cell. Some progress has been made in the treatment of Class 5 mutations with the development of compounds known as "amplifiers." This class of compound was discovered by Proteostasis Therapeutics in 2016 and work by stabilizing CFTR mRNA in the cell. Interestingly, they found that their compounds do not stabilize all mRNA in the cell. Their preliminary amplifier is "PTI-428" and is currently undergoing phase I clinical trails. Amplifiers may also be useful for other classes of mutations since they are said to have additive effects with clinically available correctors and potentiators (116).

Class 6 – This represents a relatively new classification and describes mutations that reduce the plasma membrane residence time of CFTR. There are examples of mutations that solely lead to this effect, for example the Q1412X mutation; however, this problem has become more prominent with the discovery that corrected F508del-CFTR also displays this phenotype. In regard to the treatment of patients with the F508del mutation, this finding suggests that restoring the ability of the channel to traffic will not be sufficient to fully restore function (116).

Therapeutics that target this problem have been classified as "stabilizers" and, in theory, this problem could be corrected in multiple ways. First, Valentine and colleagues showed that the rescued F508del protein has reduced levels of PDZ interactions (74) suggesting that reduced cytoskeletal interaction may play a role in its short plasma membrane residence time. Consistent with this hypothesis, multiple groups have shown that increasing the interaction of CFTR with NHERF-1 stabilizes the protein at the PM (117-119). An additional approach may be to inhibit specific chaperone proteins. This idea is based on the observation that rescued F508del-CFTR stability was improved by reducing its interaction with Hsp70/Hsp90 organizing proteins. Ultimately, finding stabilizers will be crucial to effectively increase CFTR activity in the majority of CF patients (i.e., F508del homozygotes).

Gene therapy – a mutation-independent approach

The proverbial "holy grail" of treating monogenetic diseases is to permanently correct the condition through the use of gene therapy. In theory there are multiple ways to achieve this goal: 1) gene transfer using viral and non-viral DNA vectors and, 2) gene editing using endonuclease complexes (120; 121). Multiple groups have successfully restored CFTR

channel function *in vitro* and a few others have successfully restored activity in the nasal

epithelial cells of CF patients (122-125). However, their *in vivo* effect on pulmonary function

has been limited by difficulties in vector delivery and the fact that pulmonary epithelial cells

are terminally differentiated (120; 121). Additionally, treatment with viruses and non-viral

complexes often leads to inflammatory responses that could exacerbate an already

hyperinflamed CF lung. Despite these current hurdles, the high potential reward of a

permanent cure drives continued research in the CF-focused gene therapy. In fact, multiple

pharmaceutical companies have recently increased their gene-therapy funding, particularly

since the discovery of the CRISPR/Cas9 system (investors.vrtx.com).

1.4) Sphingolipids in Epithelia and CF

The goal of section 1.4 is to introduce the relationship between CFTR and the lipid environment of epithelial cells, specifically that of sphingolipids. Due to the evidence for a functional interaction between sphingolipids and CFTR, time will be spent discussing sphingolipid metabolism, as well as their roles in signaling and as structural molecules in the membrane. Discussion of other lipid classes will be included where appropriate but, for brevity, will be relatively brief. Evidence of disruptions in sphingolipid metabolism in CF will then be discussed along with their potential contributions to CF disease. Finally, this section will discuss the published evidence for an interaction between CFTR function and sphingolipid metabolism.

1.4.1) General Lipid Considerations:

It has been known for decades that lipids are an integral part of the cellular plasma membrane. As in all other mammalian cells, epithelial cells rely on various lipid systems to function properly. Lipid bilayers delineate the boundaries of cells and organelles, acting as a barrier to the free diffusion of the numerous charged molecules that are required for life, for example DNA, ATP, ions, and proteins. Additionally, the metabolism of specific membrane lipids can modulate intracellular processes, for example phosphatidylinositol 4,5-bisphophate (PIP_2) cleavage into diacylglycerol (DAG) and inositol triphosphate (IP_3) in response to the activation of Gq-coupled GPCRs (126), or the breakdown of sphingomyelin stimulated by the activation of TNF-R1 (127). However, compared to the influence of small charged molecules and enzymes, relatively little is known about the influence of lipid homeostasis on cellular physiology.

The lipids found in cell membranes can be divided into eight groups total (128), with

the predominant three being glycerolipids, sphingolipids, and sterols. Examples of each are shown in Figure 1.4. Glycerolipids are characterized by a glycerol backbone and often contain three modifications, like the two acyl chains and phosphocholine headgroup of phosphatidylcholine (shown in the middle panel of Figure 1.4a). Sphingolipids are characterized by the "sphingoid base," this simplest of which is sphingosine and is shown in Figure 1.4a. Sterols are characterized by the quaternary ring backbone and have crucial roles in hormone signaling.
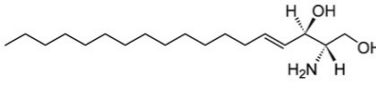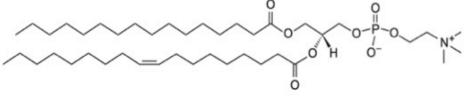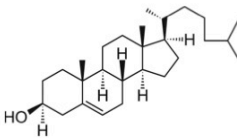
Interestingly, lipids are not randomly distributed in the plasma membrane. A subset of lipids known as phospholipids, which are characterized by a phosphodiester bond-linked headgroup on the C1 carbon, are asymmetrically distributed between the inner and outer leaflet of the bilayer (Fig. 1.4b). Specifically, phosphatidylcholine (PC), sphingomyelin (SM), and glycosphingolipids (GSL) reside in the outer leaflet, while phosphatidylserine (PS), phosphatidylinositol (PI), and phosphatidylethanolamine (PE) reside predominantly in the inner leaflet (129). This heterogeneity is maintained by ABC transporters that are colloquially called "flippases" and "floppases" (130; 131). Conversely, activation of proteins called "scramblases" can collapse this heterogeneity in response to specific cellular signals. The most notable scramblase dependent process is the movement of PS to the outer leaflet of the membrane preceding apoptosis (132; 133). The energy-dependent and tightly controlled nature of lipid asymmetry speaks to its importance in cellular homeostasis.

In addition to leaflet asymmetry, some evidence suggests that a heterogeneous distribution of lipids exists across the lateral face of the plasma membrane as well. It is believed that this effect might create lipid-specific nanodomains, or "lipid rafts", in the cell membrane that could assist in protein organization and/or signaling (134). The size, lifetime, and role of these domains are active areas of study and the concept of "lipid rafts"

Figure 1.4) Major mammalian cell lipids: The three major lipids classes are shown in panel a. Sphingolipids are characterized by the presence of sphingosine, the simplest sphingolipid that is often referred to as a "sphingoid base" and is shown in the top row of panel a. Sphingosine can be acylated at the C2 amine to form ceramide. The C1 hydroxyl can also be modified with one of several headgroups including phosphate, phosphocholine, glucose, or galactose. Glycerolipids are characterized by the glycerol backbones (hydroxyl groups at C1, C2, and C3). Phosphatidylcholine is shown in which the C2 and C3 hydroxyls are acylated and the C1 hydroxyl is conjugated to a phosphocholine headgroup. Sterols make up the third most abundant class of lipid in the cell membrane and are characterized by the quaternary ring backbone. Panel b shows the asymmetric distribution of phospholipids that is characteristic of eukaryotic cells. Adapted from Daleke 2008 (129).

Figure 1.4) Major mammalian cell lipids

a)

Class	Example	Example structure
Sphingolipid	Sphingosine	
Glycerolipid	Phosphatidylcholine	
Sterol	Cholesterol	

b)
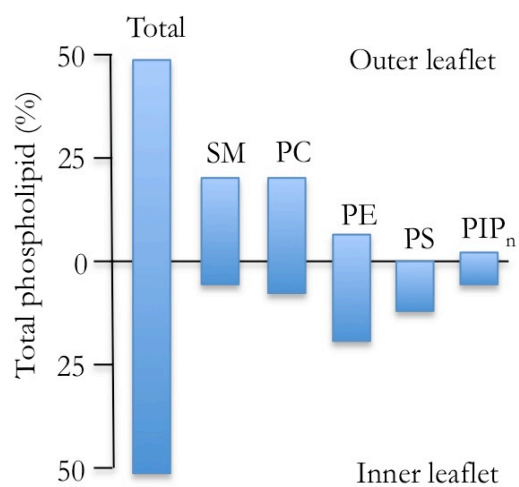
has evolved over the last couple decades. Lipid partitioning can be clearly seen when vesicles are made from purified lipids, but their stability decreases with increasing lipid complexity and temperature, two factors that clearly influence lipid behavior in cells (135). Early biochemical evidence for the existence of lipid rafts in cells was the observation that some proteins and lipids coalesced into detergent-resistant, low-density fractions following cellular lysis with nonionic detergents like Triton X-100. These detergent resistant membranes (DRMs) were rich in sphingolipids and dependent upon the presence of cholesterol. They also contained specific membrane proteins like caveolin-1 (136). Given that some signaling events correlated with the movement of specific proteins into DRMs and depended upon cholesterol, DRM microdomains seemed to be important for some types of physiologic events. Recent evidence using TIRF and high-resolution microcopy in live cells at 37°C have supported the idea of transient, nanometer-sized lipid domains. One piece of evidence is that fluorescently tagged sphingolipids localize to specific membrane domains and colocalize with protein-based lipid specific probes in live erythrocytes (134). Additionally, protein sorting into sphingolipid rich domains has been observed in live B lymphocytes following activation (137; 138). Thus, current evidence suggests that the distribution of proteins and lipids in the cell membrane is complex and tightly controlled with potential mechanisms for protein/lipid crosstalk yet to be fully elucidated.

1.4.2) Sphingolipid Handling in Epithelial Cells:

Sphingolipid synthesis and trafficking:

Sphingolipids are a diverse class of lipid molecules characterized by the presence of the sphingoid base backbone (128) . First described in 1884 by J.L.W. Thudichum, the sphingolipid structure remained unknown until 1947 when the structure of sphingosine was

described (shown in Figure 1.4) (139). Since then, the role of sphingosine in cellular

signaling as well as its metabolism into hundreds of other species has uncovered (139-141).

The predominant sphingosine species in mammals consists of an 18 carbon sphingoid base,

though species containing anywhere from 14 to 26 carbons in numerous saturation states

have been described. The amide group at position C2 can be acylated to form the

intermediate ceramide. As is seen in sphingosine, the length of the amide-linked acyl chain

can vary depending on the subcellular location and synthetic enzyme. Finally, the hydroxyl

group at position C1 can be modified with one of numerous possible headgroups ranging

from a phosphate, a small organic moiety like phosphocholine, or a carbohydrate (142).

This huge variety of end products is the culmination of numerous synthetic enzymes

functioning in multiple cellular organelles.

A schematic of sphingolipid metabolism is shown in Figure 1.5 and can generally be

divided into two parts. The first is synthesis of ceramide (N-acyl sphingosine) in the ER.

The initial steps in sphingolipid synthesis are catalyzed by enzymes localized in the ER

membrane. The first reaction is catalyzed by serine palmitoyl transferase (SPT) and involves

condensation of serine with palmitoyl-CoA to form 3-ketosphinganine + CoA + CO_2 (143;

144). The palmitoyl group (C16:0) is the most common fatty acid-CoA in mammalian cells

and therefore is most often utilized in the synthesis of most mammalian sphingolipids.

When present, C15- and C17-linked CoA groups can also be used by SPT to make 2

additional sphingolipid species via the same condensation reaction (145). The 3-

ketosphinganine product is then reduced to form sphinganine and the majority of

sphinganine is acylated by 1 of 6 ceramide synthase (CerS) enzymes to form

dihydroceramide. Each member of the CerS family is specific for substrates with a particular

acyl chain length. In all cases, the N-linked sphinganine is called dihydroceramide despite

Figure 1.5) Sphingolipid synthesis and major metabolic pathways: The initial steps of sphingolipid synthesis occur in the ER (bottom) where serine and two fatty acyl-CoA molecules are conjugated to form ceramide, the diacyl sphingolipid that is central to all sphingolipid metabolic pathways. Ceramide is transported from the ER to the Golgi by the ceramide transport protein (CERT) where it is further conjugated to one of multiple headgroups. The 2 most common reactions involve the addition of either a phosphocholine to make sphingomyelin (SM) or a hexose to form a glycosphingolipid (GSL). The newly formed complex sphingolipids are transported to the outer leaflet of the plasma membrane by vesicular transport. Some plasma membrane turnover is constitutive but specific cellular signals, particularly those associated with cellular stress, can accelerate the process. SM and GSLs can also be internalized and broken down in lysosomal compartments. The sphingosine that results from breakdown can either be phosphorylated and irreversibly broken down or can reenter the synthetic pathway and be recycled. Enzymes are denoted by boxes.

Figure 1.5) Sphingolipid synthesis and major metabolic pathways

nCDase

aCDase

aSMase

Cer

S-1-P ← Sph ← Cer

EthAP
+
FattyAld

nSMase

SM/GSL

PM

SM/GSL

aSMase

Cer

aCDase

Sph

SM/GSL

SM

GSL

SM ← Cer

GSL

Golgi

Sph

S-1-P

CERT

"Salvage"

Serine

3-ketoSpha → 3-Spha → dhCer → Cer

Palm-CoA

EthAP + FattyAld

ER
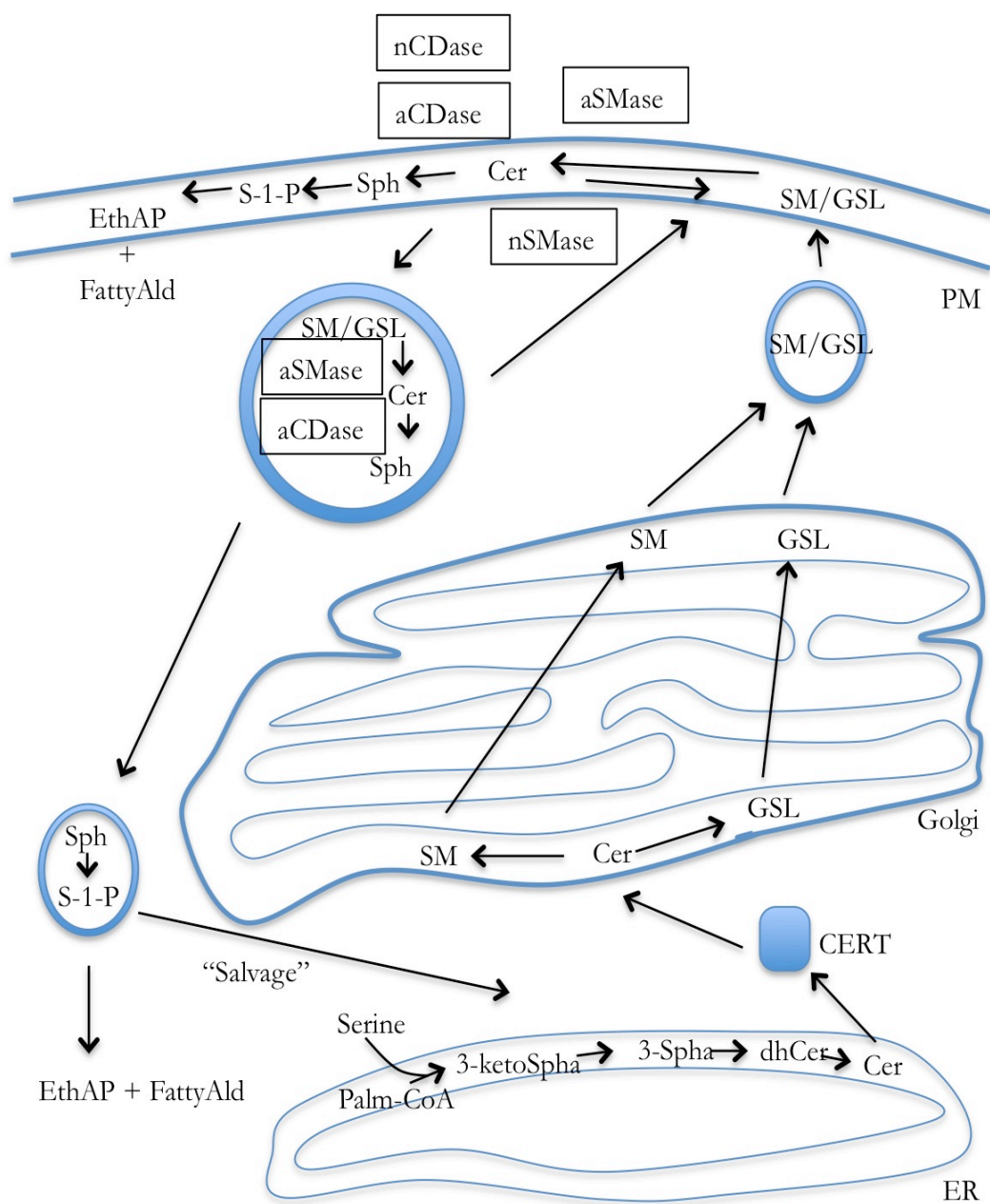
the variability in the N-linked acyl chain length (ranging from 14-26 carbons) (141). In the airway, the predominant ceramide species contains a C18 N-linked acyl group (C18 Cer) (146) suggesting that C18-CoA is the predominant substrate and that CerS1 in the most highly expressed. The resulting dihydroceramide is then desaturated to form ceramide, which contains the 4,5-trans double bond found in most mammalian sphingolipids (147; 148). Ceramide serves as a junction in sphingolipid metabolism and the C1 carbon can be modified with 1 of 5 different head groups. Synthesis of these more complex sphingolipids occurs in various parts of the cell depending on the pathway and the two predominant products are glycoceramide and sphingomyelin (142).

Most complex sphingolipids are synthesized in the Golgi. Ceramide is transported to the Golgi from the ER by either a vesicular trafficking mechanism or the ceramide transport protein CERT (149; 150). At this point the ceramide is utilized by one of two synthetic pathways to form either glycoceramides or sphingomyelin. Glycoceramides encompass a class of hundreds of different molecules and their biological importance and complexity is still being uncovered (151). In all cases, their synthesis begins with addition of a hexose to the C1 position of ceramide. The addition of glucose is catalyzed by Glucosylceramide (GlcCer)-synthase, whereas the addition of a galactose moiety is catalyzed by Galactosylceramide (GalCer)-synthase. GlcCer is the first step in the synthesis of gangliosides, for example GM3 and GM1. GM3 contains three carbohydrate groups (Glucose+Galactose+N-acetylneuraminic acid) while GM1, a product of GM3 modification, contains five carbohydrate groups. Gangliosides are present in the lung and have been shown to influence cell proliferation, migration, toxin binding, and potentially microbe binding (152-154). Subsequent addition and branching of more carbohydrate groups leads to a incredible variety of glycoceramides, with hundreds of different molecules being

observed *in vivo* (142). Glycolipids are then trafficked to the plasma membrane via vesicular transport and inserted into the outer leaflet of the membrane.

The second major sphingolipid that is produced in the Golgi is sphingomyelin. This reaction is catalyzed by the sphingomyelin synthase 1 (SMS1) enzyme, which catalyzes the transfer of phosphocholine from PC to ceramide, thus creating diacylglycerol and sphingomyelin (142; 155). SM synthesis in the Golgi is highly dependent on CERT-mediated transport of ceramide. After synthesis, the SM is trafficked to the plasma membrane via vesicular transport. Interestingly, a role of SM in the trafficking of membrane proteins has been suggested (155-157). One mechanism by which this is thought to occur is through the specific interaction of SM with transmembrane proteins. In 2014, Contreras and colleagues characterized a SM binding motif found in p24, a protein involved in the formation of COPI vesicles (158). They found that mutation of the motif decreased SM binding and accelerated tracking of a vesicular transport protein to the plasma membrane by decreasing the activity of the retrograde COPI trafficking. SM can also be synthesized in the plasma membrane by sphingomyelin synthase 2 (142; 155). This arm of metabolism is not dependent upon CERT-mediated trafficking of ceramide from the ER and is primarily thought to restore PM sphingomyelin following the formation of ceramide by PM associated or extracellular SMase-mediated breakdown of SM.

Early work by Garrett van Meer and colleagues suggested that sphingolipid trafficking in polarized MDCK epithelial cells was a tightly controlled process (159; 160). By monitoring the localization and metabolism of fluorescently labeled ceramide (NBD-Cer) they discovered that during a low temperature incubation, signal accumulated in the ER, but after shifting cells to 37° the signal migrated to the plasma membrane. The redistribution was nearly complete after 1 hour and corresponded with the appearance of NBD-

sphingomyelin and NBD-glucosylceramide in a ratio of 5:1. Interestingly, the glucosylceramide was asymmetrically redistributed, with 2-fold more being trafficked to the apical membrane than the basolateral membrane. Consistent with tight control of localization, the NBD-labeled sphingolipids were not freely mobile. Selective depletion in either membrane did not lead to a redistribution of lipid from the other. Thus, like proteins, sphingolipids are selectively trafficked in polarized epithelial cells (161). Upon arrival, both become fixed in their respective cellular compartments. Localization of both lipids and proteins in the plasma membrane is subject to modification by the actions of signaling pathways.

Sphingolipid turnover:

Plasma membrane associated SM and glycoceramides can be converted back to ceramide by a variety of enzymes called galactosidases and sphingomyelinases. Many of these catabolic enzymes were discovered because loss-of-function mutations commonly lead to disease (162-164). Glycosphingolipids and SM are broken down constitutively in endosomes and lysosomes by lysosome-associated enzymes with low pH optima, such as acid sphingomyelinase (aSMase). Specific signaling events can also facilitate SM catalysis at the plasma membrane by either of two sphingomyelinases. As will be discussed later, secretion of aSMase by epithelial cells occurs after membrane disruption or microbe binding (32; 165). Extracellular aSMase catalyzes the breakdown of SM present in the outer leaflet of the plasma membrane and can facilitate membrane budding. In addition, the sphingomyelin can be broken down by neutral sphingomyelinase (nSMase) present on the inner leaflet after membrane scrambling. This process has been implicated in the apoptotic signaling that follows CD95 ligation and phospholipid scrambling in Jurkat cells (166). The resulting

ceramide can then broken down to sphingosine and a free fatty acid by ceramidase (CDase) or it can be converted back to SM by SMS2 (enzyme not shown in Figure 1.5). Like SMase, numerous different CDase enzymes have been discovered with varying pH optima (167; 168). Both aCDase and nCDase are secreted by mammalian cells independent of, and in conjunction with, SMases (169). Intracellular sphingosine can then be converted back into ceramide (the salvage pathway), or can be phosphorylated to form sphingosine-1-phosphate (S-1-P). S-1-P is actively exported to the outer leaflet of the membrane where it can act on specific GPCRs, or, if it remains in the inner leaflet, it can be irreversibly broken down into fatty aldehyde and ethanolamine phosphate by S-1-P lyase (142; 170).

Exogenous Sphingomyelinases

Some pathogenic bacteria secrete an ortholog of nSMase during infection. Bacterial SMase has been linked to pathogenicity of numerous microbes including *P. aeruginosa*, *S. aureus*, and *B. cereus* (171; 172) (173). For example, KO of SMase decreases virulence and improves survivability in mice following intraperitoneal injection of *S. aureus* or *B. cereus* (171; 174). Some of this effect likely results from inhibition of macrophage function (171). The *S. aureus and B. cereus* orthologs share 56% sequence identity and are SM-specific whereas the *P. aeruginosa* variant shares only 20% homology with the *S. aureus* ortholog and cleaves both PC and SM (175). Multiple lines of evidence suggest that SMase is secreted by lung-resident pathogens. Specifically, the SMase transcript of *S. aureus* is upregulated following instillation of this bacterium into mouse trachea (176) and transcript of the *P. aeruginosa* ortholog is expressed in isolates from CF patient lungs (177). Additionally, antibodies against the *P. aeruginosa* variant have been measured in the serum of CF patients (178).

The functional consequence of bacterial SMase in the lungs of CF patients has not

been thoroughly studied; however, a few studies suggest that SMase could negatively impact lung function. Vasil and colleagues showed that the *P. aeruginosa* homolog of SMase (PlcHR) decreases pulmonary elasticity in mice following tracheal instillation. Consistent with this, inhibition or KO of the enzyme reduces the associated pulmonary pathology(173). This negative effect on lung function cannot be tied directly to cleavage of SM, however, because PlcHR can also hydrolyze PC. Further studies with SM-specific PlcHR will be required to determine whether SMase activity is directly involved in this pathology. Unlike the *P. aeruginosa* homolog, *S. aureus* SMase has been directly linked to lung pathology (179). Hayashida and colleagues showed that *S. aureus* SMase can induce lung injury by recruiting activated neutrophils. They found that knocking out SMase significantly reduced lung injury and fibrosis. This is potentially relevant to CF given that activated neutrophils are thought to be a major contributor to the progression of lung disease.

1.4.3) Evidence for a Functional Interaction Between CFTR and Sphingolipid Metabolism: *CFTR expression affects sphingolipid levels*:

A few studies have suggested a direct link between CFTR expression and sphingolipid metabolism. Hamai and colleagues published the first evidence of a functional interaction between CFTR expression and sphingolipid levels (180). They compared the rate of sphingolipid synthesis between cell lines expressing either no detectable CFTR (16HBEσ⁻) or F508del CFTR (IB3) with their respective matched lines expressing WT CFTR. Using radiolabeled serine, they found that knockdown of WT-CFTR or expression of F508del-CFTR led to a significant increase in ceramide synthesis during a 2-hour incubation. The change did not result from increases in sphingomyelin catalysis as they also saw a concomitant increase in SM levels as detected by incorporation of radiolabeled

phosphocholine. Interestingly not all ceramides were affected equally, with C16-cer and those containing very long N-linked acyl chains (C22-26) showing more dramatic increases. Conversely, they found that virally driven overexpression of WT-CFTR, but not the related transporter ABCA7 decreased ceramide synthesis. These data suggest a link between expression of functional CFTR protein and ceramide homeostasis.

Other sphingolipids are influenced by CFTR expression as well. Itokazu and colleagues showed that knockdown of CFTR in the Calu3 airway cell line using shRNA reduced levels of the ganglioside GM1 (181). GM1 levels could be rescued in a concentration-dependent manner by transfection of GFP-labeled CFTR. The resulting decrease in cellular GM1 levels impaired β1-integrin activation, phosphorylation of focal adhesion kinase, and phosphorylation of Crk-associated substrate. Functionally, the reduced levels of GM1 and integrin signaling prevented normal cell migration and "wound repair" following electrical disruption of the cell monolayer. Importantly, introducing exogenous GM1 could restore these dysfunctions in migration and signaling. These results could have clinical implications, given that epithelial damage is high in the CF lung. Any dysfunction in wound repair could exacerbate fibrosis and pulmonary decline.

Disruptions in sphingolipid metabolism also have been observed in animal models of CF. Teichgräber and colleagues reported that two CFTR KO mouse strains accumulate pulmonary ceramide in an age-dependent manner and they attributed the change to alterations in lysosomal sphingolipid metabolism (182). Specifically, using a pH-sensitive dye, they reported an increase in the pH of lysosomes (from 4.5 to ~ 6) in the CFTR KO mice. The effect was also observed following treatment with the CFTR inhibitor INH_{172}. (A potential role for CFTR in the acidification of vesicles has been around for decades and involves the movement of Cl^- ions to act as a counter ion to H^+ (183; 184)). Using

lysosomal preparations, they found that a pH change of that magnitude reduced the activity of both acid ceramidase and acid sphingomyelinase. However, while the aSMase retained some activity, aCDase activity was nearly undetectable. They reasoned that this imbalance contributes to the accumulation of ceramide observed in CF cells. Treating cells with the acid SMase (aSMase) inhibitor Amitriptyline normalized cellular ceramide levels, as did generating an aSMase heterozygote CFTR KO mouse. These data suggest that aSMase is contributing to the observed ceramide imbalance, though it does not exclude the contribution of other factors.

Importantly, in 2010 Brodlie and colleagues showed that ceramide levels are abnormal in lungs from CF patients (185). Using mass spectrometry and immunohistochemistry (IHC), they compared the ceramide content in explanted lungs from CF patients with samples from patients diagnosed with pulmonary hypertension or chronic obstructive pulmonary disease (COPD), and used healthy lung donors as controls. By both metrics, they observed significantly more ceramide in the lungs from CF patients, with 2 - 4-fold increases in C16, C18 and C20 ceramide. Interestingly, this study also reported significantly higher levels of ceramide in the lungs of COPD patients as compared to the pulmonary hypertension and healthy lung donor controls. Smoking is the leading cause of COPD and cigarette smoke has been shown to reduce CFTR activity and expression (186-192). While the authors did not present any data on the abundance of CFTR in the COPD lung, or the donors' smoking status, it is interesting to consider that perhaps the increased levels of ceramide measured in the COPD lungs may be linked to a diminished CFTR activity. Consistent with this idea, Petrache et al showed that lung samples from ex-smokers showed an abundance of C16 (~20%), C22 (~10%), and C24 (~60%) ceramides (193) – a pattern similar to that reported in CF cells by Brodlie and collegaues (185).

1.4.4) Functional consequences of abnormal SL metabolism in CF cells - infection:

Abnormal aSMase function in CF cells has also been linked to an abnormal innate immunity response in epithelial cells. One possible contributor to innate immunity in epithelia is internalization of invading pathogens followed by apoptosis (194-196). Early work by Goldberg and colleagues provided evidence that pathogen internalization was defective in CF human airway cells expressing F508del-CFTR as compared to the matching line in which WT-CFTR had been introduced (31; 197). The F508del phenotype could be rescued by low temperature incubation, which allows trafficking of F508del CFTR to the cell membrane, and led to an accumulation of *P. aeruginosa* in murine lungs for two days following inoculation. Yu and colleagues linked internalization to aSMase activity in 2008 by showing that KD of aSMase in an immortalized epithelial cell line using RNAi led to a similar reduction in *P. aeruginosa* internalization (32). Of note, Teichgräber and colleagues reported a different result (182). Specifically, they found that treating CFTR KO mice with Amitriptyline, or creating aSMase heterozygotes in the CFTR KO, facilitated *P. aeruginosa* clearance and improved survival following tracheal instillation. These seemingly contradictory results have yet to be clarified but might suggest that epithelial cell-mediated internalization is only a minor component of pathogen clearance in the murine lung.

What links aSMase activity to CFTR-dependent pathogen internalization? One potential explanation lies in the observation that CFTR is shuttled into DRMs following exposure of epithelial cells to *P. aeruginosa* (198-200). Activation and translocation of aSMase to the plasma membrane has been shown to underlie clustering and activation of multiple receptors including CD95 (201), FcγRII (202), and CD40 (203). Upon exposure of epithelial cells to *P. aeruginosa*, CFTR is rapidly moved into DRM fractions and the effect could be

abolished by treating cells with methyl-beta-cyclodextrin (mβCD), a cholesterol chelating

agent that been shown to prevent the formation of DRMs (199). Translocation of CFTR

correlated with microbe internalization and could also be diminished by mβCD.

Interestingly, mβCD treatment also diminished activation of NF-κB-mediated

proinflammatory signaling. This CFTR mediated internalization of microbes was also

shown to be dependent upon caveolin-1 (33). Microbe internalization generally leads to

desquamation and apoptosis (194-196). Consistent with reduced microbe internalization in

CF epithelial cells, CF cells are less prone to apoptosis following exposure to *P. aeruginosa*

(204). Taken together these observations lead to a possible model wherein infection and

microbe binding leads to mobilization of aSMase to the plasma membrane where its activity

facilitates CFTR clustering and microbe internalization. This model has yet to be

systematically tested.

There is some evidence that CFTR is dynamically trafficked into and out of

membrane microdomains in live cells as well. The first evidence of CFTR sequestration was

published by Verkman and colleagues who used fluorescence recovery after photobleaching

to measure the diffusion of GFP-tagged CFTR in MDCK cells (75). They found that

heterologously expressed GFP-CFTR diffused significantly faster after deletion of its C-

terminal PDZ binding domain, though this study relied on overexpression and thus likely

overestimated the mobility of WT CFTR. After construction of a stable cell line expressing

low levels of CFTR containing an extracellular epitope, they showed that under these

expression conditions, CFTR is nearly immobilized at the cell's surface and that this

immobilization could be prevented by either expressing a CFTR construct lacking the C-

terminal PDZ, or by coexpressing a CFTR C-terminal peptide (76). A similar observation

was made by Verkman and colleagues who found that the small fraction of mobile CFTR

observed in their system was occasionally "captured" in microdomains (205). Recent data from Hanrahan and colleagues implicated lipids, specifically cholesterol, in this confinement process as well (77). Using TIRF microscopy and image correlation spectroscopy, they were able to quantify net flux of tagged CFTR at the plasma membrane of epithelial cells. They found that CFTR clustering was significantly reduced following treatment with cholesterol oxidase, which effectively removes cholesterol from the membrane. Conversely, treatment with cholesterol esterase, which synthesizes cholesterol from the ester precursor, increased the prevalence of large CFTR-containing clusters with relatively slow diffusion rates. Importantly, this study was performed at 37°C to avoid temperature-dependent lipid aggregation. While they did not test the effect of *P. aeruginosa* on CFTR clustering in their system, they did show that viral infection (which has also been shown to activate aSMase and lead to ceramide accumulation) led to the formation of large CFTR-containing clusters. These data suggest that the location of CFTR in the plasma membrane is tightly controlled and can be affected by both PDZ-mediated protein interactions, the surrounding lipid environment, and the presence of pathogens. How the cytoskeletal components and lipid systems cross talk is yet to be clearly elucidated, but Canals and colleagues have shown that the formation of ceramide can alter the activity of PDZ proteins (ERMs in particular) by activating phosphatases that altering their phosphorylation state (206; 207).

A second factor that might contribute to the increased susceptibility of CF patients to lung infections is a reduction in sphingosine. Sphingosine has be shown to have antimicrobial properties (an active area of dermatological research) (208; 209) and some evidence suggests that pulmonary sphingosine levels are reduced in the lungs of CFTR KO mice and CF patients (210). This is consistent with the observation that aCDase activity is reduced with loss of CFTR function and, interestingly, Pewzner-Jung and colleagues found

that treating CFTR KO mice with exogenous sphingosine reduced their susceptibility to infection.

1.4.5) Functional consequences of abnormal SL metabolism in CF cells - inflammation:

The abnormal sphingolipid levels that are seen with the loss of CFTR function likely contribute to the hyperinflammatory state seen in the CF lung as well. Multiple groups have reported that CF cells secrete higher levels of proinflammatory cytokines following exposure to stress (32; 182). Yu and colleagues showed that the IB3-1 cell line, which is homozygous for F508del, secretes nearly 2-fold more IL-8 following exposure to *P. aeruginosa* than a matching cell line that had been complimented with WT CFTR (32). They implicated aSMase dysfunction by demonstrating that WT cells showed a similar phenotype when aSMase was inhibited with desipramine or knocked down with RNAi. Additionally, a normal phenotype could be elicited in the CF cell line by including low levels of *S. aureus* SMase during the infection period. Teichgräber and colleagues also showed a hyperinflammatory state in CFTR KO mice as measured by increased IL-1β secretion in the lungs as well as increased neutrophil and macrophage infiltration (182). Unlike Yu and colleagues, however, they found that treatment with amitriptyline or knocking out one aSMase allele in CFTR KO mice reduced the inflammatory markers.

While both groups demonstrated increased markers of inflammation they found seemingly contradictory evidence for the role of aSMase in their measured phenotypes. This discrepancy has not been explained to date; however, it is important to consider that they were testing different aspects of the inflammatory response in different systems. Teichgräber and colleagues implicated an imbalance in aSMase and aCDase activities in resting hyperinflammation (though the activities of both enzymes was reduced relative to

WT). Given that the mice were not challenged with bacteria, this likely corresponds with increased intracellular (lysosomal) ceramide concentrations. Conversely, Yu and colleagues found that reduced aSMase activity at the outer leaflet of the membrane exacerbated release of inflammatory cytokines following exposure to bacteria. This suggests that extracellular aSMase activity may be involved in termination of inflammatory signaling following exposure to proinflammatory stressors. Taken together, these studies consistently implicate sphingolipid imbalance to the hyperinflammatory phenotype that is seen in CF cells; however, they seem to suggest that both the location (outer leaflet vs. lysosome) and timing (resting vs. stimulated) of ceramide formation might be important in regulating the inflammatory state of epithelial cells.

1.4.6) Evidence for Direct interactions between CFTR and sphingolipids:

As discussed, there are multiple lines of evidence to suggest that CFTR interacts with sphingolipid metabolism to affect cellular processes. However, a complete mechanistic understanding of how CFTR expression and/or function overlaps with sphingolipid metabolism has not been well described. One intriguing possibility is that CFTR facilitates the transport of sphingolipids across the cell membrane. Boujaoude and colleagues reported evidence for CFTR-mediated S-1-P transport in 2001 (211). They found that expression of WT CFTR, but not F508del, CFTR led to a time-dependent, saturable accumulation of S-1-P in the murine C127 epithelial cell line. Interestingly, the uptake was not affecting by activating cellular PKA with FSK and IBMX suggesting that this transport may be independent of the chloride channel activity of CFTR.

A direct interaction between CFTR and sphingolipids has not been described, but some circumstantial evidence exists. First, CFTR is a membrane protein that is

evolutionarily related to numerous lipid flippases and floppases. Second, a decane molecule was present in the recently published structure of zebrafish CFTR (79). The decane was not discussed in the text nor was it described as a key part of purification in the Methods section. Interestingly, it resided in a hydrophobic cleft at the junction of helices making up TMs 9, 10, 11, and 12 that contains a motif reminiscent of a sphingomyelin-binding motif described by Contreras and colleagues (this observation and potential binding pocket will be explored more thoroughly in the Discussion). It remains to be seen whether other sphingolipids could recognize the motif because the authors did not test the specificity (158).

1.4.7) SMase activity inhibits CFTR channel function in some cell systems:

One of the most interesting interactions between sphingolipid metabolism and CFTR was published in 2007 when Lu and colleagues showed that CFTR channel activity could be acutely inhibited by bacterial sphingomyelinase (212). The authors found that CFTR currents recorded from *Xenopus* oocytes using Two Electrode Voltage Clamp (TEVC) were slowly and completely shut down upon exposure to WT bacterial sphingomyelinase but not an enzyme-dead mutant. Inhibition did not result from liberation of the phosphocholine headgroup of SM but did occur in multiple CF-associated CFTR variants. The most interesting aspect of their study was the observation that inhibition did not result from dephosphorylation of the R-domain because the phosphorylation-independent variant of CFTR, split-ΔR-CFTR, could be inhibited by SMase. This result suggested that inhibition was occurring through a novel mechanism. The full mechanism was not determined but these observations are consistent with two possibilities. The first is that CFTR channel function is lipid dependent with either SM being required for channel function or that CFTR is inhibited by one of the metabolic lipid products. The lipid dependence of CFTR gating

has never been systematically tested using purified protein in artificial bilayers so either could conceivably be possible. The second possibility is that the SMase-induced formation of ceramide inhibits CFTR channel function by stimulating a second-messenger signaling cascade that blocks channel function. This possibility is intriguing because no signaling event other than phosphorylation of the R-domain has been shown to acutely affect CFTR channel function.

A second study conducted in polarized airway epithelial cells seemed to overlap with the results published by Ramu and colleagues and suggested that SMase-mediated modulation of CFTR might be conserved and clinically relevant. Specifically, Ito and colleagues found that application of bacterial sphingomyelinase to the basolateral side of the immortal pulmonary epithelial Calu-3 cell line significantly reduced the FSK-stimulated transepithelial currents (213). Inhibition of transepithelial currents in Calu-3 cells could be recapitulated by pure ceramide. In 2014, Lu and colleagues published a follow-up study that also showed inhibition of CFTR currents in unpolarized Calu-3 cells (214).

The ability of SMase activity to inhibit CFTR currents in multiple cell systems piqued our interest and facilitated the experiments outlined in the first part of this dissertation. We hypothesized that these effects might represent a conserved interaction between sphingolipid metabolism and CFTR channel function. However, multiple basic questions remained. For example, how does SMase affect the CFTR protein to elicit its effect, i.e. does it affect channel gating, membrane expression, or channel conductance? Do the effects observed in each cell system result from the same process? To answer this question, a full elucidation of mechanism would be required, but, short of that, a comparison of defining characteristics could offer some clues. Finally, does inhibition occur in primary pulmonary epithelial cells? If so, the process could conceivably affect the outcomes of patients with CF or COPD. The

first Results section will describe our findings as we explored this interaction between SMase activity and CFTR channel function.

2) Summary

The CFTR anion channel is crucial to physiologic homeostasis as evidenced by the severe pathologies associated with the loss of function mutations in CFTR that lead to CF. The use of small molecules that directly impact CFTR function has improved outcomes in a subset of CF patients and prompts new questions regarding the interactions these drugs, the CFTR protein, and the milieu of the CF lung. For example, the presence of persistent bacterial infections and inflammatory cells could introduce proteins that interact with the lung epithelial cells and directly inhibit CFTR channel function. Modulation of sphingolipid metabolism is of particular interest because CFTR function and sphingolipid homeostasis are interconnected and sphingomyelinase has been shown to directly inhibit CFTR channel function in some model systems, as noted above. If this effect occurs in the bronchial epithelial cells of patients it could directly influence therapeutic efficacy.

Given our interest in the chloride channel function of CFTR and our knowledge of CFTR electrophysiology, we set out to better understand how SMase activity affects CFTR channel function and tried to determine how ubiquitous this novel regulatory mechanism might be by testing multiple cell model systems. The experiments discussed in the first Results section of this dissertation suggest that SMase inhibits CFTR by locking the channel into a closed state at the cell membrane and that sensitivity to SMase-mediated inhibition is affected by the channel's gating state. Further, inhibited channels are insensitive to subsequent treatment with VX-770 suggesting that, if this inhibitory mechanism occurs in patients, it could diminish the efficacy of the treatment. Finally, we show that basolateral

SMase can diminish transepithelial current in primary HBEs in a similar, activity-dependent way that is seen in the oocyte.

The small molecule VX-770 is unique in its ability to potently and effectively potentiate CFTR function. Elucidating how it works could guide future efforts in CF-drug discovery but relatively little is known about its mechanism at this point in time. Experiments reported in the second Results section describe our observation that the efficacy of VX-770-mediated potentiation of both WT and mutant CFTR channels is related to their basal channel activity. This observation is important to consider when designing a drug-screening assay for CFTR modulators because it directly limits the range of signal that is possible. Thus, by informing on the best activation condition to detect effective potentiation, it will enable the discovery of potentiators that will otherwise seem ineffective when tested on maximally activated CFTR channels.

The Discussion will review our findings and touch on possible explanations. Interestingly, our observation that the efficacy of both the indirect inhibitor, SMase, and the small molecule potentiator, VX-770, affect CFTR dynamics in an activity-dependent manner, suggest that one must fully consider the activation state of CFTR when searching for and trying to understand molecules and interactions that influence CFTR gating, either positively or negatively.

Works Cited:

1. Castellani C, Assael BM. 2016. Cystic fibrosis: a clinical view. *Cellular and Molecular Life Sciences* 74:129--40
2. Md DCC, Fracp PJM, PhD MS, PhD PKWS. 2016. Newborn screening for cystic fibrosis. *The Lancet Respiratory* 4:653--61
3. Frizzell RA, Hanrahan JW. 2012. Physiology of Epithelial Chloride and Fluid Secretion. *Cold Spring Harbor Perspectives in Medicine* 2:a009563--a
4. Frizzell RA, Rechkemmer G, Shoemaker RL. 1986. Altered regulation of airway epithelial cell chloride channels in cystic fibrosis. *Science* 233:558--60
5. Marino CR, Matovcik LM, Gorelick FS, Cohn JA. 1991. Localization of the cystic fibrosis transmembrane conductance regulator in pancreas. *The Journal of clinical investigation* 88:712--6
6. Kopelman H, Durie P, Gaskin K, Weizman Z, Forstner G. 1985. Pancreatic fluid secretion and protein hyperconcentration in cystic fibrosis. *The New England journal of medicine* 312:329--34
7. Davis PB. 2006. Cystic fibrosis since 1938. *American Journal of Respiratory and Critical Care Medicine* 173:475--82
8. Darling RC, Pa DA, Perera GA, Dh A. 1953. Electrolyte Abnormalities of the Sweat in Fibrocystic Disease of the Pancreas. *American Journal of Medical Science* 225:67--70
9. Mscs ETZMD, PhD LRHMD. 2016. Cystic Fibrosis. *Pediatric Clinics of NA* 63:617--36
10. Elborn JS. 2016. Cystic fibrosis. *Lancet*
11. Saint-Criq V, Gray MA. 2016. Role of CFTR in epithelial physiology. *Cellular and Molecular Life Sciences*:1--23
12. Tarran R, Loewen ME, Paradiso AM, Olsen JC, Gray MA, et al. 2002. Regulation of Murine Airway Surface Liquid Volume by CFTR and Ca 2+-activated Cl −Conductances. *The Journal of General Physiology* 120:407--18
13. Hoegger MJ, Fischer AJ, McMenimen JD, Ostedgaard LS, Tucker AJ, et al. 2014. Impaired mucus detachment disrupts mucociliary transport in a piglet model of cystic fibrosis. *Science* 345:818--22
14. Rutland J, Cole PJ. 1981. Nasal mucociliary clearance and ciliary beat frequency in cystic fibrosis compared with sinusitis and bronchiectasis. *Thorax* 36:654--8
15. Hoegger MJ, Awadalla M, Namati E, Itani OA, Fischer AJ, et al. 2014. Assessing mucociliary transport of single particles in vivo shows variable speed and preference for the ventral trachea in newborn pigs. *Proceedings of the National Academy of Sciences* 111:2355--60
16. Tirouvanziam R, de Bentzmann S, Hubeau C, Hinnrasky J, Jacquot J, et al. 2000. Inflammation and infection in naive human cystic fibrosis airway grafts. *American journal of respiratory cell and molecular biology* 23:121--7
17. Tirouvanziam R, Khazaal I, Pault B. 2002. Primary inflammation in human cystic fibrosis small airways. *American journal of physiology. Lung cellular and molecular physiology* 283:L445--51

18. Rosenfeld M, Gibson RL, McNamara S, Emerson J, Burns JL, et al. 2001. Early pulmonary infection, inflammation, and clinical outcomes in infants with cystic fibrosis. *Pediatr Pulmonol* 32:356-66

19. Gibson RL, Burns JL, Ramsey BW. 2003. Pathophysiology and management of pulmonary infections in cystic fibrosis. *American Journal of Respiratory and Critical Care Medicine* 168:918--51

20. Zemanick ET, Emerson J, Thompson V, McNamara S, Morgan W, et al. 2014. Clinical outcomes after initial pseudomonas acquisition in cystic fibrosis. *Pediatric Pulmonology*

21. Cribbs SK, Beck JM. 2017. Microbiome in the pathogenesis of cystic fibrosis and lung transplant-related disease. *Translational research : the journal of laboratory and clinical medicine* 179:84--96

22. Md YJH, Md JJL. 2016. The Microbiome in Cystic Fibrosis. *Clinics in chest medicine* 37:59--67

23. Knowles MR, Boucher RC. 2002. Mucus clearance as a primary innate defense mechanism for mammalian airways. *The Journal of clinical investigation* 109:571--7

24. Pezzulo AA, Tang XX, Hoegger MJ, Abou Alaiwa MH, Ramachandran S, et al. 2012. Reduced airway surface pH impairs bacterial killing in the porcine cystic fibrosis lung. *Nature* 487:109--13

25. Ning F, Wang C, Berry KZ, Kandasamy P, Liu H, et al. 2014. Structural characterization of the pulmonary innate immune protein SPLUNC1 and identification of lipid ligands. *The FASEB Journal* 28:5349--60

26. Del Porto P, Cifani N, Guarnieri S, Di Domenico EG, Mariggio MA, et al. 2011. Dysfunctional CFTR alters the bactericidal activity of human macrophages against Pseudomonas aeruginosa. *PLoS One* 6:e19970

27. Haggie PM, Verkman AS. 2007. Cystic fibrosis transmembrane conductance regulator-independent phagosomal acidification in macrophages. *J Biol Chem* 282:31422-8

28. Barriere H, Bagdany M, Bossard F, Okiyoneda T, Wojewodka G, et al. 2009. Revisiting the role of cystic fibrosis transmembrane conductance regulator and counterion permeability in the pH regulation of endocytic organelles. *Mol Biol Cell* 20:3125-41

29. Steinberg BE, Huynh KK, Brodovitch A, Jabs S, Stauber T, et al. 2010. A cation counterflux supports lysosomal acidification. *J Cell Biol* 189:1171-86

30. Tirouvanziam R, Gernez Y, Conrad CK, Moss RB, Schrijver I, et al. 2008. Profound functional and signaling changes in viable inflammatory neutrophils homing to cystic fibrosis airways. *Proc Natl Acad Sci U S A* 105:4335-9

31. Pier GB, Grout M, Zaidi TS, Goldberg JB. 1996. How mutant CFTR may contribute to Pseudomonas aeruginosa infection in cystic fibrosis. *American Journal of Respiratory and Critical Care Medicine* 154:S175--82

32. Yu H, Zeidan YH, Wu BX, Jenkins RW, Flotte TR, et al. 2009. Defective acid sphingomyelinase pathway with Pseudomonas aeruginosa infection in cystic fibrosis. *American journal of respiratory cell and molecular biology* 41:367--75

33. Bajmoczi M, Gadjeva M, Alper SL, Pier GB, Golan DE. 2009. Cystic fibrosis transmembrane conductance regulator and caveolin-1 regulate epithelial cell internalization of Pseudomonas aeruginosa. *AJP: Cell Physiology* 297:C263--77

34. Quinton PM. 1989. Defective epithelial ion transport in cystic fibrosis. *Clinical chemistry* 35:726--30

35. Yan W, Samaha FF, Ramkumar M, Kleyman TR, Rubenstein RC. 2004. Cystic fibrosis transmembrane conductance regulator differentially regulates human and mouse epithelial sodium channels in Xenopus oocytes. *The Journal of biological chemistry* 279:23183--92

36. Guilbault C, Saeed Z, Downey GP, Radzioch D. 2007. Cystic fibrosis mouse models. *American journal of respiratory cell and molecular biology* 36:1--7

37. Stoltz DA, Meyerholz DK, Pezzulo AA, Ramachandran S, Rogan MP, et al. 2010. Cystic fibrosis pigs develop lung disease and exhibit defective bacterial eradication at birth. *Science translational medicine* 2:29ra31

38. Keiser NW, Engelhardt JF. 2011. New animal models of cystic fibrosis. *Current Opinion in Pulmonary Medicine*:1

39. Wernick NLB, Chinnapen DJF, Cho JA, Lencer WI. 2010. Cholera Toxin: An Intracellular Journey into the Cytosol by Way of the Endoplasmic Reticulum. *Toxins* 2:310--25

40. Gabriel SE, Brigman KN, Koller BH, Boucher RC, Stutts MJ. 1994. Cystic fibrosis heterozygote resistance to cholera toxin in the cystic fibrosis mouse model. *Science* 266:107--9

41. Md JBH, Md RCL, PhD FQ, Md PETR, Md PSBC. 2012. Cholera. *The Lancet* 379:2466--76

42. Rommens JM, Iannuzzi MC, Kerem B, Drumm ML, Melmer G, et al. 1989. Identification of the cystic fibrosis gene: chromosome walking and jumping. *Science* 245:1059--65

43. Riordan J, Collins F, Tsui L-C. 1989. Identification of the Cystic Fibrosis Gene: Cloning and Characterization of Complimentary DNA. *Science* 245:1--9

44. Kerem B, Rommens JM, Buchanan JA, Markiewicz D, Cox TK, et al. 1989. Identification of the cystic fibrosis gene: genetic analysis. *Science* 245:1073--80

45. Devor DC, Singh AK, Lambert LC, DeLuca A, Frizzell RA, Bridges RJ. 1999. Bicarbonate and chloride secretion in Calu-3 human airway epithelial cells. *The Journal of General Physiology* 113:743--60

46. Choi JY, Joo NS, Krouse ME, Wu JV, Robbins RC, et al. 2007. Synergistic airway gland mucus secretion in response to vasoactive intestinal peptide and carbachol is lost in cystic fibrosis. *The Journal of clinical investigation* 117:3118--27

47. Moran O, Zegarra-Moran O. 2008. On the measurement of the functional properties of the CFTR. *Journal of Cystic Fibrosis* 7:483--94

48. Moran O. 2016. The gating of the CFTR channel. *Cellular and Molecular Life Sciences*:1--8

49.   Bear CE, Duguay F, Naismith AL, Kartner N, Hanrahan JW, Riordan JR. 1991.
        Cl- channel activity in Xenopus oocytes expressing the cystic fibrosis gene.
        The Journal of biological chemistry 266:19142--5

50.   Bear CE, Li CH, Kartner N, Bridges RJ, Jensen TJ, et al. 1992. Purification and
        functional reconstitution of the cystic fibrosis transmembrane conductance
        regulator (CFTR). *Cell* 68:809--18

51.   Csanady L, Chan KW, Seto-Young D, Kopsco DC, Nairn AC, Gadsby DC. 2000.
        Severed channels probe regulation of gating of cystic fibrosis transmembrane
        conductance regulator by its cytoplasmic domains. *The Journal of General
        Physiology* 116:477--500

52.   Winter MC, Welsh MJ. 1997. Stimulation of CFTR activity by its
        phosphorylated R domain. *Nature* 389:294--6

53.   Bozoky Z, Krzeminski M, Chong PA, Forman-Kay JD. 2013. Structural changes
        of CFTR R region upon phosphorylation: a plastic platform for intramolecular
        and intermolecular interactions. *The FEBS journal* 280:4407--16

54.   Mense M, Vergani P, White DM, Altberg G, Nairn AC, Gadsby DC. 2006. In vivo
        phosphorylation of CFTR promotes formation of a nucleotide-binding
        domain heterodimer. *The EMBO Journal* 25:4728--39

55.   Vergani P, Lockless SW, Nairn AC, Gadsby DC. 2005. CFTR channel opening by
        ATP-driven tight dimerization of its nucleotide-binding domains. *Nature*
        433:876--80

56.   Vergani P, Basso C, Mense M, Nairn AC, Gadsby DC. 2005. Control of the CFTR
        channel's gates. *Biochemical Society Transactions* 33:1003

57.   Dousmanis AG, Nairn AC, Gadsby DC. 2002. Distinct Mg(2+)-dependent steps
        rate limit opening and closing of a single CFTR Cl(-) channel. *The Journal of
        General Physiology* 119:545--59

58.   Hwang T-C, Sheppard DN. 2009. Gating of the CFTR Cl- channel by ATP-
        driven nucleotide-binding domain dimerisation. *The Journal of Physiology*
        587:2151--61

59.   Moody JE, Millen L, Binns D, Hunt JF, Thomas PJ. 2002. Cooperative, ATP-
        dependent association of the nucleotide binding cassettes during the
        catalytic cycle of ATP-binding cassette transporters. *The Journal of biological
        chemistry* 277:21111--4

60.   Chen J, Lu G, Lin J, Davidson AL, Quiocho FA. 2003. A tweezers-like motion of
        the ATP-binding cassette dimer in an ABC transport cycle. *Molecular cell*
        12:651--61

61.   Oldham ML, Khare D, Quiocho FA, Davidson AL, Chen J. 2007. Crystal
        structure of a catalytic intermediate of the maltose transporter. *Nature*
        450:515--21

62.   Lewis HA, Buchanan SG, Burley SK, Conners K, Dickey M, et al. 2004.
        Structure of nucleotide-binding domain 1 of the cystic fibrosis
        transmembrane conductance regulator. *The EMBO Journal* 23:282--93

63.   Gregory RJ, Rich DP, Cheng SH, Souza DW, Paul S, et al. 1991. Maturation and
        function of cystic fibrosis transmembrane conductance regulator variants
        bearing mutations in putative nucleotide-binding domains 1 and 2. *Molecular
        and cellular biology* 11:3886--93

64. Carson MR, Travis SM, Welsh MJ. 1995. The two nucleotide-binding domains of cystic fibrosis transmembrane conductance regulator (CFTR) have distinct functions in controlling channel activity. *The Journal of biological chemistry* 270:1711--7

65. Aleksandrov L. 2002. The First Nucleotide Binding Domain of Cystic Fibrosis Transmembrane Conductance Regulator Is a Site of Stable Nucleotide Interaction, whereas the Second Is a Site of Rapid Turnover. *Journal of Biological Chemistry* 277:15419--25

66. Tsai MF, Li M, Hwang TC. 2010. Stable ATP binding mediated by a partial NBD dimer of the CFTR chloride channel. *The Journal of General Physiology* 135:399--414

67. Hwang TC, Nagel G, Nairn AC, Gadsby DC. 1994. Regulation of the gating of cystic fibrosis transmembrane conductance regulator C1 channels by phosphorylation and ATP hydrolysis. *Proceedings of the National Academy of Sciences of the United States of America* 91:4698--702

68. Szollosi A, Muallem DR, Csandy L, Vergani P. 2011. Mutant cycles at CFTR's non-canonical ATP-binding site support little interface separation during gating. *The Journal of General Physiology* 137:549--62

69. Chaves LAP, Gadsby DC. 2015. Cysteine accessibility probes timing and extent of NBD separation along the dimer interface in gating CFTR channels. *The Journal of General Physiology* 145:261--83

70. Hall RA, Ostedgaard LS, Premont RT, Blitzer JT, Rahman N, et al. 1998. A C-terminal motif found in the beta2-adrenergic receptor, P2Y1 receptor and cystic fibrosis transmembrane conductance regulator determines binding to the Na+/H+ exchanger regulatory factor family of PDZ proteins. *Proceedings of the National Academy of Sciences of the United States of America* 95:8496--501

71. Sun F, Hug MJ, Bradbury NA, Frizzell RA. 2000. Protein kinase A associates with cystic fibrosis transmembrane conductance regulator via an interaction with ezrin. *The Journal of biological chemistry* 275:14360--6

72. Naren AP, Cobb B, Li C, Roy K, Nelson D, et al. 2003. A macromolecular complex of beta 2 adrenergic receptor, CFTR, and ezrin/radixin/moesin-binding phosphoprotein 50 is regulated by PKA. *Proceedings of the National Academy of Sciences of the United States of America* 100:342--6

73. Milewski MI, Mickle JE, Forrest JK, Stafford DM, Moyer BD, et al. 2001. A PDZ-binding motif is essential but not sufficient to localize the C terminus of CFTR to the apical membrane. *Journal of Cell Science* 114:719--26

74. Valentine CD, Lukacs GL, Verkman AS, Haggie PM. 2012. Reduced PDZ Interactions of Rescued Delta F508CFTR Increases its Cell Surface Mobility. *Journal of Biological Chemistry*

75. Haggie PM, Stanton BA, Verkman AS. 2004. Increased diffusional mobility of CFTR at the plasma membrane after deletion of its C-terminal PDZ binding motif. *The Journal of biological chemistry* 279:5494--500

76. Haggie PM, Kim JK, Lukacs GL, Verkman AS. 2006. Tracking of quantum dot-labeled CFTR shows near immobilization by C-terminal PDZ interactions. *Molecular biology of the cell* 17:4937--45

77. Abu-Arish A, Pandzic E, Goepp J, Matthes E, Hanrahan JW, Wiseman PW. 2015. Cholesterol Modulates CFTR Confinement in the Plasma Membrane of Primary Epithelial Cells. *Biophysj* 109:85--94

78. Mornon JP, Lehn P, Callebaut I. 2008. Atomic model of human cystic fibrosis transmembrane conductance regulator: Membrane-spanning domains and coupling interfaces. *Cellular and Molecular Life Sciences* 65:2594--612

79. Zhang Z, Chen J. 2016. Atomic Structure of the Cystic Fibrosis Transmembrane Conductance Regulator.1--22

80. He L, Aleksandrov AA, Serohijos AWR, Hegedus T, Aleksandrov LA, et al. 2008. Multiple Membrane-Cytoplasmic Domain Contacts in the Cystic Fibrosis Transmembrane Conductance Regulator (CFTR) Mediate Regulation of Channel Gating. *Journal of Biological Chemistry* 283:26383--90

81. Serohijos AWR, Hegeds T, Aleksandrov AA, He L, Cui L, et al. 2008. Phenylalanine-508 mediates a cytoplasmic-membrane domain contact in the CFTR 3D structure crucial to assembly and channel function. *Proceedings of the National Academy of Sciences* 105:3256--61

82. Cui L. 2006. The role of cystic fibrosis transmembrane conductance regulator phenylalanine 508 side chain in ion channel gating. *The Journal of Physiology* 572:347--58

83. McCarty NA, Zhang ZR. 2001. Identification of a region of strong discrimination in the pore of CFTR. *American journal of physiology. Lung cellular and molecular physiology* 281:L852--67

84. Hille B. 2001. *Ion Channels of Excitable Membranes*. Sunderland, MA: Sinauer Associates, Inc.

85. Cotten JF, Welsh MJ. 1999. Cystic fibrosis-associated mutations at arginine 347 alter the pore architecture of CFTR. Evidence for disruption of a salt bridge. *The Journal of biological chemistry* 274:5429--35

86. Smith SS, Liu X, Zhang ZR, Sun F, Kriewall TE, et al. 2001. CFTR: covalent and noncovalent modification suggests a role for fixed charges in anion conduction. *The Journal of General Physiology* 118:407--31

87. Liu X, Zhang Z-R, Fuller MD, Billingsley J, McCarty NA, Dawson DC. 2004. CFTR: a cysteine at position 338 in TM6 senses a positive electrostatic potential in the pore. *Biophysical Journal* 87:3826--41

88. Cui G, Zhang Z-R, O'Brien ARW, Song B, McCarty NA. 2008. Mutations at Arginine 352 Alter the Pore Architecture of CFTR. *The Journal of Membrane Biology* 222:91--106

89. Linsdell P, Hanrahan JW. 1996. Disulphonic stilbene block of cystic fibrosis transmembrane conductance regulator Cl- channels expressed in a mammalian cell line and its regulation by a critical pore residue. *The Journal of Physiology* 496 (Pt 3):687--93

90. Infield DT, Cui G, Kuang C, McCarty NA. 2016. Positioning of extracellular loop 1 affects pore gating of the cystic fibrosis transmembrane conductance regulator. *AJP: Lung Cellular and Molecular Physiology* 310:L403--14

91. Cui G, Freeman CS, Knotts T, Prince CZ, Kuang C, McCarty NA. 2013. Two Salt Bridges Differentially Contribute to the Maintenance of Cystic Fibrosis

Transmembrane Conductance Regulator (CFTR) Channel Function. *The Journal of biological chemistry* 288:20758--67

92. Wangemann P, Wittner M, Di Stefano A, Englert HC, Lang HJ, et al. 1986. Cl(-)-channel blockers in the thick ascending limb of the loop of Henle. Structure activity relationship. *Pflugers Arch* 407 Suppl 2:S128-41

93. Sheppard DN, Robinson KA. 1997. Mechanism of glibenclamide inhibition of cystic fibrosis transmembrane conductance regulator Cl- channels expressed in a murine cell line. *The Journal of Physiology* 503 (Pt 2):333--46

94. Muanprasat C, Sirianant L, Soodvilai S, Chokchaisiri R, Suksamrarn A, Chatsudthipong V. 2012. Novel Action of the Chalcone Isoliquiritigenin as a Cystic Fibrosis Transmembrane Conductance Regulator (CFTR) Inhibitor: Potential Therapy for Cholera and Polycystic Kidney Disease. *Journal of Pharmacological Sciences* 118:82--91

95. Hwang TC, Sheppard DN. 1999. Molecular pharmacology of the CFTR Cl-channel. *Trends in Pharmacological Sciences* 20:448--53

96. McCarty NA, McDonough S, Cohen BN, Riordan JR, Davidson N, Lester HA. 1993. Voltage-dependent block of the cystic fibrosis transmembrane conductance regulator Cl- channel by two closely related arylaminobenzoates. *The Journal of General Physiology* 102:1--23

97. McDonough S, Davidson N, Lester HA, McCarty NA. 1994. Novel pore-lining residues in CFTR that govern permeation and open-channel block. *Neuron* 13:623--34

98. Walsh KB, Long KJ, Shen X. 1999. Structural and ionic determinants of 5-nitro-2-(3-phenylprophyl-amino)-benzoic acid block of the CFTR chloride channel. *British Journal of Pharmacology* 127:369--76

99. Ma T. 2002. Thiazolidinone CFTR inhibitor identified by high-throughput screening blocks cholera toxin-induced intestinal fluid secretion. *Journal of Clinical Investigation* 110:1651--8

100. Kopeikin Z, Sohma Y, Li M, Hwang TC. 2010. On the mechanism of CFTR inhibition by a thiazolidinone derivative. *The Journal of General Physiology* 136:659--71

101. Veit G, Avramescu RG, Chiang AN, Houck SA, Cai Z, et al. 2016. From CFTR biology toward combinatorial pharmacotherapy: expanded classification of cystic fibrosis mutations. *Molecular biology of the cell* 27:424--33

102. Hamosh A, Rosenstein BJ, Cutting GR. 1992. CFTR nonsense mutations G542X and W1282X associated with severe reduction of CFTR mRNA in nasal epithelial cells. *Human molecular genetics* 1:542--4

103. Will K, Drk T, Stuhrmann M, von der Hardt H, Ellemunter H, et al. 1995. Transcript analysis of CFTR nonsense mutations in lymphocytes and nasal epithelial cells from cystic fibrosis patients. *Human mutation* 5:210--20

104. Kerem E, Hirawat S, Armoni S, Yaakov Y, Shoseyov D, et al. 2008. Effectiveness of PTC124 treatment of cystic fibrosis caused by nonsense mutations: a prospective phase II trial. *The Lancet* 372:719--27

105. Cheng SH, Gregory RJ, Marshall J, Paul S, Souza DW, et al. 1990. Defective intracellular transport and processing of CFTR is the molecular basis of most cystic fibrosis. *Cell* 63:827--34

106. Van Goor F, Hadida S, Grootenhuis PDJ, Burton B, Stack JH, et al. 2011. Correction of the F508del-CFTR protein processing defect in vitro by the investigational drug VX-809. *Proceedings of the National Academy of Sciences* 108:18843--8

107. Zegarra-Moran O, Galietta LJV. 2016. CFTR pharmacology. *Cellular and Molecular Life Sciences*:1--12

108. Wainwright CE, Elborn JS, Ramsey BW, Marigowda G, Huang X, et al. 2015. Lumacaftor-Ivacaftor in Patients with Cystic Fibrosis Homozygous for Phe508del CFTR. *The New England journal of medicine* 373:220--31

109. Logan J, Hiestand D, Daram P, Huang Z, Muccio DD, et al. 1994. Cystic fibrosis transmembrane conductance regulator mutations that disrupt nucleotide binding. *The Journal of clinical investigation* 94:228--36

110. Accurso FJ, Rowe SM, Clancy JP, Boyle MP, Dunitz JM, et al. 2010. Effect of VX-770 in persons with cystic fibrosis and the G551D-CFTR mutation. *The New England journal of medicine* 363:1991--2003

111. Ramsey BW, Davies J, McElvaney NG, Tullis E, Bell SC, et al. 2011. A CFTR potentiator in patients with cystic fibrosis and the G551D mutation. *The New England journal of medicine* 365:1663--72

112. Eckford PDW, Li C, Ramjeesingh M, Bear CE. 2012. Cystic fibrosis transmembrane conductance regulator (CFTR) potentiator VX-770 (ivacaftor) opens the defective channel gate of mutant CFTR in a phosphorylation-dependent but ATP-independent manner. *Journal of Biological Chemistry* 287:36639--49

113. Van Goor F, Yu H, Burton B, Hoffman BJ. 2014. Effect of ivacaftor on CFTR forms with missense mutations associated with defects in protein processing or function. *Journal of Cystic Fibrosis* 13:29--36

114. Sheppard DN, Rich DP, Ostedgaard LS, Gregory RJ, Smith AE, Welsh MJ. 1993. Mutations in CFTR associated with mild-disease-form Cl- channels with altered pore properties. *Nature* 362:160--4

115. Brodlie M, Haq IJ, Roberts K, Elborn JS. 2015. Targeted therapies to improve CFTR function in cystic fibrosis. *Genome Medicine*:1--16

116. Fajac I, De Boeck K. 2016. New horizons for cystic fibrosis treatment. *Pharmacology \& Therapeutics*:1--7

117. Arora K, Moon C, Zhang W, Yarlagadda S, Penmatsa H, et al. 2014. Stabilizing rescued surface-localized deltaf508 CFTR by potentiation of its interaction with Na(+)/H(+) exchanger regulatory factor 1. *Biochemistry* 53:4169-79

118. Loureiro CA, Matos AM, Dias-Alves n, Pereira JF, Uliyakina I, et al. 2015. A molecular switch in the scaffold NHERF1 enables misfolded CFTR to evade the peripheral quality control checkpoint. *Science Signaling* 8:ra48

119. Lobo MJ, Amaral MD, Zaccolo M, Farinha CM. 2016. EPAC1 activation by cAMP stabilizes CFTR at the membrane by promoting its interaction with NHERF1. *J Cell Sci* 129:2599-612

120. Sondhi D, Stiles K, De BP, Crystal RG. 2016. Genetic Modification of the Lung Directed Toward Treatment of Human Disease. *Human gene therapy*

121.   Griesenbach U, Davies JC, Alton E. 2016. Cystic fibrosis gene therapy: a mutation-independent treatment. *Current Opinion in Pulmonary Medicine* 22:602--9
122.   Drumm ML, Pope HA, Cliff WH, Rommens JM, Marvin SA, et al. 1990. Correction of the cystic fibrosis defect in vitro by retrovirus-mediated gene transfer. *Cell* 62:1227-33
123.   Rosenfeld MA, Yoshimura K, Trapnell BC, Yoneyama K, Rosenthal ER, et al. 1992. In vivo transfer of the human cystic fibrosis transmembrane conductance regulator gene to the airway epithelium. *Cell* 68:143-55
124.   Hyde SC, Gill DR, Higgins CF, Trezise AE, MacVinish LJ, et al. 1993. Correction of the ion transport defect in cystic fibrosis transgenic mice by gene therapy. *Nature* 362:250-5
125.   Zabner J, Couture LA, Gregory RJ, Graham SM, Smith AE, Welsh MJ. 1993. Adenovirus-mediated gene transfer transiently corrects the chloride transport defect in nasal epithelia of patients with cystic fibrosis. *Cell* 75:207-16
126.   Taylor CW, Merritt JE, Putney JW, Jr., Rubin RP. 1986. A guanine nucleotide-dependent regulatory protein couples substance P receptors to phospholipase C in rat parotid gland. *Biochem Biophys Res Commun* 136:362-8
127.   Tchikov V, Bertsch U, Fritsch J, Edelmann B, Schtze S. 2011. Subcellular compartmentalization of TNF receptor-1 and CD95 signaling pathways. *European journal of cell biology* 90:467--75
128.   Fahy E, Subramaniam S, Brown HA, Glass CK, Merrill AH, et al. 2005. A comprehensive classification system for lipids. *Journal of lipid research* 46:839--61
129.   Daleke DL. 2008. Regulation of phospholipid asymmetry in the erythrocyte membrane. *Current opinion in hematology* 15:191--5
130.   Aye ILMH, Singh AT, Keelan JA. 2009. Transport of lipids by ABC proteins: Interactions and implications for cellular toxicity, viability and function. *Chemico-Biological Interactions* 180:327--39
131.   Neumann J, Rose-Sperling D, Hellmich UA. 2017. Diverse relations between ABC transporters and lipids: An overview. *Biochimica et biophysica acta* 1859:605--18
132.   Bevers EM, Williamson PL. 2016. Getting to the Outer Leaflet: Physiology of Phosphatidylserine Exposure at the Plasma Membrane. *Physiol Rev* 96:605-45
133.   Nagata S, Suzuki J, Segawa K, Fujii T. 2016. Exposure of phosphatidylserine on the cell surface. 23:952--61
134.   Carquin M, D'Auria L, Pollet H, Bongarzone ER, Tyteca D. 2016. Recent progress on lipid lateral heterogeneity in plasma membranes: From rafts to submicrometric domains. *Progress in lipid research* 62:1--24
135.   Dietrich C, Bagatolli LA, Volovyk ZN, Thompson NL, Levi M, et al. 2001. Lipid rafts reconstituted in model membranes. *Biophysical Journal* 80:1417--28
136.   Simons K, Vaz WLC. 2004. Model systems, lipid rafts, and cell membranes. *Annual review of biophysics and biomolecular structure* 33:269--95

137. Stone MB, Shelby SA, Nez MF, Wisser K, Veatch SL. 2017. Protein sorting by lipid phase-like domains supports emergent signaling function in B lymphocyte plasma membranes. *eLife* 6

138. Stone MB, Shelby SA, Veatch SL. 2017. Super-Resolution Microscopy: Shedding Light on the Cellular Plasma Membrane. *Chemical reviews*

139. Merrill AH, Sandhoff K. 2002. *Sphingolipids: Metabolism and Cell signaling*. Elsevier

140. Pruett ST, Bushnev A, Hagedorn K, Adiga M, Haynes CA, et al. 2008. Biodiversity of sphingoid bases (sphingosines) and related amino alcohols. *Journal of lipid research* 49:1621--39

141. Hannun YA, Obeid LM. 2011. Many ceramides. *Journal of Biological Chemistry* 286:27855--62

142. Merrill AH. 2011. Sphingolipid and glycosphingolipid metabolic pathways in the era of sphingolipidomics. *Chemical reviews* 111:6387--422

143. Braun PE, Snell EE. 1967. The biosynthesis of dihydrosphingosine in cell-free preparations of Hansenula ciferri. *Proc Natl Acad Sci U S A* 58:298-303

144. Stoffel W, LeKim D, Sticht G. 1968. Metabolism of sphingosine bases. 8. Distribution, isolation and properties of D-3-oxosphinganine reductase. Stereospecificity of the NADPH-dependent reaction of 3-oxodihydrospingosine (2-amino-1-hydroxyoctadecane-3-one). *Hoppe Seylers Z Physiol Chem* 349:1637-44

145. Haynes CA, Allegood JC, Sims K, Wang EW, Sullards MC, Merrill AH, Jr. 2008. Quantitation of fatty acyl-coenzyme As in mammalian cells by liquid chromatography-electrospray ionization tandem mass spectrometry. *J Lipid Res* 49:1113-25

146. Zehethofer N, Bermbach S, Hagner S, Garn H, Mller J, et al. 2014. Lipid Analysis of Airway Epithelial Cells for Studying Respiratory Diseases. *Chromatographia* 78:403--13

147. Merrill AH, Jr., Wang E, Mullins RE. 1988. Kinetics of long-chain (sphingoid) base biosynthesis in intact LM cells: effects of varying the extracellular concentrations of serine and fatty acid precursors of this pathway. *Biochemistry* 27:340-5

148. Michel C, van Echten-Deckert G, Rother J, Sandhoff K, Wang E, Merrill AH, Jr. 1997. Characterization of ceramide synthesis. A dihydroceramide desaturase introduces the 4,5-trans-double bond of sphingosine at the level of dihydroceramide. *J Biol Chem* 272:22432-7

149. Hanada K, Kumagai K, Tomishige N, Kawano M. 2007. CERT and intracellular trafficking of ceramide. *Biochim Biophys Acta* 1771:644-53

150. Hanada K, Kumagai K, Yasuda S, Miura Y, Kawano M, et al. 2003. Molecular machinery for non-vesicular trafficking of ceramide. *Nature* 426:803-9

151. Lingwood CA. 2011. Glycosphingolipid Functions. *Cold Spring Harbor Perspectives in Biology* 3:a004788--a

152. Mansson JE, Fredman P, Bigner DD, Molin K, Rosengren B, et al. 1986. Characterization of new gangliosides of the lactotetraose series in murine xenografts of a human glioma cell line. *FEBS Lett* 201:109-13

153. Krivan HC, Ginsburg V, Roberts DD. 1988. Pseudomonas aeruginosa and Pseudomonas cepacia isolated from cystic fibrosis patients bind specifically to gangliotetraosylceramide (asialo GM1) and gangliotriaosylceramide (asialo GM2). *Arch Biochem Biophys* 260:493-6

154. Aureli M, Schiumarini D, Loberto N, Bassi R, Tamanini A, et al. 2016. Unravelling the role of sphingolipids in cystic fibrosis lung disease. *Elsevier Ireland Ltd* 200:94--103

155. Slotte JP. 2013. Biological functions of sphingomyelins. *Progress in lipid research* 52:424--37

156. Sharpe HJ, Stevens TJ, Munro S. 2010. A comprehensive comparison of transmembrane domains reveals organelle-specific properties. *Cell* 142:158-69

157. Surma MA, Klose C, Simons K. 2012. Lipid-dependent protein sorting at the trans-Golgi network. *Biochim Biophys Acta* 1821:1059-67

158. Contreras FX, Ernst AM, Haberkant P, Bjrkholm P, Lindahl E, et al. 2012. Molecular recognition of a single sphingolipid species by a protein's transmembrane domain. *Nature* 481:525--9

159. van Meer G, Stelzer EH, Wijnaendts-van-Resandt RW, Simons K. 1987. Sorting of sphingolipids in epithelial (Madin-Darby canine kidney) cells. *The Journal of Cell Biology* 105:1623--35

160. van Genderen I, van Meer G. 1995. Differential targeting of glucosylceramide and galactosylceramide analogues after synthesis but not during transcytosis in Madin-Darby canine kidney cells. *The Journal of Cell Biology* 131:645--54

161. Cao X, Surma MA, Simons K. 2012. Polarized sorting and trafficking in epithelial cells. *Cell Res* 22:793-805

162. Kolter T. 2011. A view on sphingolipids and disease. *Chem Phys Lipids* 164:590-606

163. Kolter T, Sandhoff K. 2010. Lysosomal degradation of membrane lipids. *FEBS Lett* 584:1700-12

164. Xu YH, Barnes S, Sun Y, Grabowski GA. 2010. Multi-system disorders of glycosphingolipid and ganglioside metabolism. *J Lipid Res* 51:1643-75

165. Tam C, Idone V, Devlin C, Fernandes MC, Flannery A, et al. 2010. Exocytosis of acid sphingomyelinase by wounded cells promotes endocytosis and plasma membrane repair. *The Journal of Cell Biology* 189:1027--38

166. Tepper AD, Ruurs P, Wiedmer T, Sims PJ, Borst J, van Blitterswijk WJ. 2000. Sphingomyelin hydrolysis to ceramide during the execution phase of apoptosis results from phospholipid scrambling and alters cell-surface morphology. *The Journal of Cell Biology* 150:155--64

167. Saied EM, Arenz C. 2015. Inhibitors of Ceramidases. *Elsevier Ireland Ltd*:1--23

168. Nikolova-Karakashian M, Merrill AH. 2000. Ceramidases. *Methods in enzymology* 311:194--201

169. Canals D, Perry DM, Jenkins RW, Hannun YA. 2011. Drug targeting of sphingolipid metabolism: sphingomyelinases and ceramidases. *British Journal of Pharmacology* 163:694--712

170. Kitatani K, Idkowiak-Baldys J, Hannun YA. 2008. The sphingolipid salvage pathway in ceramide metabolism and signaling. *Cellular Signalling* 20:1010--8

171. Oda M, Hashimoto M, Takahashi M, Ohmae Y, Seike S, et al. 2012. Role of sphingomyelinase in infectious diseases caused by Bacillus cereus. *PLoS ONE* 7:e38054

172. Martinez-Pulgarin S, Dominguez-Bernal G, Orden JA, de la Fuente R. 2009. Simultaneous lack of catalase and beta-toxin in Staphylococcus aureus leads to increased intracellular survival in macrophages and epithelial cells and to attenuated virulence in murine and ovine models. *Microbiology* 155:1505--15

173. Wargo MJ, Gross MJ, Rajamani S, Allard JL, Lundblad LKA, et al. 2011. Hemolytic phospholipase C inhibition protects lung function during Pseudomonas aeruginosa infection. *American Journal of Respiratory and Critical Care Medicine* 184:345--54

174. Herrera A, Vu BG, Stach CS, Merriman JA, Horswill AR, et al. 2016. Staphylococcus aureusβ-Toxin Mutants Are Defective in Biofilm Ligase and Sphingomyelinase Activity, and Causation of Infective Endocarditis and Sepsis. *Biochemistry* 55:2510--7

175. Stonehouse MJ, Cota-Gomez A, Parker SK, Martin WE, Hankin JA, et al. 2002. A novel class of microbial phosphocholine-specific phospholipases C. *Molecular microbiology* 46:661--76

176. Chaffin DO, Taylor D, Skerrett SJ, Rubens CE. 2012. Changes in the Staphylococcus aureus transcriptome during early adaptation to the lung. *PLoS ONE* 7:e41329

177. Son MS, Matthews WJ, Kang Y, Nguyen DT, Hoang TT. 2007. In vivo evidence of Pseudomonas aeruginosa nutrient acquisition and pathogenesis in the lungs of cystic fibrosis patients. *Infection and immunity* 75:5313--24

178. Hollsing AE, Granstrm M, Vasil ML, Wretlind B, Strandvik B. 1987. Prospective study of serum antibodies to Pseudomonas aeruginosa exoproteins in cystic fibrosis. *Journal of clinical microbiology* 25:1868--74

179. Hayashida A, Bartlett AH, Foster TJ, Park PW. 2010. Staphylococcus aureus Beta-Toxin Induces Lung Injury through Syndecan-1. *The American journal of pathology* 174:509--18

180. Hamai H, Keyserman F, Quittell LM, Worgall TS. 2009. Defective CFTR increases synthesis and mass of sphingolipids that modulate membrane composition and lipid signaling. *Journal of lipid research* 50:1101--8

181. Itokazu Y, Pagano RE, Schroeder AS, O'Grady SM, Limper AH, Marks DL. 2014. Reduced GM1 ganglioside in CFTR-deficient human airway cells results in decreased β1-integrin signaling and delayed wound repair. *AJP: Cell Physiology* 306:C819--30

182. Teichgrber V, Ulrich M, Endlich N, Riethmller J, Wilker B, et al. 2008. Ceramide accumulation mediates inflammation, cell death and infection susceptibility in cystic fibrosis. *Nature medicine* 14:382--91

183. Gottlieb RA, Dosanjh A. 1996. Mutant cystic fibrosis transmembrane conductance regulator inhibits acidification and apoptosis in C127 cells:

possible relevance to cystic fibrosis. *Proceedings of the National Academy of Sciences of the United States of America* 93:3587--91

184. Bradbury NA. 1999. Intracellular CFTR: localization and function. *Physiological reviews* 79:S175--91
185. Brodlie M, McKean MC, Johnson GE, Gray J, Fisher AJ, et al. 2010. Ceramide is increased in the lower airway epithelium of people with advanced cystic fibrosis lung disease. *American Journal of Respiratory and Critical Care Medicine* 182:369--75
186. Welsh MJ. 1983. Cigarette smoke inhibition of ion transport in canine tracheal epithelium. *Journal of Clinical Investigation*
187. Cantin AM, Hanrahan JW, Bilodeau G, Ellis L, Dupuis A, et al. 2006. Cystic fibrosis transmembrane conductance regulator function is suppressed in cigarette smokers. *American Journal of Respiratory and Critical Care Medicine* 173:1139--44
188. Clunes LA, Davies CM, Coakley RD, Aleksandrov AA, Henderson AG, et al. 2012. Cigarette smoke exposure induces CFTR internalization and insolubility, leading to airway surface liquid dehydration. *The FASEB Journal* 26:533--45
189. Rab A, Rowe SM, Raju SV, Bebok Z, Matalon S, Collawn JF. 2013. Cigarette smoke and CFTR: implications in the pathogenesis of COPD. *AJP: Lung Cellular and Molecular Physiology* 305:L530--41
190. Raju SV, Jackson PL, Courville CA, McNicholas CM, Sloane PA, et al. 2013. Cigarette smoke induces systemic defects in cystic fibrosis transmembrane conductance regulator function. *American Journal of Respiratory and Critical Care Medicine* 188:1321--30
191. Moran AR, Norimatsu Y, Dawson DC, MacDonald KD. 2014. Aqueous cigarette smoke extract induces a voltage-dependent inhibition of CFTR expressed in Xenopus oocytes. *AJP: Lung Cellular and Molecular Physiology* 306:L284--91
192. Raju SV, Solomon GM, Dransfield MT, Rowe SM. 2016. Acquired Cystic Fibrosis Transmembrane Conductance Regulator Dysfunction in Chronic Bronchitis and Other Diseases of Mucus Clearance. *Clinics in chest medicine* 37:147--58
193. Petrache I, Berdyshev EV. 2016. Ceramide Signaling and Metabolism in Pathophysiological States of the Lung. *Annual Review of Physiology* 78:463--80
194. Mulvey MA, Lopez-Boado YS, Wilson CL, Roth R, Parks WC, et al. 1998. Induction and evasion of host defenses by type 1-piliated uropathogenic Escherichia coli. *Science* 282:1494-7
195. Cywes C, Stamenkovic I, Wessels MR. 2000. CD44 as a receptor for colonization of the pharynx by group A Streptococcus. *J Clin Invest* 106:995-1002
196. Tsai PJ, Lin YS, Kuo CF, Lei HY, Wu JJ. 1999. Group A Streptococcus induces apoptosis in human epithelial cells. *Infect Immun* 67:4334-9
197. Schroeder TH, Reiniger N, Meluleni G, Grout M, Coleman FT, Pier GB. 2001. Transgenic cystic fibrosis mice exhibit reduced early clearance of

Pseudomonas aeruginosa from the respiratory tract. *Journal of immunology (Baltimore, Md. : 1950)* 166:7410--8

198. Grassm. 2003. Host defense against Pseudomonas aeruginosa requires ceramide-rich membrane rafts. *Nature medicine* 9:322--30

199. Kowalski MP, Pier GB. 2004. Localization of cystic fibrosis transmembrane conductance regulator to lipid rafts of epithelial cells is required for Pseudomonas aeruginosa-induced cellular activation. *Journal of immunology (Baltimore, Md. : 1950)* 172:418--25

200. Ni I, Ji C, Vij N. 2015. Second-hand cigarette smoke impairs bacterial phagocytosis in macrophages by modulating CFTR dependent lipid-rafts. *PLoS ONE* 10:e0121200

201. Grassm. 2001. CD95 signaling via ceramide-rich membrane rafts. *The Journal of biological chemistry* 276:20589--96

202. Abdel Shakor AB, Atia MM, Kwiatkowska K, Sobota A. 2012. Cell surface ceramide controls translocation of transferrin receptor to clathrin-coated pits. *Cellular Signalling* 24:677--84

203. Gulbins E, Dreschers S, Wilker B, Grassme H. 2004. Ceramide, membrane rafts and infections. *J Mol Med (Berl)* 82:357-63

204. Cannon CL, Kowalski MP, Stopak KS, Pier GB. 2003. Pseudomonas aeruginosa-induced apoptosis is defective in respiratory epithelial cells expressing mutant cystic fibrosis transmembrane conductance regulator. *American journal of respiratory cell and molecular biology* 29:188--97

205. Bates IR, Hbert B, Luo Y, Liao J, Bachir AI, et al. 2006. Membrane lateral diffusion and capture of CFTR within transient confinement zones. *Biophysical Journal* 91:1046--58

206. Canals D, Jenkins RW, Roddy P, Hernndez-Corbacho MJ, Obeid LM, Hannun YA. 2010. Differential effects of ceramide and sphingosine 1-phosphate on ERM phosphorylation: probing sphingolipid signaling at the outer plasma membrane. *Journal of Biological Chemistry* 285:32476--85

207. Canals D, Roddy P, Hannun YA. 2012. Protein phosphatase 1α mediates ceramide-induced ERM protein dephosphorylation: a novel mechanism independent of phosphatidylinositol 4, 5-biphosphate (PIP2) and myosin/ERM phosphatase. *The Journal of biological chemistry* 287:10145--55

208. Arikawa J, Ishibashi M, Kawashima M, Takagi Y, Ichikawa Y, Imokawa G. 2002. Decreased Levels of Sphingosine, a Natural Antimicrobial Agent, may be Associated with Vulnerability of the Stratum Corneum from Patients with Atopic Dermatitis to Colonization by Staphylococcus aureus. *The Journal of investigative dermatology* 119:433--9

209. Fischer CL, Walters KS, Drake DR, Blanchette DR, Dawson DV, et al. 2013. Sphingoid Bases Are Taken Up by Escherichia coliand Staphylococcus aureusand Induce Ultrastructural Damage. *Skin Pharmacology and Physiology* 26:36--44

210. Pewzner-Jung Y, Tavakoli Tabazavareh S, Grassme H, Becker KA, Japtok L, et al. 2014. Sphingoid long chain bases prevent lung infection by Pseudomonas aeruginosa. *EMBO molecular medicine* 6:1205--14

211. Boujaoude LC, Bradshaw-Wilder C, Mao C, Cohn J, Ogretmen B, et al. 2001. Cystic fibrosis transmembrane regulator regulates uptake of sphingoid base phosphates and lysophosphatidic acid: modulation of cellular activity of sphingosine 1-phosphate. *The Journal of biological chemistry* 276:35258--64

212. Ramu Y, Xu Y, Lu Z. 2007. Inhibition of CFTR Cl- channel function caused by enzymatic hydrolysis of sphingomyelin. *Proceedings of the National Academy of Sciences of the United States of America* 104:6448--53

213. Ito Y, Sato S, Ohashi T, Nakayama S, Shimokata K, Kume H. 2004. Reduction of airway anion secretion via CFTR in sphingomyelin pathway. *Biochemical and Biophysical Research Communications* 324:901--8

214. Ramu Y, Xu Y, Shin H-G, Lu Z. 2014. Counteracting suppression of CFTR and voltage-gated K+ channels by a bacterial pathogenic factor with the natural product tannic acid. *eLife* 3:e03683

3) Methods

3.1) Protein Purification

To facilitate our study of CFTR modulation by bacterial Sphingomyelinase C (SMase), we purified the enzyme to obtain large quantities of active protein that we would easily characterize. The gene encoding *S. aureus* SMase was amplified out of ATCC strain 29213 and inserted into the pET28b inducible expression vector (Novagen) using the Gibson Assembly Method (New England BioLabs) according to the manufacturer's instructions. *S. aureus* genomic DNA was isolated using the Wizard Genomic DNA purification kit (Promega). The SMase N-terminal signal sequence (AAs 1-34) was removed to prevent secretion and thereby simplify purification. Primers to amplify SMase were as follows: Forward –CTTTAAGAAGGAGATATACCATGGAATCTAAGAAAGATG-ATACTG; Reverse – GCTCGAGTGCGGCCGCAAGCTTTTTACTATAGGCTTTG-ATTGG. Primers to amplify pET28b were as follows: Forward- AAGCTTGCGGC-CGCACTCGAGC; Reverse – CCATGGTATATCTCCTTCTTAAAG. The inactivating H322A mutation was introduced using QuikChange mutagenesis (Agilent Technologies). The expression host was BL21(DE3) *E. coli* and protein production was induced with 0.1 mM IPTG at 16° C overnight. Cells were pelleted, resuspended in PBS + bacterial protease inhibitor cocktail (Goldbio), and lysed with three passes in a French press. Insoluble material was cleared via centrifugation at 10,000×g for 10 minutes. Protein was purified from the cleared lysate using "cOmplete" His-Tag Purification Resin (Roche) and Poly-prep chromatography columns (Bio-Rad) according to the Roche protocol. Imidazole was removed via serial dialyses in 1L volumes at 4°C so that the final concentration was below 1 pM. Eluate was stored in 250 mM sodium phosphate (final concentration)/50% glycerol at 4° C. SMase C activity was quantified using the Amplex Red sphingomyelinase assay

described below. Experiments testing the effect of SMase on CFTR variants were always

matched with same-day controls using WT-CFTR.

3.2) Amplex Red SMase assay

The fluorometric assay kit was purchased from Invitrogen (MP12220) and

set up according to the manufacturer's instructions. Briefly, the indicated amount of purified

SMase protein was mixed with reaction buffer to a final volume of 100 µL and the reaction

was initiated by injecting an equal volume of the reaction mixture containing sphingomyelin,

Amplex Red, alkaline phosphatase, choline oxidase, and horseradish peroxidase for a final

volume of 200 µL. In my experience, 100 ng of pure SMase provides adequate signal

without saturating the assay. This assay indirectly measures SMase activity via enzyme-

dependent oxidation of the phosphocholine (ChoP) product to form H_2O_2, and subsequent

formation of resorufin from Amplex Red. In all experiments, equimolar ChoP was used as a

positive control to determine the maximum signal and the useful range. It also ensured that

our treatments (e.g., exposure to VX-770) did not alter the assay independent of SMase

activity.

3.3) Preparation of oocytes and cRNA

The mutants used in this study were prepared using the QuikChange site-directed

mutagenesis method (Agilent Technologies). Mutant constructs were verified by sequencing

across the entire open reading frame before use. All cRNAs for electrophysiology

experiments were prepared from a construct encoding WT-CFTR in the pGEMHE vector

provided by D. Gadsby (The Rockefeller University, New York, NY) using the mMessage

mMachine T7 *in vitro* transcription kit (Ambion). *Xenopus* oocytes were injected with a range

of 0.5 - 15 ng CFTR cRNAs and were incubated at 17°C in modified Leibovitz's L-15 media

plus 21.8 mM HEPES, pH 7.5, with penicillin, and streptomycin(1). Recordings were made

18–72 h after the injection of cRNAs. Methods of animal handling are in accordance with

the National Institutes of Health guidelines, and the protocol was approved by the

Institutional Animal Care and Use Committee of Emory University.

3.4) Oocyte Electrophysiology (TEVC and Patch Clamp)

In all cases data were acquired using pClamp software and analyzed using Clampfit.

For Two Electrode Voltage Clamp (TEVC), CFTR currents were recorded using a

Geneclamp 500B amplifier equipped with a virtual ground and pClamp 10.2 software

(Axon). Electrodes were pulled from borosilicate glass with a filament and filled with 3M

KCl. Resistances were $0.2 – 0.5$ MΩ. Bath solution was standard ND96 containing (in

mM): 96 NaCl, 2 KCl, 1 MgCl2, and 5 HEPES, pH 7.5. Cells were held at $V_m = -20$ mV and

currents were elicited at 0.1 Hz using a 500 ms ramp from $V_m = -60 – 0$ mV. Data were

acquired at 1 kHz and software-filtered at 100 Hz. Current amplitudes reported in the

'Results' section were measured at $V_m = -60$ mV. SMase was diluted in ND96 at room

temperature immediately before application and applied at 2 mL/min using a gravity-fed

perfusion system into a recording chamber holding approximately 300 µL of solution.

GlyH-101 was applied at 30 µM to ensure that residual current was CFTR. To control for

batch-to-batch variation in sensitivity of cells to SMase, equal numbers of cells expressing

WT and mutant CFTR were utilized each week. For excised macropatch experiments, the

vitelline membrane was removed and the cell was submerged in a recording solution

containing (in mM): 150 NMDG-Cl, 1.1 $MgCl_2$, 2 Tris-EGTA, and 10 TES, pH 7.4. After

patch excision, inside-out patches were exposed to recording solution containing 1 mM ATP and 25 units PKA. Pipette solution contained 150 NMDG-Cl, 5 $MgCl_2$, and 10 TES, pH 7.4. For cell-attached macropatch recordings, a window was generated in the vitelline membrane and the cells were submerged in the pipette solution outlined above. The recording pipette accessed the plasma membrane via the tear in the vitelline membrane. To activate CFTR channels, 2 μL of 30 mM IBMX was added to the chamber containing ~300 μL for a final IBMX concentration of 0.2 mM. For these experiments, SMase was diluted 1:1 in recording solution before addition to the chamber to facilitate diffusion of the protein. After the CFTR currents in the cell-attached patch were fully activated, 6 μL of the diluted SMase was pipetted into the chamber containing ~300 μL of solution for a final concentration of 10 μg/mL SMase. Note that the volume of SMase added to the chamber will depend on the initial protein concentration. Currents were elicited with a 0.6 Hz ramp from V_m = -100 mV to +100 mV for both the I/O patch and the cell-attached patch experiments.

3.5) Voltage Clamp Fluorometry

For real-time measurement of the plasma membrane localization of CFTR via voltage clamp fluorometry, oocytes were injected with cRNA encoding CFTR that was tagged with GFP, either on the intracellular N-terminus[2] or within extracellular loop 4 [3]. Acidic ND96 solution (pH 5.5) was buffered with 10 mM MES instead of HEPES, but was otherwise prepared as described for ND96 above. The voltage clamp fluorometry rig was built similarly as described by Pless.[4] Briefly, fluorescence from oocytes was measured via a photomultiplier tube (Hamamatsu no. H9306-02), and the signal was digitized into pClamp 9 in parallel with the ionic current. The photomultiplier tube was controlled by an Oriel power supply (Newport no. 70703) and set to 650 volts via a 10-kOhm potentiometer. To

minimize photobleaching, excitation from the halogen lamp (Lumen Dynamics Xcite no. 120Q) was reduced via a neutral density filter (Thorlabs no. NE03B) and shuttered via TTL pulses from pCLAMP 9 to a shutter driver (Vincent Associates no. VCM-D1) and Uniblitz shutter (Vincent Associates no. 9002-0212), such that the oocytes were exposed to excitation for 100 ms/s. Oocytes were placed in the custom built chamber with the animal side (dark side) down and positioned such that the plasma membrane was in focus. The oocyte was the inpaled as normal for TEVC. This is a bit more difficult on the inverted microscope and care should be taken to not "crash" the electrodes into anything. After impaling the oocytes, recording commenced with electrical stimulation identical to that used in the TEVC experiments discussed previously; namely, cells were held at V_m = -20 mV and currents were elicited at 0.1 Hz with a ramp from V_m = -60 mV to V_m = 0 mV. A custom ramp protocol was designed to include additional channels for the TLL pulse out to the shutter and in from the PMT. Once it was clear that the cell was stable, the iris was opened so that fluorescence measurements could be made. Once a stable baseline was clear, perfusion was switched from the pH 7.5 ND96 to the pH 5.5 solution and fluorescence was continually monitored until the change was stable (usually 30 seconds is adequate). At that point, the solutions were switched back and, as before, fluorescence was monitored until a stable reading was achieved. At this point the iris was closed to prevent bleaching. The cell was then activated with 0.1 mM IBMX until stable and then treated with 10 μg/mL SMase for 10 minutes. Once stable inhibition had occurred, another fluorescence measurement was made by opening the iris and monitoring the fluorescence change that occurred with application of the pH 5.5 solution as described previously. Note that if IBMX is included in the pH 5.5 solution, quenching does not occur so it is important to omit IBMX from that solution and to perfuse the cell with ND96 without IBMX during the pH 7.5 reading. It is also important

to measure the fluorescence of uninjected oocytes on the day of experimentation so that the background fluorescence of the oocytes can be accounted subtracted.

3.6) Xenopus oocyte cell-ELISA

Oocytes were injected with exGFP-CFTR and inGFP-CFTR mRNA at the beginning of the week and the cell-ELISA experiment was performed 4 days post injection. Expression was verified by TEVC the day before the cell-ELISA experiment was run. Cells were washed with ND96 solution and 20 cells were used for each replicate. The washed cells were treated with 10 μg/mL SMase in ND96 for 10 minutes at RT. After treatment, the SMase-containing solution was removed, and cells were fixed in 4% paraformaldehyde in PBS for 20 minutes at room temperature. The fixed oocytes were then blocked nonspecific in 10% bovine calf serum in PBS for 45 minutes. Oocytes were then treated with an anti-GFP antibody (Novus #NB600-308 at 1:500 in blocking solution) for 2 hours at room temperature. Primary antibody was removed, cells were washed 2 times for 10 minutes each in PBS, and a 1:1000 dilution of HRP-conjugated secondary antibody in blocking solution was added and the cells were incubated for 2 hours at RT (Cell Signaling #7074). Cells were then washed 2X in PBS/Serum and 2X in PBS alone. TMB-ELISA substrate (Biolegend) was then added to the cells to develop the signal. Signal was read after a 20-minute incubation at room temperature (blue color should be clear by this point). 200 μL samples were removed at 20 minutes and sulfuric acid was added to the sample to quench the reaction. The solution changes from blue to yellow with addition of the sulfuric acid.

3.7) *Xenopus* oocyte biotinylation

Cells were injected with 1 μg of WT-CFTR RNA and incubated at 17°C until the day

of the experiment (4 days). Each treatment group was made up of 20 oocytes and treatments were performed in triplicate. Streptavidin resin was washed in PBS and incubated in oocyte solubilization buffer containing 5% BSA until needed (Solubilization buffer: 20 mM TRIS, 10% v/v glycerol, 5 mM EDTA, 1% w/v Na^+ deoxycholate, 1 mM PMFS; pH 6.8). Cells were moved to 35 mm dishes, washed 2 times in ND96, and then treated with the appropriate enzyme (WT-SMase or H322A-SMase). After 10 minutes at RT, solution was removed and cells were washed 3 times in PBS without Ca^{2+} and Mg^{2+} to quench the SMase activity. Sulfa-NHS-SS-Biotin was added to a final concentration of 0.5 mg/mL and then the cells were incubated at RT for 30 minutes. After labeling, the biotinylation solution was removed and the reaction was quenched with 3 TBS washes. Oocytes were moved to homogenization buffer (20 mM TRIS, 5 mM $MgCl_2$, 5 mM $NaHPO_4$, 1 mM EDTA, 80 mM sucrose, 1 mM PMSF; pH 7.4), and lysed with fine scissors and serial trituration. Homogenate was then centrifuged at 16,200xg for 30 minutes at 4°C to pellet membranes and separate yolk. Supernatant was then aspirated, the pellet was resuspended in solubilization buffer, and the samples was centrifuged 16,200xg for 30 minutes at 4°C. A small fraction of the supernatant was removed as the "total CFTR" control. The remaining supernatant was moved to a new tube, mixed with preblocked streptavidin beads, and rotated for 2 hours at 4°C. After binding, beads were separated using a centrifugation filter, washed with 20 volumes of PBS, and eluted in Laemmli buffer. Eluate was incubated at 37°C for 30 minutes and then separated on a precast 4-20% gradient polyacrylamide gel. Protein was transferred onto PVDF membranes, blocked with 5% nonfat dry milk, and probed with a CFTR primary antibody (UNC #596) and an anti-mouse HRP secondary antibody. Membranes were developed using luminescent HRP substrate and imaged on a BioRad Gel Doc imager.

3.8) Ussing Chamber Electrophysiology

Cells were seeded onto Transwell or Snapwell permeable supports according to the experimental requirements. Calu-3 cells were plated at either $1*10^6$ cells per Snapwell or $5*10^5$ cells per Snapwell as specified in the Results section. After polarization, Calu-3 cells were transitioned to an air/liquid interface. Primary bronchial epithelial cells (HBEs) or nasal epithelial cells (NBEs) were obtained from the CF@LANTA RDP cell models core already plated on filters. Calu3 cells were cultured in DMEM/F12 media supplemented with 10% FBS and Penicillin/Streptomycin. Primary epithelial cells were maintained at an air/liquid interface and cultured in "Emory ALI" media purchased from the RDP cell models core. For experiments in which SMase was incubated on the cells overnight, enzyme was diluted in KRH buffer. All equipment was sourced from Physiologic Instruments: Amplifier – VCC-MC6; electrodes – P2020-S; Chambers – EM-RSYS-2; Sliders – P2302 for Snapwells and P2302T for Transwells. On the day of experimentation, electrode tips were prepared by adding ~1 cm of 3M KCL/3% agar to the electrode tips according to the manufacturers' protocol. The voltage offset and fluid resistance compensation were set according to manufacturers' instructions with a blank filter in the chamber. Filters were inserted into the appropriate slider (NOTE: Transwells must be trimmed before they will fit into the chambers) and inserted into the chambers. The following solutions were then added to the chambers (mM): basolateral – 115 NaCl, 5 KCL, 1 $MgCl_2$, 2 $CaCl_2$, 10 glucose, 10 HEPES, 25 $NaHCO_3$; apical – 115 NaGluconate, 5 KCl, 1 $MgCl_2$, 4 $CaCl_2$, 10 glucose, 10 HEPES, 25 N_AHCO_3. Both solutions were bubbled with a 95/5 mixture of O_2/CO_2 and heated to 37°C. Data were acquired using the Acquire and Analyze software and exported to excel for analysis.

3.9) Statistics

Data were compared using an unpaired t-test, paired t-test, 1-way, or 2-way ANOVA analysis as indicated in the figure legends. In all cases, error bars represent S.E.M. and differences were considered significant when $p \leq 0.05$.

Works Cited:

1.   Cui G, Rahman KS, Infield DT, Kuang C, Prince CZ, McCarty NA. 2014. Three charged amino acids in extracellular loop 1 are involved in maintaining the outer pore architecture of CFTR. In *The Journal of General Physiology*, pp. 159-79
2.   Moyer BD, Loffing J, Schwiebert EM, Loffing-Cueni D, Halpin PA, et al. 1998. Membrane trafficking of the cystic fibrosis gene product, cystic fibrosis transmembrane conductance regulator, tagged with green fluorescent protein in madin-darby canine kidney cells. *The Journal of biological chemistry* 273:21759-68
3.   Haggie PM, Verkman AS. 2008. Monomeric CFTR in plasma membranes in live cells revealed by single molecule fluorescence imaging. *The Journal of biological chemistry* 283:23510-3
4.   Pless SA, Dibas MI, Lester HA, Lynch JW. 2007. Conformational variability of the glycine receptor M2 domain in response to activation by different agonists. *The Journal of biological chemistry* 282:36057-67

4) Results

4.1) *State dependent inhibition of CFTR by bacterial SMase*

4.1.1) *Introduction*

The Cystic Fibrosis Transmembrane conductance Regulator (CFTR) chloride channel mediates hydration of the airway epithelium and loss-of-function mutations in CFTR lead to cystic fibrosis (CF), a disease characterized by bronchiectasis, mucus plugging, and persistent bacterial infections that induce a chronic inflammatory state (1). Many CF therapeutics in the pipeline target CFTR with the goal of restoring channel function, but recent findings suggest that the bacterial virulence factor sphingomyelinase (SMase) can diminish CFTR activity in the *Xenopus* oocyte expression system and polarized Calu-3 cells (2; 3). Given the potentially antagonistic effects that bacterial SMase could have on pharmacological rescue of CFTR channel function, it is important to understand how SMase affects CFTR channel activity.

Lu and coworkers (2)found that two catalytically distinct orthologs of SMase inhibited CFTR channel function in the *Xenopus* oocyte expression system. The first was SMase C, which breaks down sphingomyelin to form phosphocholine and ceramide, and the second was SMase D, which forms choline and ceramide 1-phosphate. Ramu *et al.* established that inhibition relies on catalysis of sphingomyelin by demonstrating that both an inactive SMase mutant and preparations of wildtype SMase lacking the requisite Mg^{2+} cofactor left CFTR currents unaffected. However, the underlying mechanism by which SMase enzymatic activity inhibits CFTR activity remains unknown. SMase activity leads to multiple biochemical and biophysical changes in cells; specifically, catalysis of sphingomyelin reduced the prevalence of positive charge in the outer-leaflet of the cell membrane (4), activates various signaling pathways in numerous cell types (5-10), facilitates the formation

of membrane microdomains (11-13), and induces plasma membrane internalization (14; 15),
It is currently unclear which of these processes may be responsible for inhibition of CFTR
chloride currents in the *Xenopus* expression system.

In Section 4.1, we show that SMase C inhibits CFTR channels expressed in *Xenopus*
oocytes without inducing internalization of the channel and present evidence for the
requirement of a mobile cytosolic component. Additionally, we show that channel activation
state directly affects inhibition rate suggesting that SMase modifies CFTR gating activity. We
also show that SMase-mediated inhibition reduces the efficacy of modulation of CFTR by
VX-770, a CFTR-targeted therapeutic. Finally we present evidence that basolateral
application of SMase to primary bronchial epithelial cells reduces FSK and VX-770
stimulated currents. These results suggest that SMase inhibits CFTR channels via a novel,
state-dependent mechanism and that the presence of SMase in the pulmonary interstitial
space may diminish the ability to activate CFTR.

4.1.2) *Results*

Purification of S. aureus SMase

We cloned a HIS-tagged variant of *S. aureus* SMase to facilitate our study and avoid the need to purchase large quantities of recombinant protein. To this end, we utilized the BL21(DE3) strain of *E. coli* as our expression host and the SMase protein was enriched to >80% using a HIS-purification column as outlined in the Methods section. A representative Coomassie blue-stained SDS-PAGE gel is shown in Figure 4.1b. In addition to the WT protein, we purified an enzyme dead mutant of SMase (H322A SMase). A crystal structure of *S. aureus* is shown in Figure 4.1a (PDB 3I48) and the mutated histidine at position 322 is shown in orange. We chose to mutate this particular residue because Obama and colleagues found that the corresponding histidine in the closely related *B. cereus* enzyme (H296) is a requisite general base in the acid/base phosphodiesterase catalysis mechanism (16). As expected, our purified WT SMase was able to catalyze the breakdown of sphingomyelin in an Amplex Red-based SMase assay, indicated by the time dependent accumulation of fluorescence after injection of reaction buffer, while the H322A mutant showed no activity (Figure 4.1c, d).

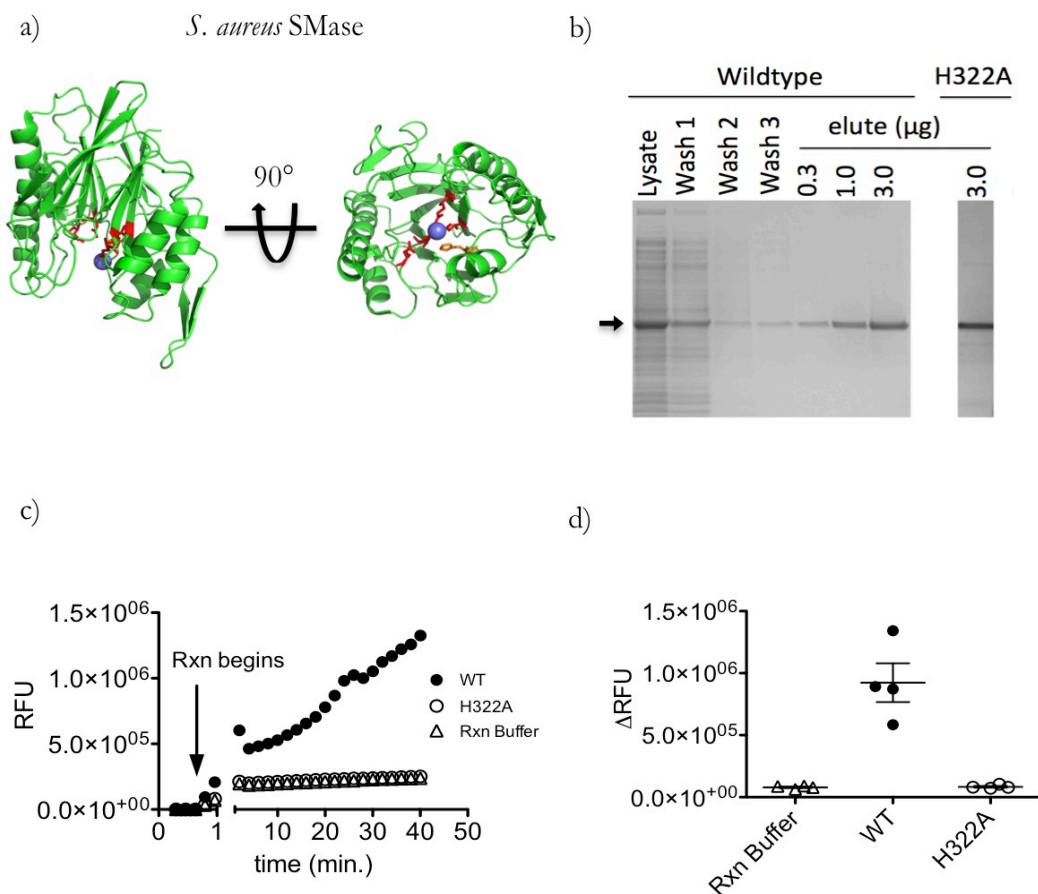Figure 4.1) Purification and characterization of WT and H322A Sphingomyelinase

Figure 4.1) Purification and characterization of WT and H322A sphingomyelinase: (a) The crystal structure of *S. aureus* SMase (PDB 3I48) with the required catalytic histidine H322 shown in orange. A bound Mg^{2+} ion is shown in blue and all other active site residues are shown as red sticks. (b) A Coomassie stained polyacrylamide gel showing purification of both the wild-type and enzyme-dead mutant (H322A) SMase proteins. (c) Activity of 100 ng of the WT protein was verified using the commercially available fluorometric SMase assay and is apparent by the time-dependent increase in fluorescence. An equal amount of H322A protein showed no activity. (d) Cumulative data from four independent replicates of the Amplex Red assay. Data are shown as ΔRFU, which represents the change in fluorescent signal from 30s after initiation of the reaction to the final measurement.

CFTR currents in Xenopus oocytes are inhibited by WT SMase but not H322A SMase

To investigate the effect of *S. aureus* sphingomyelinase C (SMase) on CFTR channel activity, the two-electrode voltage clamp (TEVC) method was used to measure whole-cell CFTR currents in *Xenopus* oocytes heterologously expressing the CFTR channel (Figure 4.2). Currents were activated by exposure of the cell to the phosphodiesterase inhibitor IBMX (0.1 mM), which stimulates protein kinase A (PKA)-mediated signaling (Figure 4.3). After currents reached steady-state activation, cells were exposed to 2 µg/mL wildtype (WT) or enzyme-dead (H322A) SMase in the continuing presence of IBMX. As shown in Figure 4.3a, and consistent with previous observations (2), CFTR current decreased slowly in the presence of WT SMase but not H322A SMase, suggestive of enzymatic activity and possibly the initiation of a signaling cascade that impinged upon CFTR over time, rather than the rapid block of the channel pore (17; 18). Inhibition was voltage independent, which is consistent with altered channel gating activity and not pore block (Fig. 4.3b). Holding the duration of exposure constant at 10 minutes, both the rate and extent of SMase-mediated inhibition of CFTR currents by the active protein were dependent upon SMase concentration (Fig. 4.3c,d). In these experiments, residual currents were shown to be CFTR-mediated by their sensitivity to inhibition by the pore blocker GlyH-101 (19).
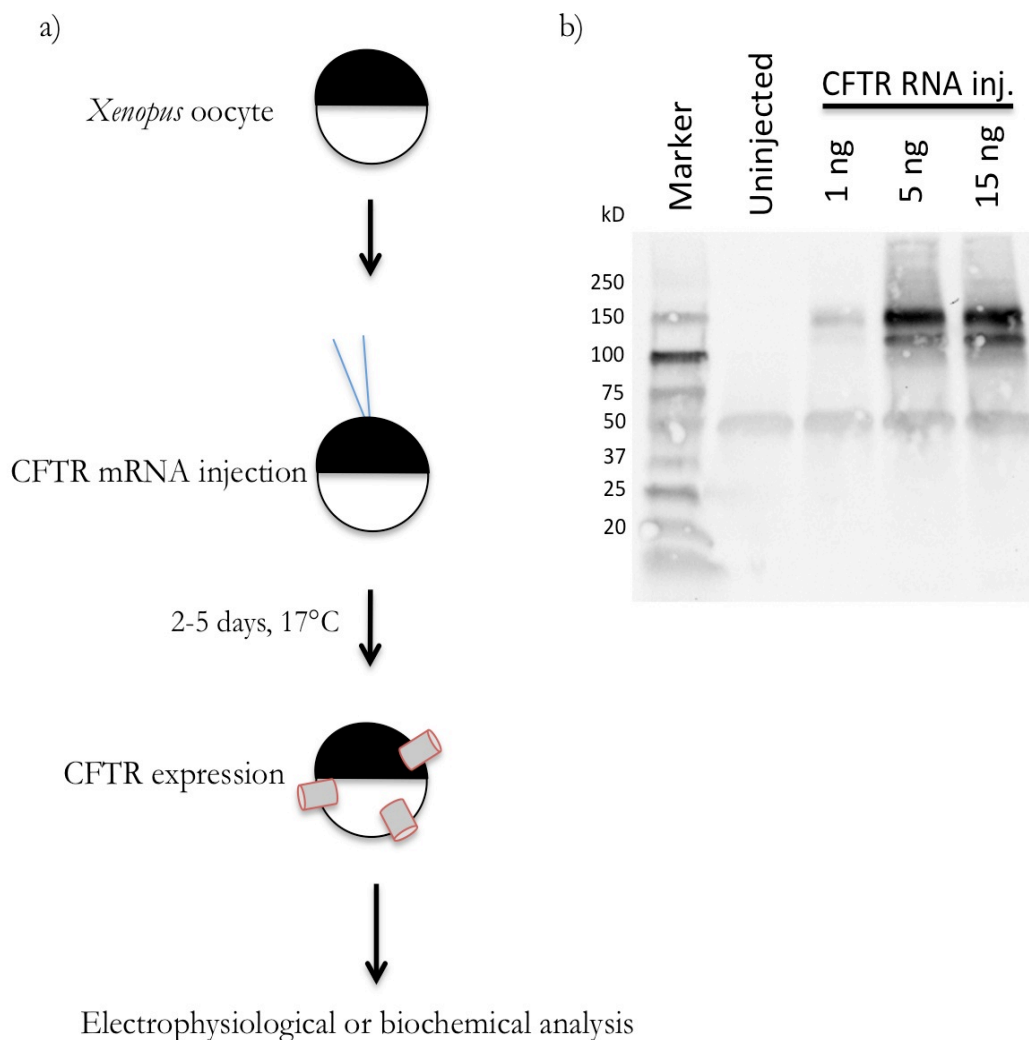
Figure 4.2) Expression of CFTR in *Xenopus laevis* oocytes

Figure 4.2) Expression of CFTR in *Xenopus laevis* oocytes (a) *Xenopus* oocytes were isolated from sexually mature female frogs via surgical removal of the ovary followed by defolliculation using collagenase. Individual oocytes were then injected with mRNA encoding WT or mutant CFTR and incubated at 17°C until the day of experimentation. Incubation period and mRNA mass were adjusted to acheive the desired expression level. (b) A western blot shows expression of CFTR protein in *Xenopus* oocytes injected with increasing masses of CFTR mRNA.

Figure 4.3) Inhibition of CFTR channel activity in *Xenopus* oocytes requires enzymatic activity
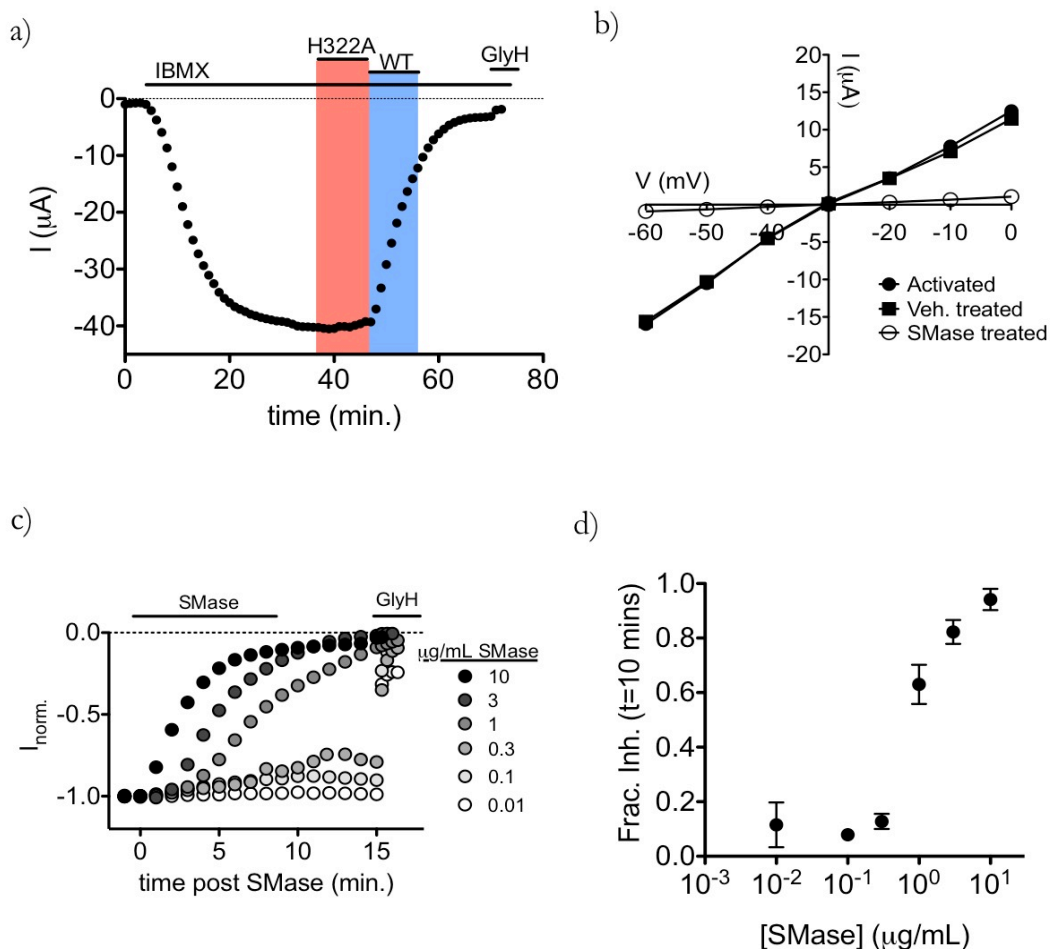

Figure 4.3) Inhibition of CFTR channel activity in *Xenopus* oocytes requires enzymatic activity: (a) WT-human-CFTR currents elicited with 0.1 mM IBMX and a voltage step to V_m = -60 mV were inhibited by 2 μg/mL WT SMase but not by the inactive H322A mutant (n=6). (b) Current voltage relationships of CFTR before and after inhibition by SMase show that inhibition is voltage independent. (c) Example traces show that inhibition rate was proportional to SMase concentration. For display, currents were normalized to the amplitude 1 minute prior to application of enzyme. SMase was applied from 0 - 10 minutes. Sensitivity to GlyH-101 applied at the end of the experiment shows that remaining currents represented uninhibited CFTR channels. (d) Summary data showing that fractional inhibition at 10 minutes was proportional to SMase concentration (n=4-6).

Inhibition is not membrane-delimited

The results from TEVC experiments as shown in Figure 4.3 indicate that inhibition of CFTR by extracellular SMase developed after a brief delay of duration inversely related to the bath enzyme concentration, and continued after washout of enzyme from the bath solution for concentrations ≥1 µg/mL; both of these observations are consistent with the activation of a signaling cascade. To investigate the requirement for cytosolic signaling components, we compared the sensitivity of channels to SMase in two configurations of the macropatch voltage clamp technique (20) (Fig. 4.4). In cell-attached macropatch recordings, SMase was added to the solution bathing the entire cell outside of the patch of membrane within the pipette (Fig. 4.4a). In this configuration, currents reflect the activity of only those channels in the membrane patch protected from direct exposure to SMase by the pipette. Channels were activated by exposure of the cell to 0.2 mM IBMX in the bath and subsequent exposure to 10 µg/mL of SMase in the bath led to reduction in channel currents. Figure 4.4b shows an example of the second configuration, the excised inside-out patch clamp. For excised patch experiments, channels were activated by direct exposure to exogenous PKA at a concentration of 25 U/mL and 1 mM ATP, an approach we have used extensively in the past (21), and then directly exposed to 10 µg/mL of SMase backfilled in the pipette-filling solution. Inhibition did not develop over the course of the experiment (45 minutes). As before, currents were shown to arise from CFTR by their sensitivity to inhibitor, in this case the cell-permeant INH_{172} (22). These results, summarized in Figure 4.4c, suggest that SMase-mediated inhibition of CFTR channels is not membrane-delimited but instead utilizes mobile signaling components that are lost from the cytoplasmic face of the membrane upon excision of the membrane patch. Additionally, it provides evidence that

Figure 4.4) Inhibition is not membrane-delimited: (a) CFTR currents recorded in the cell-attached configuration after activation with 0.2 mM IBMX were inhibited by 10 μg/ml SMase in the recording chamber. (b) WT-CFTR channels activated with 25 U PKA (expected activation of ~50% max) (34), and recorded in the excised inside-out patch configuration were insensitive to 10 μg/mL SMase backfilled into the recording pipette. (c) Summary data showing that cell attached patches were inhibited while excised patches were not, and that the presence of the PI3K inhibitor LY294002 or the JNK inhibitor SP600125 had no effect. These data were acquired by Dr. Guiying Cui.
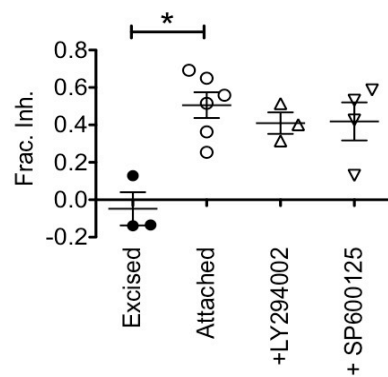
Figure 4.4) Inhibition is not membrane delimited

a) Cell-attached
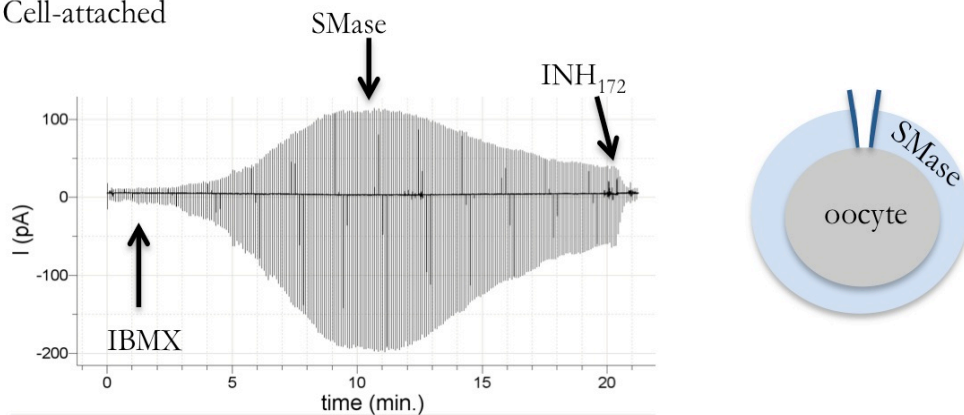
b) Inside/Out Patch
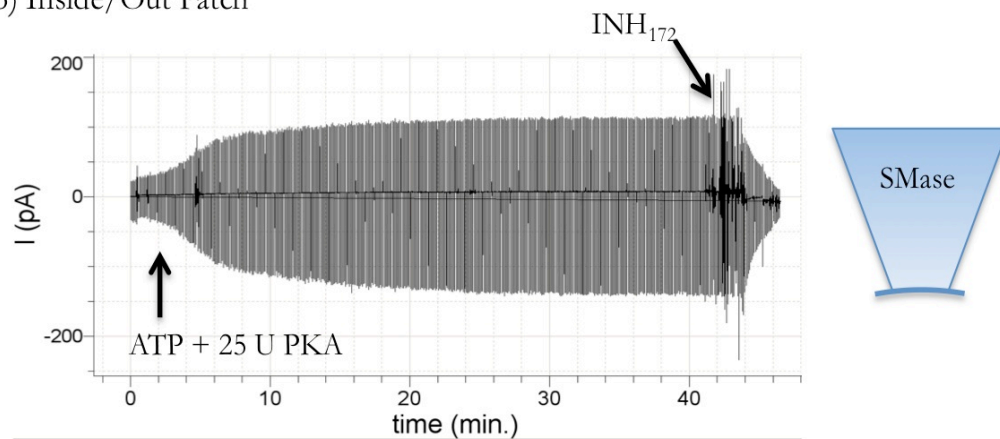
c)

inhibition does not rely on SMase-mediated catalysis of sphingomyelin molecules that may be directly associated with gating CFTR channels.

Ceramide is known to activate multiple signaling cascades, as are its metabolic products ceramide-1-phosphate and sphingosine. Affected cascades include JNK, PI3K, KSR, MEK/ERK, CAPK, PKCζ, and PP2A (5-10). To implicate one of these cascades, we have started screening small molecule inhibitors in the cell-attached systems. At this point, we have not found a compound that significantly affected inhibition by SMase (Fig. 4.4c). So far, we have tested the PI3K inhibitor LY294002 and the JNK inhibitor SP600125 at IC_{90} concentrations, both of which have been previously shown to be effective in *Xenopus* oocytes (23; 24).

Channel internalization does not underlie SMase-mediated inhibition of CFTR

One potential mechanism by which activation of SMase-induced signaling pathways could lead to loss of CFTR current is by the reduction of channel density in the plasma membrane. SMase has been shown to facilitate internalization in models of membrane repair (14), so we tested this possibility in three different ways. First, we used a novel assay for CFTR channels resident in the plasma membrane that relies upon the pH sensitivity of a GFP tag in the fourth extracellular loop (25). Fluorescence of CFTR proteins tagged with this exofacial GFP (exGFP-CFTR; Fig. 4.5a) was reversibly quenched by perfusion with acidic bath solution (Fig. 4.5b, c) while fluorescence of an intracellularly-tagged CFTR (inGFP-CFTR) was unaffected by pH in this timeframe (Fig. 4.5b). Thus, fluorescence quenching is a readout of the abundance of exGFP-CFTR at the plasma membrane. Fluorescence was monitored via a fluorescence microscope coupled to a photomultiplier tube and is shown as a voltage (V_{PMT}). To determine whether SMase-mediated inhibition of current corresponded with a proportional reduction in cell surface exGFP-CFTR, we compared the pH-dependent fluorescence change (ΔV) before and after exposure to 10 μg/mL SMase. As shown in Figure 4.5e, the pH-dependent change in fluorescence of exGFP-CFTR was not significantly affected by bath SMase despite nearly complete inhibition of the CFTR-mediated current, which was measured simultaneoulsy in the same cells (fractional current inhibition = 0.95 ± 0.056).

Figure 4.5) Voltage clamp fluorometry shows that inhibition does not correlate with internalization: (a) *Left* – A model of the exGFP-CFTR protein shows the exofacial GFP tag in ECL4 of the McCarty et al. 2013 homology model of CFTR. *Right* – A model of the inGFP-CFTR constructed using CHIMERA v1.11.2 based on the unpublished cryo-EM structure of human CFTR. GFP tags are circled in red. (b) Fluorescence measured from oocytes expressing exGFP-CFTR was sensitive to a 30-second exposure to low extracellular pH. Representative background-subtracted voltage from the photomultiplier tube (PMT) during a short exposure to pH 5.5 recording solution is shown. (c) Perfusion of cells expressing the extracellularly-tagged GFP construct with an acidic recording solution led to reversible quenching while the fluorescence of cells expressing the intracellularly-tagged construct was unaffected in this time domain. (d) Cells expressing the intracellular or extracellular GFP-tagged CFTR variants showed significant fluorescence signal. (e) Treatment with 10 μg/mL SMase led to inhibition of currents (p=0.0012) while the pH-dependent fluorescence change was not significantly affected (p=0.4437, paired t-test).
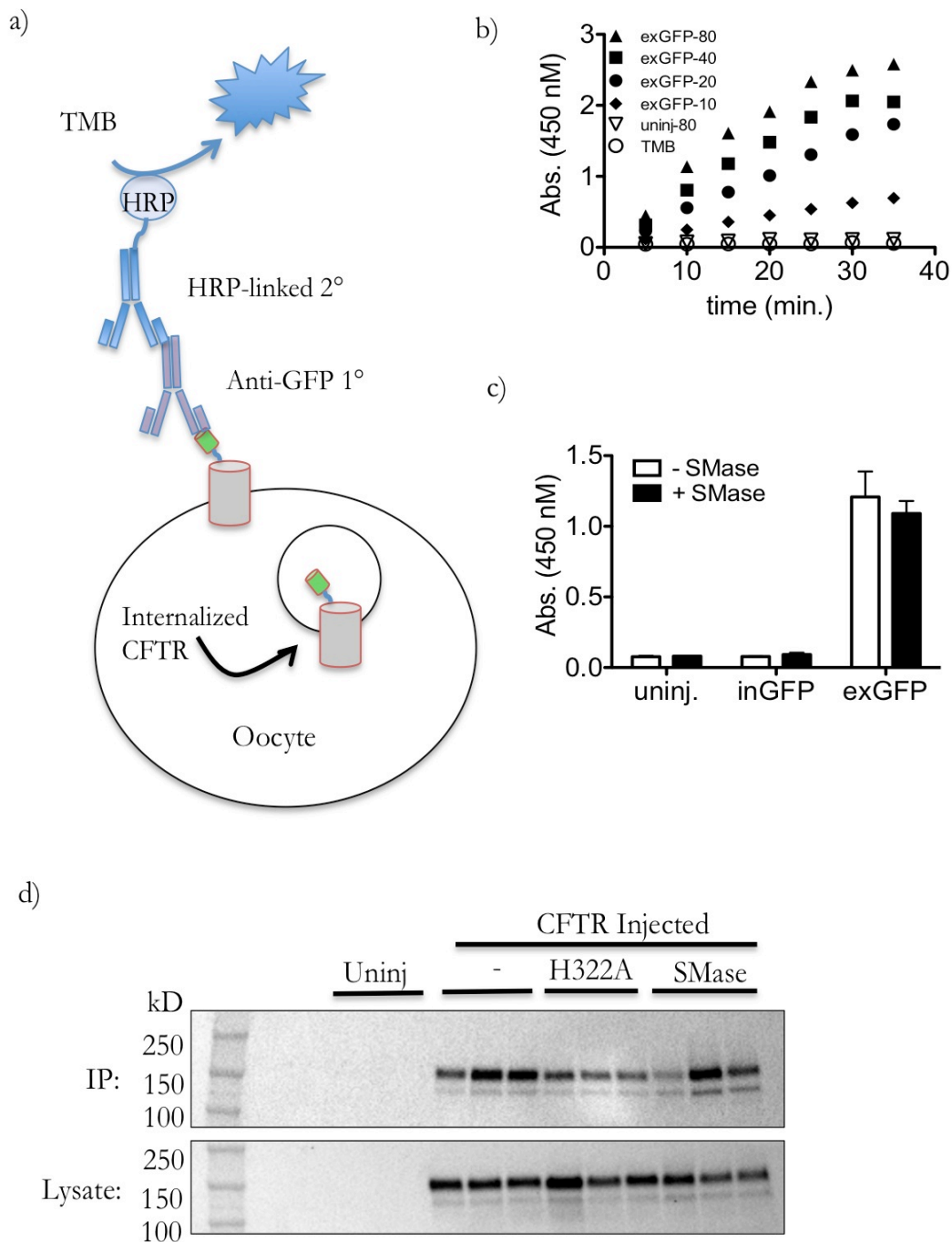
Figure 4.5) Voltage clamp fluorometry shows that inhibition does not correlate with internalization

a)

b)

c)

d)

e)
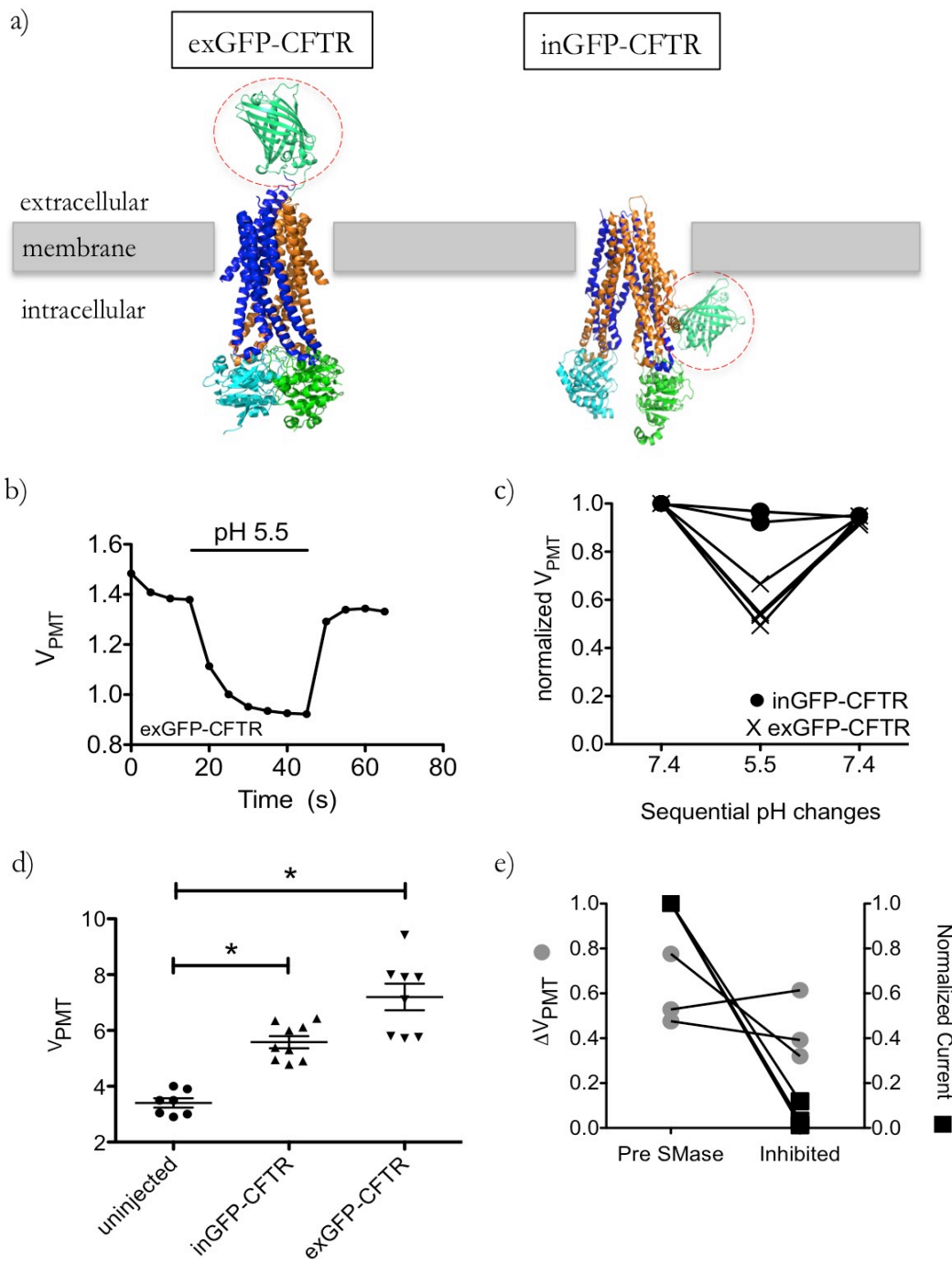
We verified this finding using cell-ELISA and biotinylation approaches (Fig. 4.6) (26). For the cell-ELISA experiments the relative surface expression of exGFP-CFTR on oocyte membranes was monitored via binding of a GFP primary antibody and subsequent development with an HRP-conjugated secondary antibody, and the colorimetric TMB substrate. As expected, signal was proportional to the number of exGFP-CFTR expressing cells tested and did not develop when uninjected or inGFP-CFTR cells were used (Fig. 4.6b, c). We found that pretreating cells with 10 µg/mL SMase for 10 minutes did not significantly affect the colorimetric signal indicative of exGFP-CFTR at the cell surface (Fig. 4.6c). Similarly, we found that SMase treatment did not significantly affect labeling of WT-CFTR with the cell impermanent biotinylation reagent sulfo-HNS-SS-biotin (Fig. 4.6d). These results suggest that SMase-mediated inhibition of CFTR does not arise from removal of CFTR proteins from the plasma membrane and instead prevents the normal gating of membrane-embedded channels.

Figure 4.6) Cell-ELISA and biotinylation confirm that SMase treatment does not facilitate CFTR internalization on the same time scale as inhibition: (a) Schematic of cell-ELISA experiment shows enzyme-linked immunolabeling of extracellular GFP in a live exGFP-CFTR-expressing oocyte. Internalized exGFP-CFTR is inaccessible due to the integrity of the plasma membrane. (b) Accumulation of colorimetric substrate in the cell-ELISA experiment is proportional to the number of exGFP-CFTR expressing cells in the well. In the figure, exGFP-# refers to the number of oocytes expressing exGFP-CFTR in each well of the plate. Uninjected cells did not produce any signal demonstrating that signal is specific for exGFP-CFTR. (c) Treatment with 10 μg/mL SMase for 10 minutes did not change the accessibility of the extracellular GFP on exGFP-CFTR. Uninjected cells and cells expressing inGFP-CFTR showed minimal signal following incubation with the TMB substrate (n=3). (d) Oocytes expressing WT CFTR were either untreated, treated with 10 μg/mL H322A SMase, or treated with 10 μg/mL WT SMase for 10 minutes before exposure to the membrane impermeant biotinylation reagent Sulfo-NHS-SS-biotin. This SMase treatment would be expected to decrease CFTR currents by ≥95%; however, it did not significantly change labeling of surface CFTR. Each lane represents an experimental replicate and uninjected oocytes ("uninj") were used as a control for antibody specificity.

Figure 4.6) Cell-ELISA and biotinylation confirm that SMase treatment doe not facilitate CFTR internalization on the same time scale as inhibition

a)

b)

c)

d)

Sensitivity to inhibition is modulated by IBMX concentration

Data to this point suggest that SMase inhibits CFTR activity by affecting channel gating so we next asked whether SMase preferentially affects an open or closed conformation of the channel. CFTR activity is controlled by the phosphorylation of its cytosolic regulatory domain (R-domain) and binding of ATP to the cytosolic nucleotide-binding domains (NBDs) (27; 28). R-domain phosphorylation by PKA and PKC occurs at several sites, but these sites are not apparently phosphorylated in random order and the consequences of phosphorylation at these sites are not equivalent; in fact, some phosphorylation events are inhibitory while most are stimulatory (29; 30) (31; 32). The cumulative effect of phosphorylation is graded activation of CFTR channel activity (33; 34). In the TEVC configuration, CFTR channel activity can be regulated by varying concentrations of the phosphodiesterase inhibitor IBMX in the presence or absence of forskolin (FSK). Consistent with previous reports, we found that increasing the IBMX concentration led to a dose-dependent increase in whole-cell (TEVC) currents wherein 0.01, 0.1, and 1.0 mM IBMX resulted in a fractional activity of 0.05 ± 0.01, 0.38 ± 0.07, and 0.94 ± 0.06, relative to 1 mM IBMX + 50 µM FSK (Figure 4.7a,b). Graded phosphorylation increases channel open probability (P_o) to a maximum of ~0.38 under normal conditions without changing open channel unitary conductance (27).

Lu and coworkers reported that SMase-mediated inhibition of CFTR in oocytes was reduced under strongly activating conditions, specifically in the presence of 50 µM FSK + 1 mM IBMX or with heterologous expression of the PKA catalytic subunit (2). The graded nature of phosphorylation-mediated activation of CFTR means that this effect could be due to either changes in phosphorylation itself, perhaps through a steric interaction related to

Figure 4.7) Inhibition is inversely proportional to cAMP-mediated activation of CFTR:
(a) An example trace shows the graded nature of CFTR channel function where total
cellular current increases with increasing IBMX concentration. Maximum current was
defined as that which was elicited by 1 mM IBMX + 50 µM FSK. (b) Summary data
show the fractional current elicited with each activation condition. (c) Summary traces
show the distinct kinetics associated with inhibition of channels by 1 µg/mL SMase
following activation with 0.01, 0.1, or 1.0 mM IBMX (n=4-5). (d) Summary data
showing that fractional inhibition at 10 minutes was dependent upon activation
condition (p=0.0003, 1-way ANOVA). (e) Addition of IBMX did not significantly
affect SMase activity as compared to the DMSO vehicle control (1-way ANOVA with
Dunnett's multiple comparison test, n=2-4) demonstrating that change in sensitivity is
due to effect on CFTR.

Figure 4.7) Rate of inhibition is inversely proportional to cAMP-mediated activation of CFTR
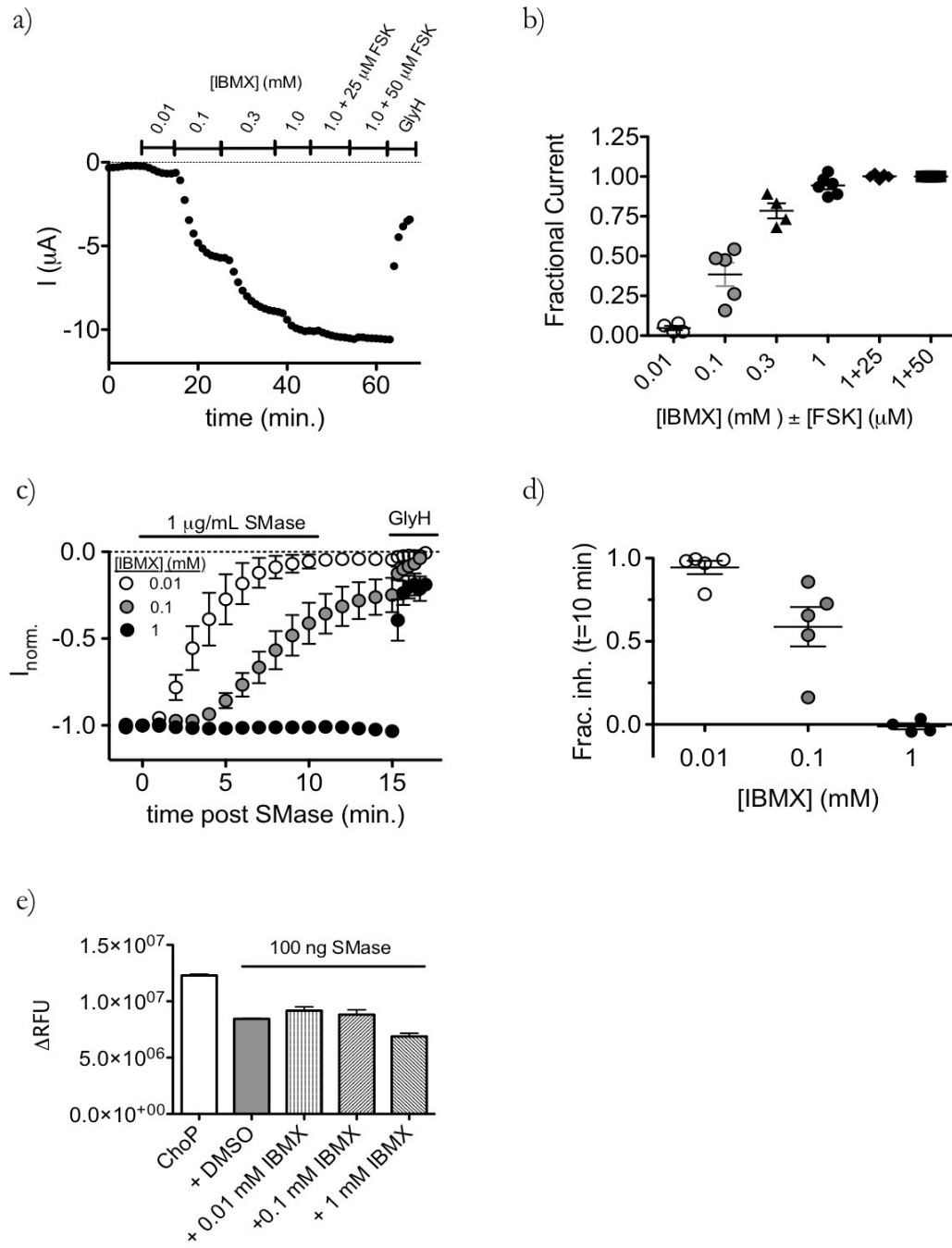
charge on the R-domain, or the increased channel open probability associated with strong phosphorylation. We also found that the rate and extent of inhibition by a ten-minute exposure to the intermediate concentration of 1 μg/mL SMase was sensitive to the concentration of IBMX used to activate CFTR (Fig. 4.7c,d). In our system, activation with 1 mM IBMX protected CFTR channels from inhibition by 1 μg/mL SMase while channels activated using 0.01 mM IBMX were rapidly inhibited. We verified that this effect did not result from direct inhibition of SMase by IBMX (Fig. 4.7e) and found that CFTR activated by exposure to forskolin alone was also inhibited by SMase (Fig. 4.8a). One important mechanistic observation reported by Ramu *et al.* was that the phosphorylation-independent CFTR variant lacking the R-domain, split-ΔR-CFTR, exhibited sensitivity to extracellular SMase, a result we have confirmed (Fig. 4.8b). This result suggests that PKA-mediated phosphorylation of the R-domain under strongly activating conditions does not protect CFTR channels from SMase-mediated inhibition via a direct interaction. Therefore, we hypothesized that SMase inhibits channels in a state-dependent manner wherein closed channels are affected and open channels are not.

Figure 4.8) FSK-activated WT CFTR and split-ΔR-CFTR are sensitive to SMase-mediated inhibition
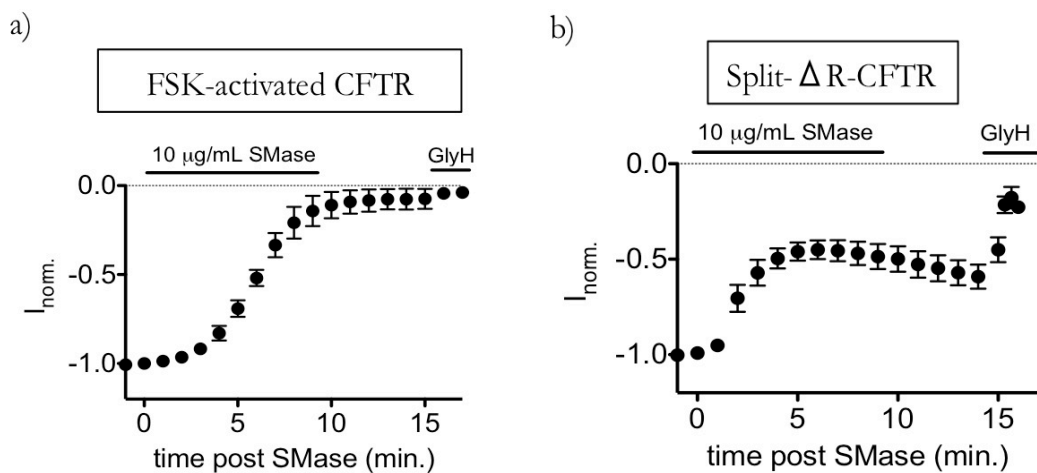
Figure 4.8) FSK-activated WT-CFTR and split-ΔR-CFTR are sensitive to SMase-mediated inhibition: (a) A summary TEVC trace showing inhibition of WT-CFTR following activation with 10 μM FSK alone, indicating that potential direct binding of IBMX to CFTR does not lead to the appearance of a state sensitive to SMase. Similarly, the presence of FSK is not leading to the result reported by Ramu et al. (n=3). (b) A summary TEVC trace shows inhibition of split-ΔR-CFTR by SMase at a high concentration (10 μg/mL, n=3).

Inhibition rate is inversely proportional to CFTR activity

To further separate the effects of phosphorylation from control of channel open state, we used a series of CFTR channel mutants known to vary in their relative occupancy of the full open state. If our hypothesis is correct, we predict that CFTR mutations that increase channel open probability (P_o, i.e. the proportion of time spend in the open state) should decrease sensitivity to inhibition by SMase in the presence of equal concentrations of IBMX. To test this hypothesis, we first compared the inhibition rate of WT-CFTR to that

of K1250A-CFTR. Lysine1250 plays an important role in ATP hydrolysis at ATP binding-site 2. Mutation to alanine increases the channel P_o by decreasing the rate of ATP catalysis and prolonging the mean burst duration (35; 36). As predicted, we found that K1250A-CFTR was less sensitive to inhibition than WT-CFTR in the presence of 0.1 mM IBMX (mean fractional inhibition = 0.01 ± 0.12 vs. 0.70 ± 0.17 for WT-CFTR, Fig. 4.9a,b) in cells studied in parallel. This result suggests that increasing the fraction of time that channels occupy the full open state protects against inhibition by SMase.

To ensure that this result did not arise from mutating the ATP binding site, we next compared the sensitivity of WT-CFTR to that of split-ΔR-CFTR. This construct has been shown to have constitutive activity with a relative open probability of approximately half that of highly phosphorylated WT channels, or P_o ~0.19 (37). If our hypothesis is correct, we would predict that split-ΔR-CFTR has a different sensitivity to SMase than WT-CFTR when the phosphorylation state of WT-CFTR is such that P_o is not 0.19. As expected, we observed constitutive chloride currents in cells expressing split-ΔR-CFTR that was indicative of phosphorylation-independent activity, but also noticed a small increase in current upon exposure of these cells to IBMX (data not shown). While the cause of this effect is not

Figure 4.9) Increased channel activity imparts resistance to SMase-mediated inhibition: (a, b) The ATP hydrolysis-deficient K1250A-CFTR mutant was resistant to inhibition by 1 μg/mL SMase (p<0.0001, unpaired t-test in parallel experiments). (c, d) The phosphorylation-independent variant split-ΔR-CFTR was less sensitive to inhibition by SMase than was WT-CFTR in the presence of 0.1 mM IBMX (p=0.034, unpaired t-test in parallel experiments). (e, f) Potentiation by VX-770 protected CFTR from inhibition by SMase (p=0.019, unpaired t-test in parallel experiments).

Figure 4.9) Increased channel activity imparts resistance to SMase-mediated inhibition
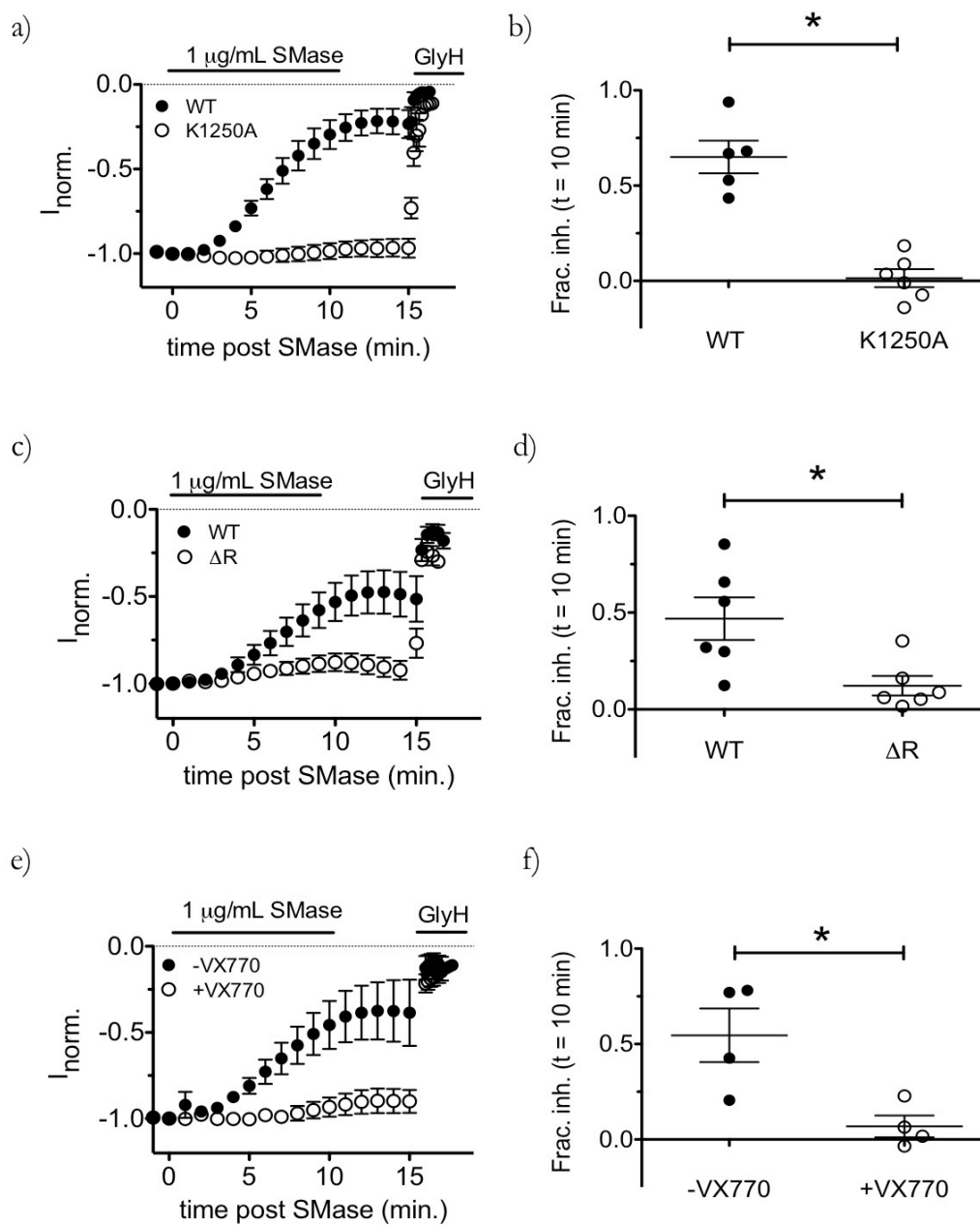
known, potentiation of split-ΔR-CFTR by PKA has been observed in excised inside-out

patches from *Xenopus* oocytes (37) and is indicative of a slight increase in channel P_o above

0.19. In our system, activation of WT-CFTR with 0.1 mM IBMX led to a fractional

activation of 0.38 ± 0.07 of maximum, leading to an expected P_o of ~0.14. Thus, we

predicted that split-ΔR-CFTR ($P_o > 0.19$) is less sensitive to inhibition than WT CFTR

activated with 0.1 mM IBMX ($P_o \approx 0.14$). Indeed, we found WT-CFTR was more sensitive

to the inhibitory effect of 1 μg/mL SMase than split-ΔR-CFTR under these conditions with

a fractional inhibition of 0.12 ± 0.12 for split-ΔR-CFTR vs. 0.46 ± 0.27 for WT-CFTR (Fig.

4.9c,d). As before, groups were measured in parallel in the same batch of oocytes. These

data are consistent with the idea that the insensitivity of K1250A-CFTR originates from its

high P_o.

  To ensure that the apparent desensitization of K1250A- and split-ΔR-CFTR did not

result from mutation of the channel, we next used VX-770 (Ivacaftor) as a pharmacological

approach to increase channel activity. VX-770 is a highly efficacious potentiator of CFTR

that increases P_o by increasing the opening rate and stabilizing the open burst duration (38;

39). Data presented thus far demonstrate that mutations in CFTR that increase gating

activity diminish the ability of SMase to inhibit channel activity, so we predicted that

potentiation of channel activity by VX-770 would also protect CFTR from SMase-mediated

inhibition. To test this, we activated WT-CFTR as before using 0.1 mM IBMX, potentiated

currents with 1 μM VX-770 ($\approx EC_{90}$) (38) and then treated with SMase. Consistent with

results obtained using mutants, channels that were pretreated with VX-770 were less

sensitive to SMase and showed a mean fractional inhibition of only 0.07 ± 0.056 vs. 0.54 ±

0.14 in untreated cells studied in parallel (Fig. 4.9e, f). Taken together, these data provide

evidence that SMase is less effective at inhibiting CFTR when channel activity is high and

suggest that SMase traps CFTR in a closed conformation.

Mutations that disrupt gating differentially affect inhibition rate

Numerous mutations have been shown to alter CFTR gating behavior through disruption of NBD dimerization and/or stability of the open pore. If SMase targets a closed state of CFTR, increasing the duration of time that channels spend in the target closed state should increase the sensitivity to inhibition by SMase. To test whether some well-characterized gating mutations increase the prevalence of the target state, we first determined the effect of the CF disease-associated mutation R117H on the sensitivity to SMase; the R117H mutation has been shown to disrupt gating behavior of CFTR by destabilizing both the pore and the NBD dimer (40). We found that R117H-CFTR was more sensitive to SMase-mediated inhibition than WT-CFTR studied in parallel with a fractional inhibition of 0.55 ± 0.14 versus 0.31 ± 0.14 for WT (Fig. 4.10a,b). These data suggest that the R117H mutation increases the occupancy of the state targeted by SMase.

Disrupting both NBD dimer stability and pore stability increases the total occupancy of multiple closed states (40). Specifically, destabilization of the pore leads to a "closed permissive" state in which the NBDs are dimerized but the pore cannot permeate chloride, while destabilization of the NBD dimer facilitates the pore closure that accompanies NBD dedimerization. Both of these states occur during normal CFTR gating, so to begin to determine whether SMase targets the closed permissive state we compared the sensitivity of D110R-CFTR channels to WT-CFTR channels. Mutations at D110 are well characterized as destabilizing the pore and thus increasing the occupancy of the closed permissive state

Figure 4.10) Mutations that disrupt channel gating had differential effects on sensitivity to SMase-mediated inhibition: (a, b) The R117H mutation, which disrupts both pore stability and NBD-dimer stability, increased sensitivity of CFTR to inhibition by SMase (p=0.0057, unpaired t-test in parallel experiments). (c-f) The D110R and R347D variants of CFTR were inhibited similarly to WT channels (p=0.348 and p=0.147, respectively, unpaired t-test in parallel experiments).

Figure 4.10) Mutations that disrupt channel pore gating have differential effects on sensitivity to SMase-mediated inhibition
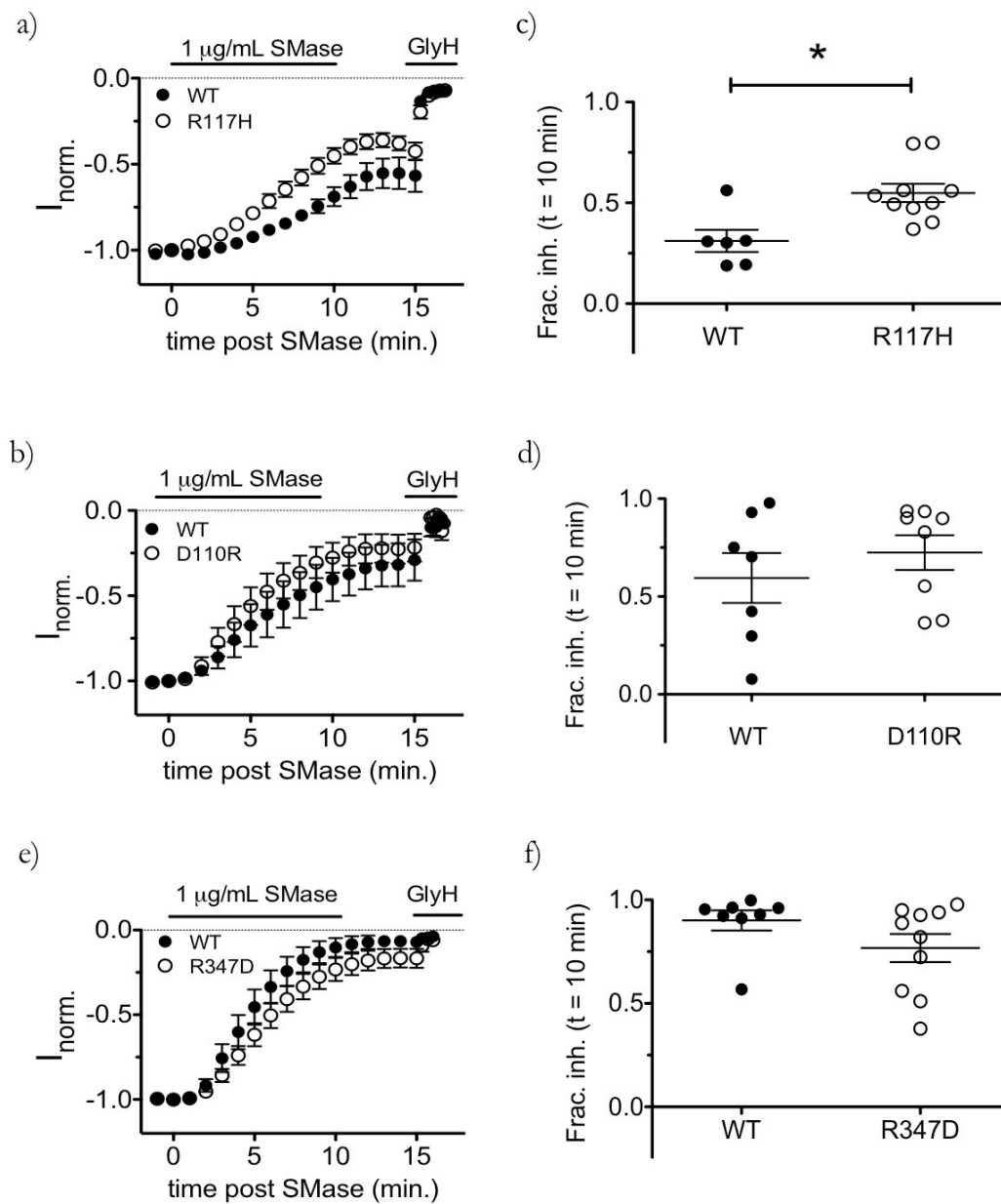
without appearing to impact NBD-mediated gating (41; 42). We found that D110R-CFTR channels were inhibited at a similar rate as WT-CFTR channels, with a fractional inhibition of 0.72 ± 0.25 versus 0.59 ± 0.34 for WT-CFTR channels studied in parallel (Fig. 4.10c,d). Consistent with published results, these data suggest that the D110R and R117H mutations have distinct deleterious effects on CFTR gating and that SMase targets an NBD-dedimerized closed state that occurs more frequently by the R117H but not the D110R mutation. To confirm this conclusion, we tested the sensitivity of R347D-CFTR, which destabilizes the open pore conformation by abolishing a salt bridge required for CFTR pore gating from the s1 substate to the full open state but maintains open durations similar to that of WT-CFTR, albeit in a substate (21; 43). Like D110R-CFTR, we found that R347D-CFTR was similar to WT-CFTR with a fractional inhibition of 0.77 ± 0.21 versus 0.90 ± 0.14 for WT-CFTR in parallel studies (Fig. 4.10e,f). Taken together, these results suggest that the R117H mutation, but not the D110R or R347D mutations, increases the occupancy of the SMase target state. Based on published data describing the defect associated with each mutation, these results suggest that SMase targets a closed state wherein the NBDs are dedimerized to inhibit CFTR chloride conductance.

We next performed a post-hoc analysis to ensure that the difference in magnitude of inhibition we observed with each mutant did not result from differences in expression level. Figure 4.11 shows that total whole-cell current for each of the groups discussed does not correlate with their relative sensitivities to inhibition (Fig. 4.11a-d). Additionally, the resistance imparted by VX-770 pretreatment did not result from direct inhibition of SMase by the potentiator as measured using the fluorometric assay (Fig. 4.11e). These control analyses support our conclusion that the differential sensitivity of mutant and potentiated channels that we tested results from changes in gating activity and not from changes in channel abundance.

Figure 4.11) Sensitivity is not proportional to current amplitude
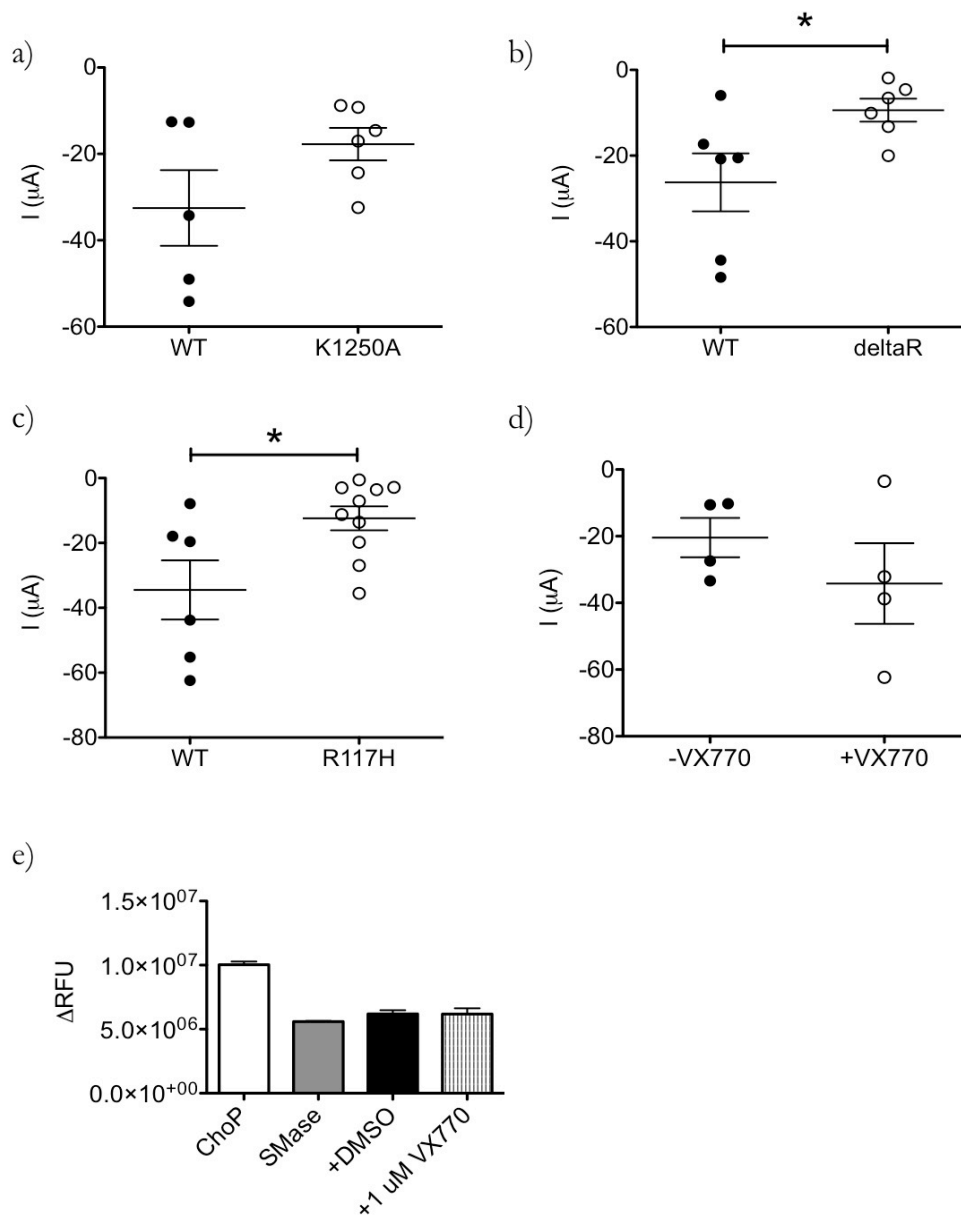
Figure 4.11) Sensitivity is not proportional to current amplitude: (a) Total current magnitude of WT and K1250A-CFTR expressing cells was not different. (b) Cells expressing WT-CFTR showed significantly more current than cells expressing split-ΔR-CFTR, but WT-CFTR currents were more sensitive to SMase (Fig. 14b, c). (c) Cells treated with VX-770 did not have significantly more current than untreated cells. This was achieved by reducing expression level in VX-770 treated cells. (d) Current magnitude of R117H-CFTR expressing cells was slightly lower than that of WT-CFTR cells. Given the gating defects associated with the R117H mutation that reduce the activity of this mutant, this likely represents a similar expression level. (e) SMase was not significantly inhibited by 1 μM VX-770 in the Amplex Red SMase assay (1-way ANOVA with Dunnett's multiple comparison test, n=4).

Murine, Cysless, and ΔPDZ CFTR are sensitive to SMase

In an effort to determine whether specific residues were involved in SMase-mediated inhibition of CFTR, we screened three functional CFTR variants. The rationale behind this blind screening was that if a particular residue is required for inhibition, mutation of that residue should abolish the effect of SMase on channel activity. For example, this might occur if inhibition resulted from a site-specific post-translational modification. The first variant that we tested was murine CFTR, which shares 78% sequence identity with human CFTR and showed clear inhibition with perfusion of SMase (Figure 4.12a). This suggests that none of the differing residues are required for inhibition to occur. We next tested cysless CFTR, a construct in which all 18 cysteines have been mutated to either alanine (16/18) or leucine (2/18) (44). The state of cysteines can be dynamically controlled at physiologic pH and therefore we hypothesized that inhibition might results from modification of an endogenous cysteine. Like murine CFTR, however, we found that the cysless CFTR is inhibited by SMase leading us to conclude that acute modification of an endogenous cysteine is not involved in SMase-mediated inhibition of CFTR (Fig. 4.12b).

CFTR is also modulated by interactions with other proteins that are facilitated by its C-terminal PDZ binding domain. PDZ-dependent interactions have been shown to control CFTR trafficking, membrane dynamics, and, to some extent, ion channel activity (45-49). To determine whether SMase-mediated inhibition resulted from a PDZ-dependent process, for example binding of an inhibitory protein, we tested whether a CFTR construct lacking the C-terminal D-T-R-L motif (ΔPDZ-CFTR) could be inhibited by SMase. Indeed, we found that ΔPDZ-CFTR was sensitive to inhibition by SMase (Fig. 4.12c).

Figure 4.12) Inhibition of murine-, cysless-, and ΔPDZ-CFTR by SMase
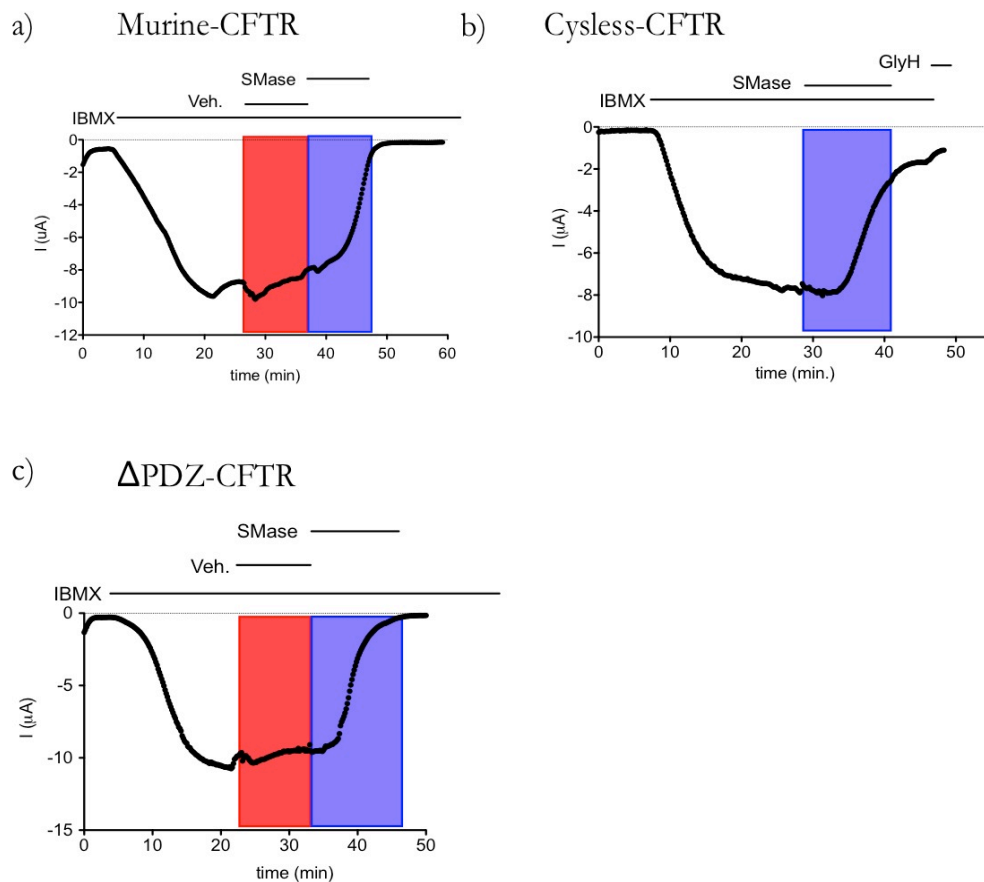

a) Murine-CFTR

b) Cysless-CFTR

c) ΔPDZ-CFTR

Figure 4.12) Inhibition of other CFTR variants by SMase: Example traces show inhibition of multiple variants of CFTR. In all cases, currents were elicited with 0.1 mM IBMX and SMase was perfused for 10 minutes as indicated by the blue box. Sensitivity of murine cysless and ΔPDZ-CFTR inform about residues that are not essential for inhibition.

SMase prevents potentiation by VX-770

Ivacaftor (VX-770) is prescribed to some CF patients over the age of 2 while bacterial infections are often measured in the first year of life, so it is likely that pulmonary epithelial cells are exposed to SMase before the patient may take VX-770. VX-770 has been shown to increase the opening rate and stabilize the open state of CFTR while data presented to this point suggest that SMase locks CFTR channels into a closed state. To better understand the potential interaction of these two CFTR modulators, we asked whether the inhibition elicited by SMase could be reversed by treatment with VX-770. In the absence of SMase, a two-minute exposure to 1 μM VX-770 (~EC_{90}) potentiated CFTR currents by 10-fold when channels were activated with 0.1 mM IBMX (Fig. 4.13a, d). However, we found that VX-770 was unable to fully restore currents following inhibition by SMase. Exposing SMase-treated channels to 1 μM VX-770 restored a small fraction of the current (0.01 ± 0.01, Fig. 4.13b-d) compared to the original IBMX-stimulated current amplitude. These data demonstrate that the effect of SMase is not immediately reversible by VX-770 and suggest that inhibition by SMase results in channels locked into a conformation that is not affected by VX-770, effectively removing channels from the druggable pool.

Figure 4.13) SMase pretreatment diminishes the effect of VX-770
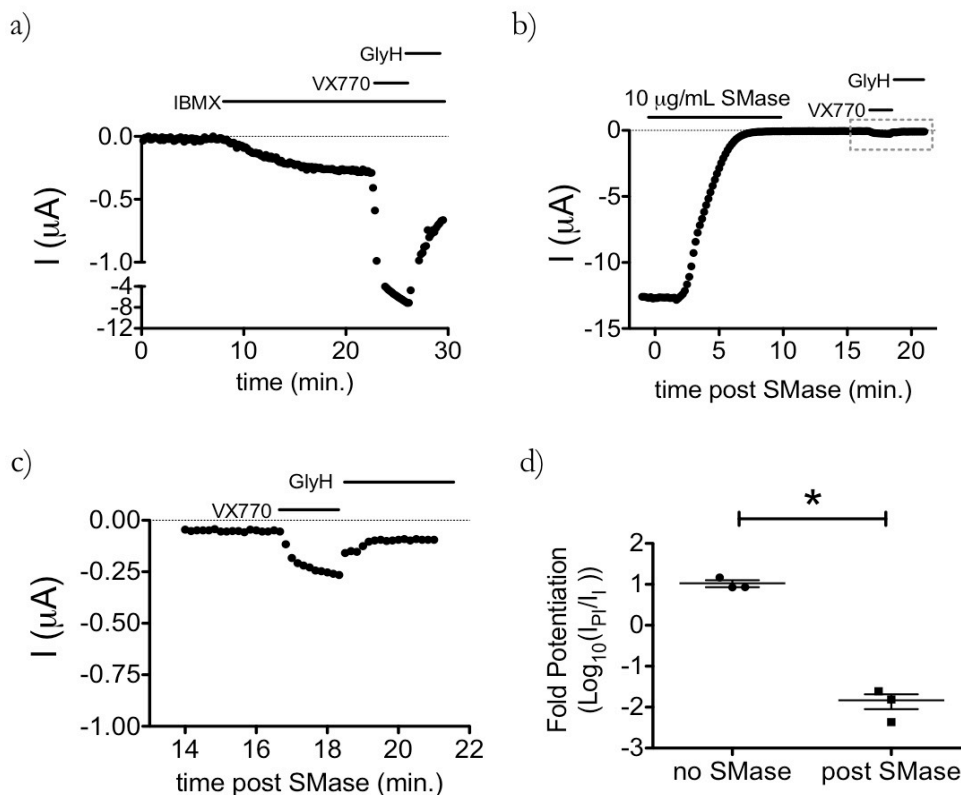
Figure 4.13) SMase pretreatment diminishes the effect of VX-770: (a) Application of VX-770 to WT-CFTR channels activated with 0.1 mM IBMX led to a 10.6 ± 3.6-fold increase in current in 2 minutes. (b) An example trace showing that 1 μ M VX-770 led to a fractional recovery of only 0.01 ± 0.01 when applied after currents were inhibited by SMase. (c) Expansion of the area denoted by the grey box in part B shows details of VX-770-mediated potentiation kinetics. (d) Summary data showing that the effect of VX-770 on CFTR currents was diminished following inhibition by SMase as compared to IBMX-stimulated currents alone (p=0.007, unpaired t-test): I_{PI} is the current elicited by VX-770 + IBMX, I_I = is the initial current elicited by 0.1 mM IBMX.

Basolateral SMase diminishes transepithelial currents in NHBEs

We next asked whether SMase treatment affects transepithelial currents in primary human bronchial epithelial cells. To test this, we treated primary NHBEs expressing WT CFTR with 1 µg/mL SMase for 30 minutes and activated currents using FSK. Because SMase inhibited currents more effectively at low activity levels in *Xenopus* oocytes, we tested multiple activation levels of CFTR by increasing the FSK concentration in a stepwise fashion to gradually increase phosphorylation. While apical application of SMase did not significantly affect currents (Fig. 4.14a, b), we found that NHBEs treated basolaterally with SMase conducted significantly less current than the control filters treated with H322A SMase (Fig. 4.14c, d). This differential sensitivity of epithelia to SMase has been reported in both Calu-3 and T84 epithelial cell lines (3; 50) and suggests the presence of either polarization-dependent accessibility of sphingomyelin or basolateral-specific signaling networks (see Discussion). Interestingly, we observed a larger fractional inhibition at 10 and 100 nM FSK (area demarcated by the grey hatch marks in Fig. 4.14c) than at 100 µM FSK (Fig. 4.14e), consistent with the inverse relationship between channel activity and SMase-mediated inhibition observed in our *Xenopus* oocyte experiments. We also observed inhibition of currents under maximally activating conditions, namely in the presence of >10 µM FSK and 1 µM VX-770. Prolonging the incubation of 1 µg/mL SMase on the apical surface to 18 hours (overnight) did not lead to an effect (Fig. 4.15), which suggests that the apical surface is inherently resistant to this effect.

Figure 4.14) Basolateral treatment with SMase diminishes transepithelial currents in human bronchial epithelial cells: (a) Example trace showing similar activation of transepithelial current in NHBEs expressing WT-CFTR following apical pretreated with either WT or H322A SMase. Scale bars represent 20 μA/cm^2 and 20 minutes. (b) Summary data showing that there was no difference in transepithelial currents following apical SMase treatment. (c) An example trace showing that pretreatment with basolateral WT SMase diminishes FSK-stimulated transepithelial currents in NHBEs expressing WT CFTR. Scale bars: 10 μA/cm^2, 10 mins. (d) Summary data showing significant difference in current amplitudes following basolateral WT SMase (p>0.0001, 2-way ANOVA). Table: summary of p-values for basolateral application

Figure 4.14) Basolateral treatment with SMase diminishes transepithelial currents in human bronchial epithelial cells

a) Apical SMase

c) Basolateral SMase

p-values (Basolat.)	[FSK]	SMase Treatment
Apical	<0.0001	0.4241
Basolateral	<0.0001	<0.0001

e)
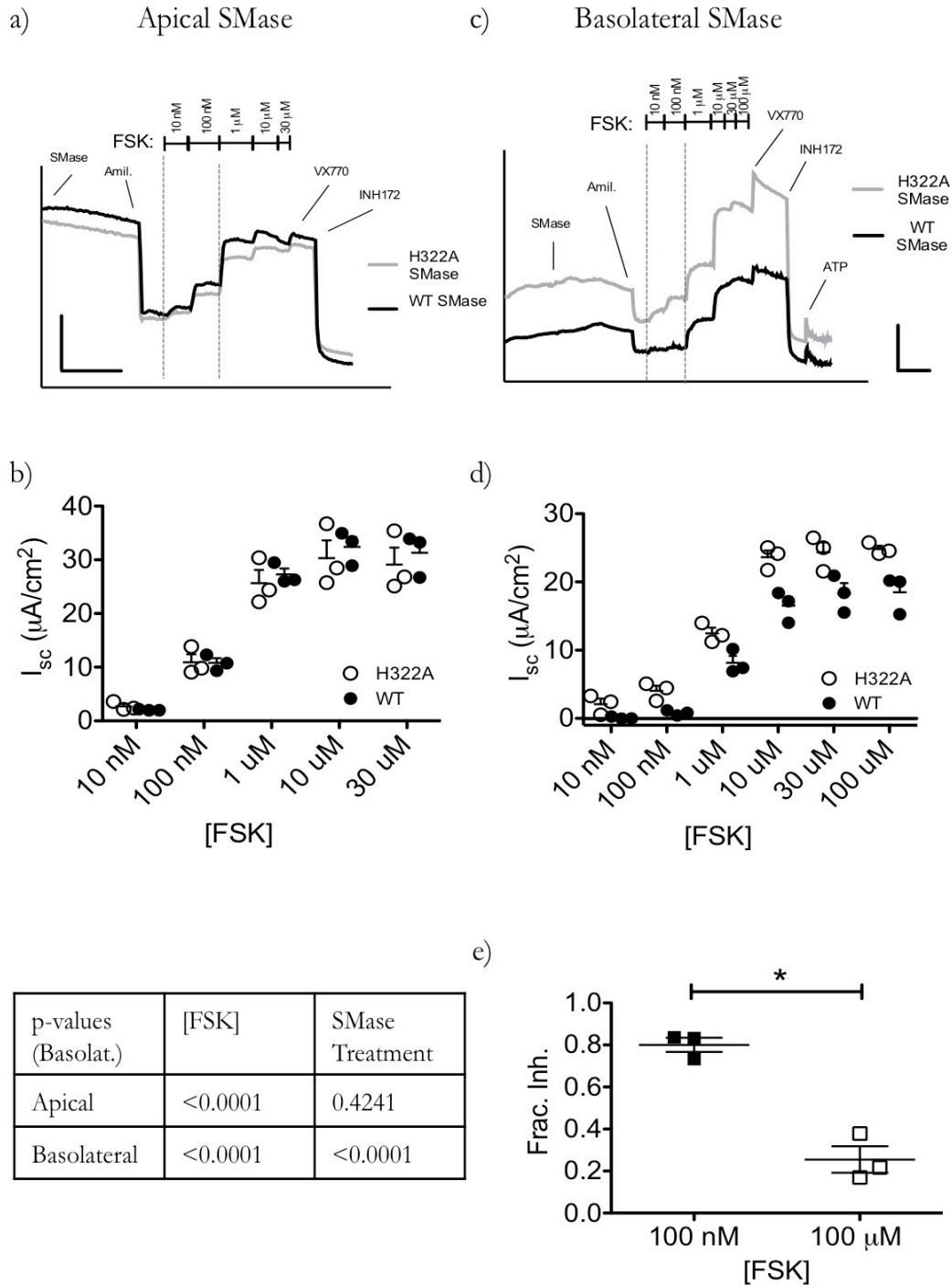
Figure 4.15) Incubation of SMase overnight on NHBE cells does not affect currents

a)

Overnight Apical SMase Trace

b)

Overnight Apical SMase Summary
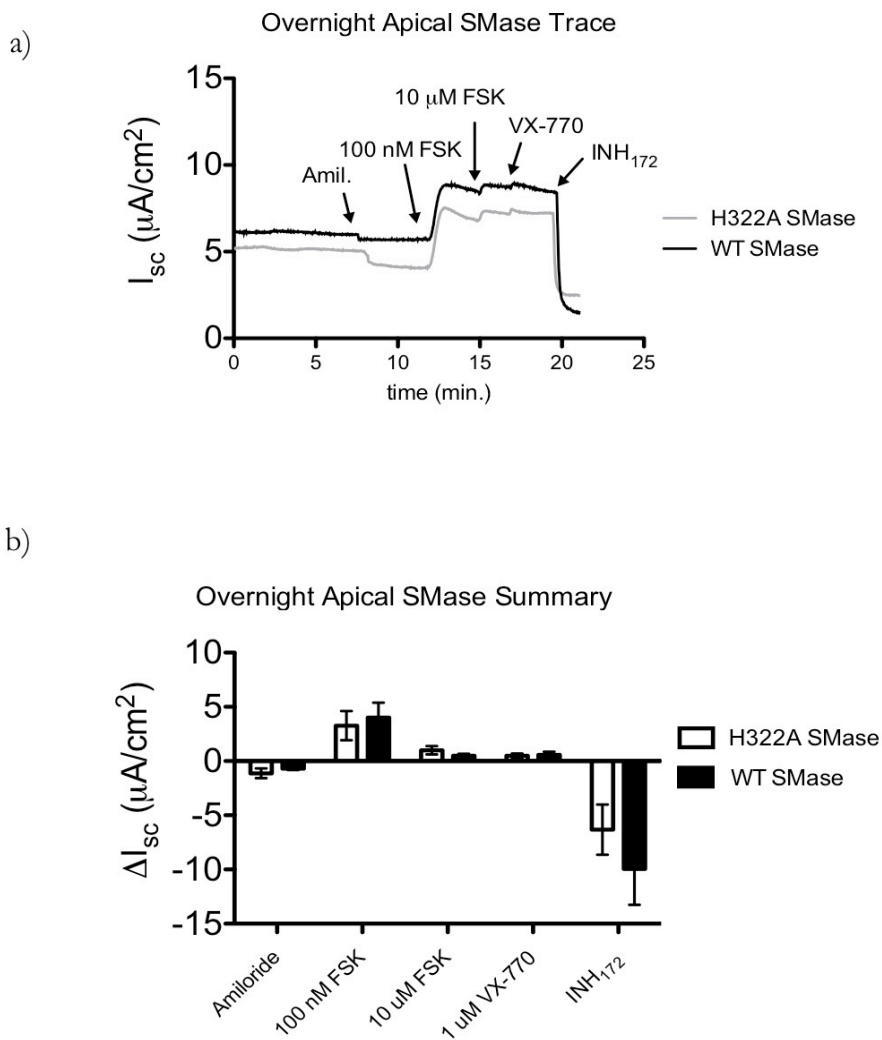
<u>Figure 4.15) Incubation of apical SMase overnight on NHBE cells does not affect currents</u>: (a) An example trace shows that an overnight incubation of 1 µg/mL SMase on the apical surface of NHBEs does not affect currents activated by 100 nM or 10 µM FSK. (b) Summary data, mean±SEM, n=5.

We next asked whether F508del CFTR homozygous CFHBEs exhibit the same sensitivity to SMase. In the absence of correction by either low temperature incubation or the small molecule corrector VX-809, CFHBEs showed no FSK- or VX-770-stimulated currents (Fig. 4.16a, b) (51; 52). Consistent with our observations in the NHBEs, we observed significant current inhibition, even in the presence of 100 μM FSK and 1 μM VX-770 (Fig. 4.16c, d). The small magnitude and lack of clear stepwise activation in these cells at low FSK concentrations made it difficult to quantify inhibition in the presence of low FSK; however, like in the NHBEs, we observed significant inhibition of currents under maximally activating conditions (>10 μM FSK + 1 μM VX-770; Fig. 4.16d).

Figure 4.16) Basolateral SMase diminishes transepithelial currents in F508del homozygous CFHBEs

a)

FSK: 10 nM 100 nM 1 μM 10 μM 30 μM 100 μM

SMase

VX770

INH172

Uncorrected CFHBEs

b)

1 μM VX770

10 μM FSK

100 nM FSK

INH172

Amil.

DMSO
VX-809

VX-809 Corrected

c)

FSK: 10 nM 100 nM 1 μM 10 μM 30 μM 100 μM

SMase

VX770

INH172

H322A SMase

WT SMase

Temperature Corrected

d)

ΔIsc (μA/cm^2) (100 μM FSK+1μM VX-770)

Pretreatment :
● H322A SMase
● WT SMase

NHBE   CFHBE   CFHBE (27°C)
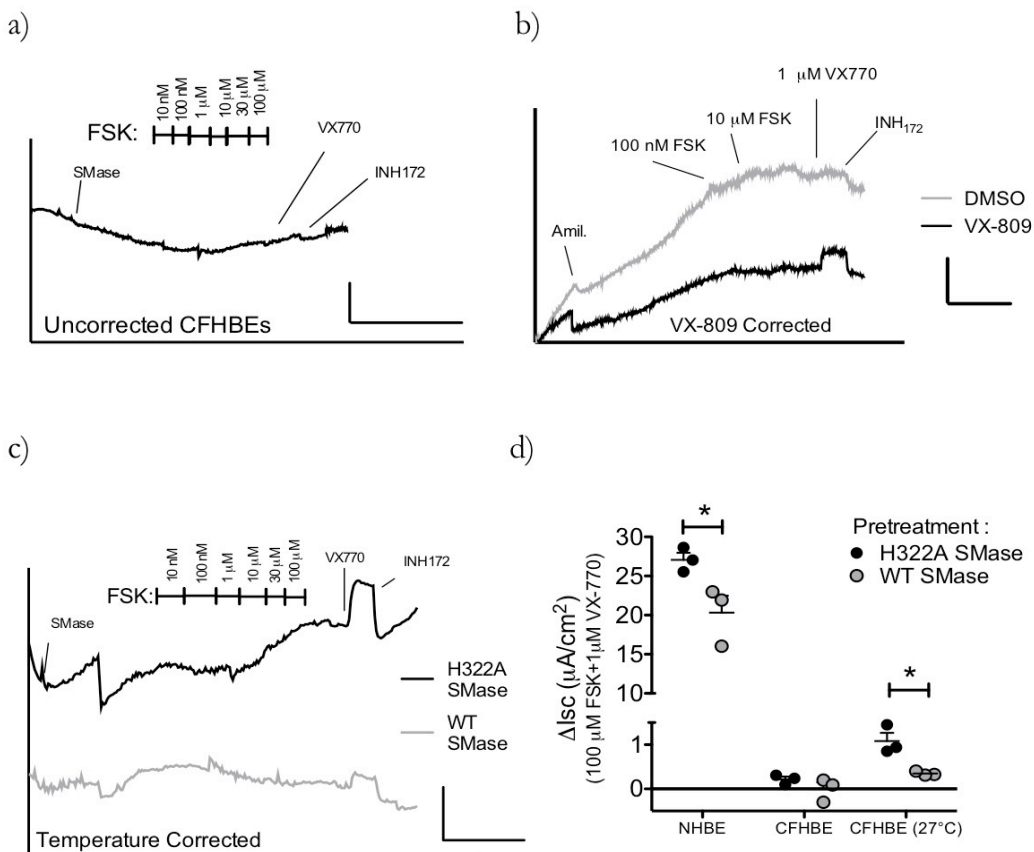
Figure 4.16) Basolateral SMase diminishes transepithelial currents in F508del homozygous CFHBEs: (a) An example trace showing that uncorrected F508del CFHBEs do not show FSK- or VX-770-stimulated currents, consistent with a lack of functional F508del CFTR at the cell surface. Scale bars: 2 μA/cm^2 and 50 minutes. (b) Example trace shows that CFHBEs corrected with 3 μM VX-809 showed a similar phenotype to the temperature corrected CFHBEs. Scale bars: 2 μA/cm^2 and 5 minutes. (c) An example trace showing that pretreatment of temperature-corrected CFHBEs with basolateral SMase leads to a reduction in maximal current that is similar to that seen in NHBEs. Scale bars: 2 μA/cm^2, 20 mins. (d) Summary data showing that basolateral treatment with WT SMase reduces currents elicited by 100 μM FSK + 1 μM VX-770 (NHBE p=0.04, CFHBE-27°C p=0.02; t-test).

Multiple groups using different epithelial cell systems have shown that basolateral SMase treatment affects ion channel function while apical treatment does not, and the reason for this discrepancy is currently unknown (3; 50). Data from early studies of sphingomyelin trafficking in epithelial cells suggest that it is present in both apical and basolateral membranes (53) so we hypothesized that the differential effect was the result of differences in sphingomyelin accessibility. To test this we used an mCherry sphingomyelin binding protein (non-toxic Lysenin) to ask how SM abundance changes following unilateral SMase treatment in primary NHBEs (54). Figure 4.17 shows that this construct is quite specific, and signal in unpolarized Calu-3 cell monolayers is reduced following WT SMase treatment. When NHBE cells were stained with purified mCherry-lysenin and imaged using confocal microscopy, we observed a homogenous staining with continuous labeling of the apical to the basolateral membrane (Fig. 4.18a). This staining pattern was also seen following pretreatment of the apical surface with SMase (Fig. 4.18b). However, basolateral SMase treatment reduced basolateral staining and led to a discontinuous and irregular pattern with the appearance of void spaces (Fig. 4.18c). Plots of mean fluorescence along the z-axis shows a depth-dependent decay in red signal that is not seen in the untreated and apically treated monolayers (Fig. 4.18d). This result suggests that only basolateral treatment leads to a marked change in sphingomyelin dynamics and distribution and offers a possible explanation to the differential effect of SMase treatment seen by us and others in the Ussing Chamber.

Figure 4.17) mCherry-NT-lysenin is a specific sphingomyelin probe
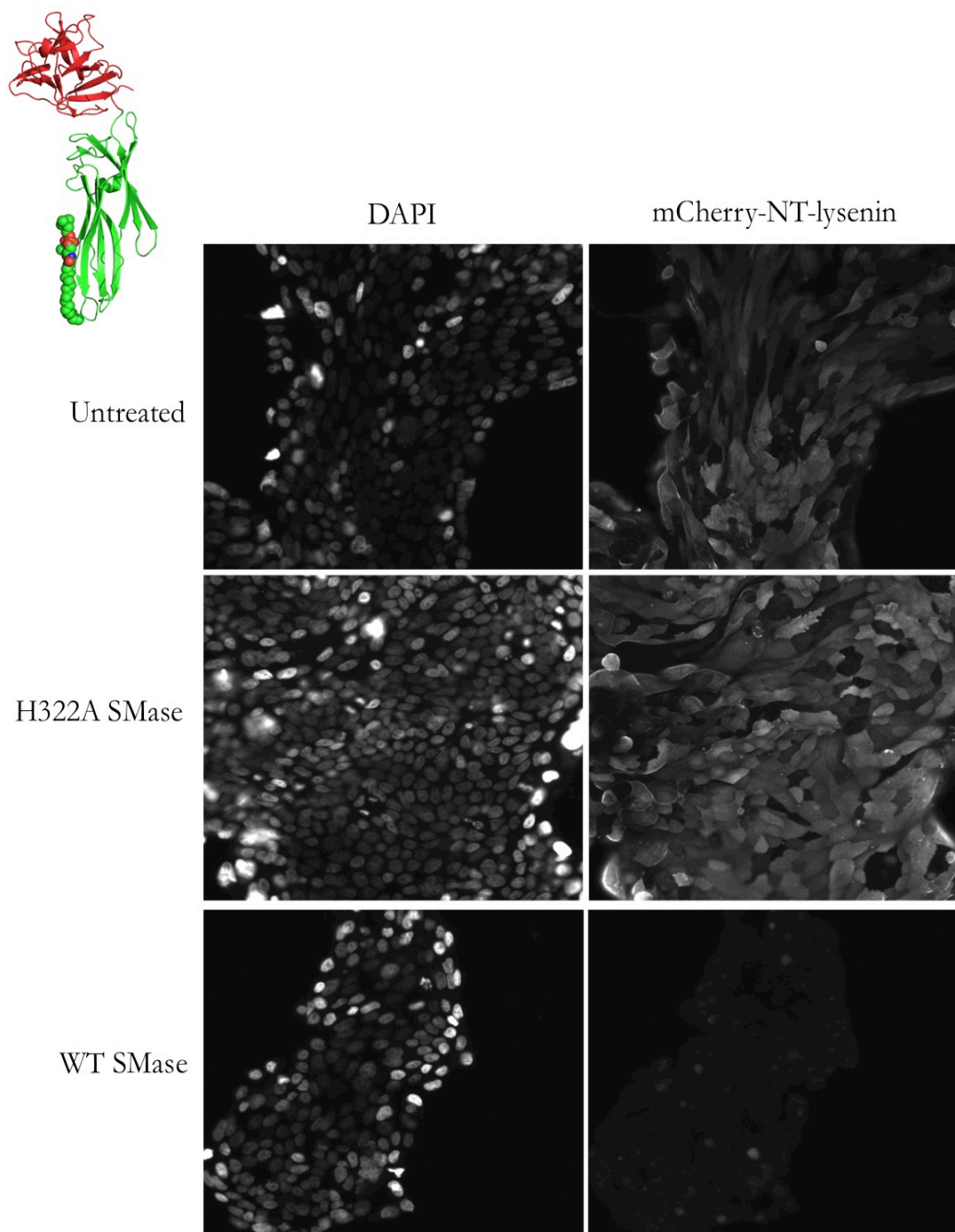
Figure 4.17) mCherry-NT-lysenin is a specific sphingomyelin probe: *Top left* – crystal structure of full length lysenin bound to sphingomyelin (PDB 3zxg). When conjugated to a fluorophore, the nontoxic (NT) phosphocholine-binding domain of lysenin (red) can be used as a sphingomyelin probe(54). *Bottom right- S*taining the Calu-3 epithelial cell line with mCherry-NT-lysenin (shown as greyscale) labels the cell membrane. Preincubation with WT SMase but not H322A SMase diminishes binding of the probe. The mCherry-NT-lysenin construct was provided by the RIKEN BRC through the National Bio-Resource Project of the MEXT, Japan.

Figure 4.18) Asymmetrical effect of SMase treatment on sphingomyelin distribution in primary NHBEs
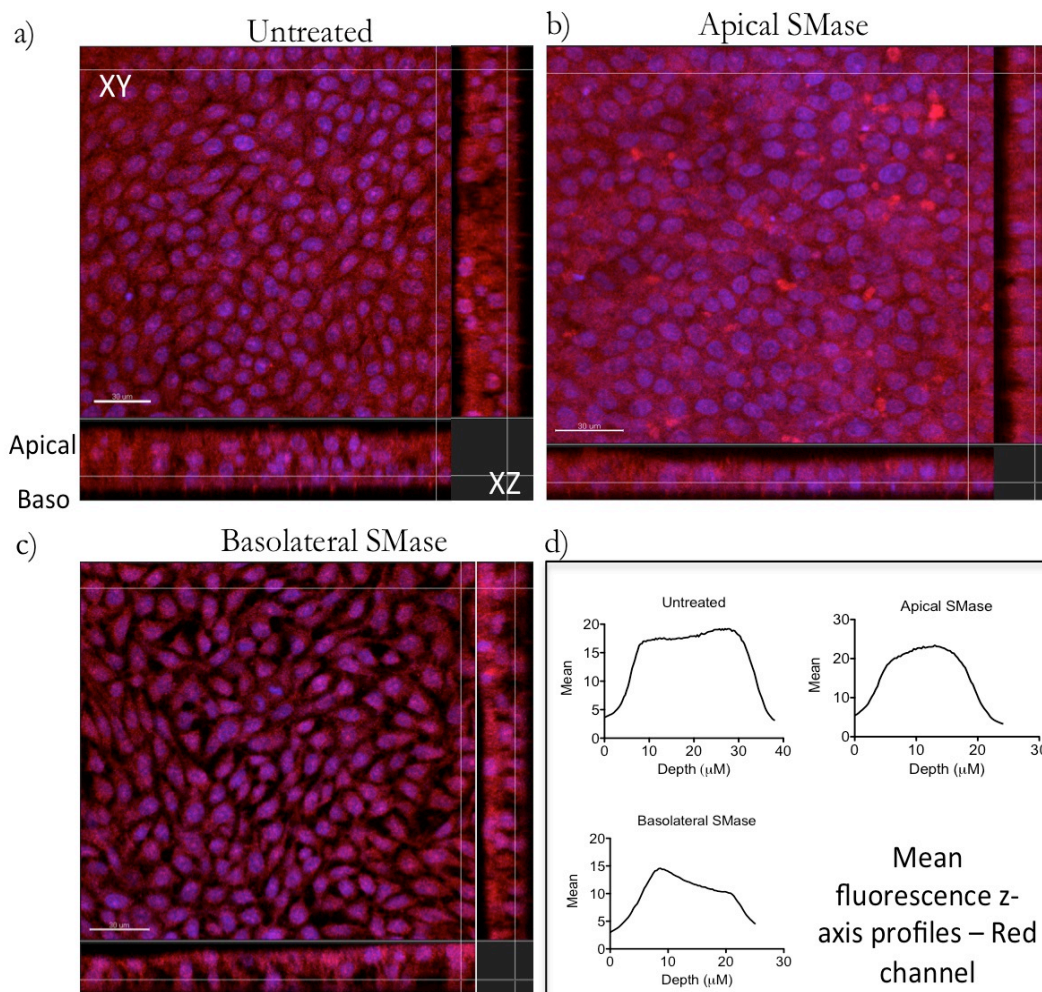
Figure 4.18) Confocal microscopy shows an asymmetrical effect of SMase treatment on sphingomyelin distribution in primary NHBEs: (a) Staining HBEs bilaterally with the sphingomyelin probe mCherry-lysenin (pseudocoloered as red, DAPI is shown as blue) results in fluorescence localized on both apical and basolateral sides. (b) Similar continuous bilateral staining can be seen in cells pretreated with apical SMase. (c) Basolateral SMase treatment results in reduced staining of the basolateral membrane and leads to an irregular fluorescence pattern. (d) Mean intensity z-axis profiles of the red channel show a depth-dependent decay in signal in the basolateral treated cells that is not apparent in the untreated or apically treated cells. Note: profile begins on the apical side and moves toward the basal side.

4.1.3) *Discussion*

Bacterial virulence factors could influence the progression of CF and COPD by altering pulmonary epithelial ion channel physiology. In this study, we began to characterize the inhibitory effect of sphingomyelinase C (SMase) on the chloride channel function of CFTR in two systems. We presented evidence that SMase is a novel gating modifier of CFTR that inhibits membrane embedded channels in *Xenopus* oocytes without relying on catalysis of CFTR-associated sphingomyelin or internalization of the channel. Our results using mutant channels suggest that SMase inhibits currents by affecting closed channels in such a way that they cannot reopen. Finally, we found that basolateral pretreatment with SMase, but not apical treatment, decreased FSK- and VX-770-stimulated currents in primary NHBEs.

SMase can influence the function of integral membrane proteins either by modulating direct lipid-protein interactions or by altering cellular signaling (4; 8; 50; 55). Our data suggest that the inhibitory effect of SMase on CFTR function in *Xenopus* oocytes relies on a mobile signaling molecule and does not result from cleavage of annular sphingomyelin. This is supported by the observation that SMase inhibited channels that were isolated from the enzyme in the cell-attached configuration while channels in excised patches were not inhibited when SMase was backfilled into the recording pipette. While our data do not rule out the possibility that inhibition occurs through a direct lipid-CFTR interaction, they do open the extremely interesting possibility that CFTR channel activity may be modulated by an uncharacterized post-translational modification because the effect does not rely on the R-domain and requires a cytosolic signal. Inhibition also occurs independent of the PDZ domain or and cysteines suggesting dynamic regulation of another

channel motif.

It remains to be seen which sphingolipid is responsible for the observed inhibition by SMase. Given that ceramide is expected to be the most abundant product in the membrane, we believe that it is the most likely effector. Ramu and coworkers began to test this possibility in oocytes by adding C8-ceramide to the recording chamber. After observing no change in CFTR current, they concluded that ceramide signaling was not responsible for inhibition. One potential issue with this approach stems from the observation that ceramide-mediated signaling can be highly dependent on acyl chain length (56) and C8-ceramide makes up a small fraction of ceramide in the *Xenopus* oocyte with the predominant species being long chain C16 and C18 ceramides (57). Ceramide can also be subsequently metabolized into other active signaling molecules to influence cellular physiology, for example ceramide 1-phosphate, sphingosine, and sphingosine 1-phosphate, so it is possible that one of these other sphingolipid species is responsible for the observed inhibition. This complex series of metabolic transformations ultimately leads to "metabolic ripple effects," as described by Hunnan and coworkers (58), and elucidating the sphingolipid species responsible for SMase-mediated inhibition of CFTR will provide valuable mechanistic insight into this novel regulatory mechanism.

Ramu and coworkers provided some intriguing mechanistic information that suggested SMase was a novel gating modifier of CFTR and, indeed, our data provide direct evidence that SMase is a state-dependent inhibitor of CFTR. This is supported by the observation that sensitivity to inhibition is influenced by channel gating kinetics. The K1250A mutation, which slows channel closure, and VX-770 pretreatment impart resistance to the inhibitory effect of SMase as compared to normally gating WT-CFTR channels.

Additionally, the R117H mutation, which accelerates channel closure in two distinct ways (40), increases the sensitivity of channels to inhibition by SMase. Our observation that D110R and R347D-CFTR are inhibited similarly to WT-CFTR leads us to hypothesize that SMase affects an NBD-dedimerized closed state of CFTR. Whether sensitivity to SMase requires loss of ATP or ADP from the ATP-binding sites following NBD dedimerization remains to be determined.

Our observation that basolateral SMase diminishes FSK-stimulated currents in primary NHBEs suggests that sphingolipid metabolism is functionally linked to CFTR in mammalian epithelial cells as well as in *Xenopus* oocytes. Several other studies have linked CFTR activity to sphingolipid metabolism in mammalian cells as well and the details of this potential pathway interaction have yet to be fully elucidated (59-64). Consistent with published results (3; 50), we found that only basolateral application of SMase affected ion channel activity in polarized epithelial cells and presented evidence that suggests this unilateral sensitivity results from differential sphingomyelin accessibility. It is also possible that apical sphingomyelin may simply be replaced more rapidly so treatment does not affect overall sphingolipid homeostasis. This remains to be seen; however, it is interesting that the unilateral effect of SMase on mCherry-NT-lysenin binding correlates so well with the functional affects presented here. Whether bacterial SMase can access the basolateral side of epithelial cells remains to be seen, though recent reports suggest that CFHBEs have dysfunctional tight junction trafficking that might enable the movement of proteins across the epithelium (65). Grassme and colleagues have also shown that lymphocytes translocate acid-SMase to the plasma membrane following activation, which opens up the possibility that transmigrating immune cells might influence the local epithelial ion channel function through this mechanism (66).

The influence of bacterial SMase on the prognosis of CF and COPD has not been clearly defined, but numerous observations suggest that SMase is a functionally conserved virulence factor that influences the pathogenicity of multiple bacteria. For example, SMase from *S. aureus* gets upregulated upon instillation into the murine lung (67), likely through the mobilization of an inactivating phage (68-70), where it can facilitate inflammatory lung damage (71). Multiple groups have shown that *B. cereus* SMase decreases macrophage phagocytosis and increases mortality in murine and ovine models of infection (72; 73). Wargo and coworkers implicated *P. aeruginosa* SMase (PlcH) in the reduction of lung function associated with bacterial instillation, though this effect cannot be directly linked to SMase activity because PlcH also hydrolyzes phosphatidylcholine (74; 75). What evolutionary benefit might stem from SMase-mediated inhibition of CFTR by bacteria? One possibility is that loss of CFTR function could slow epithelial-mediated bacterial clearance. This could occur through a reduction in ASL height and mucocilliary clearance because CFTR-mediated chloride conductance is the primary regulator of pulmonary epithelial secretion (76; 77). Functional CFTR has also been implicated in bacterial endocytosis by epithelial cells (78) an early innate immune response that is thought to contribute to clearance of low-grade bacterial infections. Finally, CFTR-mediated bicarbonate secretion is important for the activity of small-antimicrobial peptides, which are less effective following loss of CFTR and acidification of the airway (79). These results suggest that understanding the impact of SMase activity on CFTR function may be relevant to the treatment of CF.

Works Cited:

1.   Elborn JS. 2016. Cystic fibrosis. *Lancet*
2.   Ramu Y, Xu Y, Lu Z. 2007. Inhibition of CFTR Cl- channel function caused by enzymatic hydrolysis of sphingomyelin. *Proceedings of the National Academy of Sciences of the United States of America* 104:6448--53
3.   Ito Y, Sato S, Ohashi T, Nakayama S, Shimokata K, Kume H. 2004. Reduction of airway anion secretion via CFTR in sphingomyelin pathway. *Biochemical and Biophysical Research Communications* 324:901--8
4.   Ramu Y, Xu Y, Lu Z. 2006. Enzymatic activation of voltage-gated potassium channels. *Nature* 442:696--9
5.   Mller G, Ayoub M, Storz P, Rennecke J, Fabbro D, Pfizenmaier K. 1995. PKC zeta is a molecular switch in signal transduction of TNF-alpha, bifunctionally regulated by ceramide and arachidonic acid. *The EMBO Journal* 14:1961--9
6.   Bourbon NA, Sandirasegarane L, Kester M. 2002. Ceramide-induced Inhibition of Akt Is Mediated through Protein Kinase C : IMPLICATIONS FOR GROWTH ARREST. *Journal of Biological Chemistry* 277:3286--92
7.   Chalfant CE. 2003. The structural requirements for ceramide activation of serine-threonine protein phosphatases. *Journal of lipid research* 45:496--506
8.   Bao HF, Zhang ZR, Liang YY, Ma JJ, Eaton DC, Ma HP. 2007. Ceramide mediates inhibition of the renal epithelial sodium channel by tumor necrosis factor- through protein kinase C. *AJP: Renal Physiology* 293:F1178--F86
9.   Heinrich M, Neumeyer J, Jakob M, Hallas C, Tchikov V, et al. 2004. Cathepsin D links TNF-induced acid sphingomyelinase to Bid-mediated caspase-9 and -3 activation. *Cell Death and Differentiation* 11:550--63
10.   Stancevic B, Kolesnick R. 2010. Ceramide-rich platforms in transmembrane signaling. *FEBS Letters* 584:1728--40
11.   Pinto SN, Laviad EL, Stiban J, Kelly SL, Merrill AH, et al. 2013. Changes in membrane biophysical properties induced by sphingomyelinase depend on the sphingolipid N-acyl chain. *Journal of lipid research* 55:53--61
12.   Holopainen JM, Subramanian M, Kinnunen PK. 1998. Sphingomyelinase induces lipid microdomain formation in a fluid phosphatidylcholine/sphingomyelin membrane. *Biochemistry* 37:17562--70
13.   Babiychuk EB, Monastyrskaya K, Draeger A. 2008. Fluorescent annexin A1 reveals dynamics of ceramide platforms in living cells. *Traffic* 9:1757--75
14.   Tam C, Idone V, Devlin C, Fernandes MC, Flannery A, et al. 2010. Exocytosis of acid sphingomyelinase by wounded cells promotes endocytosis and plasma membrane repair. *The Journal of Cell Biology* 189:1027--38
15.   Lariccia V, Fine M, Magi S, Lin M-J, Yaradanakul A, et al. 2011. Massive calcium-activated endocytosis without involvement of classical endocytic proteins. *The Journal of General Physiology* 137:111--32
16.   Obama T, Fujii S, Ikezawa H, Ikeda K, Imagawa M, Tsukamoto K. 2003. His151 and His296 are the acid-base catalytic residues of Bacillus cereus sphingomyelinase in sphingomyelin hydrolysis. *Biological \& pharmaceutical bulletin* 26:920--6
17.   Zhang ZR, Cui G, Zeltwanger S, McCarty NA. 2004. Time-dependent Interactions of Glibenclamide with CFTR: Kinetically Complex Block of Macroscopic Currents. *The Journal of Membrane Biology* 201:139--55

18. Cui G, Song B, Turki HW, McCarty NA. 2012. Differential contribution of TM6 and TM12 to the pore of CFTR identified by three sulfonylurea-based blockers. *Pfl \ u gers Archiv - European Journal of Physiology* 463:405--18

19. Muanprasat C, Sonawane ND, Salinas D, Taddei A, Galietta LJV, Verkman AS. 2004. Discovery of glycine hydrazide pore-occluding CFTR inhibitors: mechanism, structure-activity analysis, and in vivo efficacy. *The Journal of General Physiology* 124:125--37

20. Pfaffinger PJ, Martin JM, Hunter DD, Nathanson NM, Hille B. 1985. GTP-binding proteins couple cardiac muscarinic receptors to a K channel. *Nature* 317:536-8

21. Cui G, Freeman CS, Knotts T, Prince CZ, Kuang C, McCarty NA. 2013. Two Salt Bridges Differentially Contribute to the Maintenance of Cystic Fibrosis Transmembrane Conductance Regulator (CFTR) Channel Function. *The Journal of biological chemistry* 288:20758--67

22. Ma T. 2002. Thiazolidinone CFTR inhibitor identified by high-throughput screening blocks cholera toxin-induced intestinal fluid secretion. *Journal of Clinical Investigation* 110:1651--8

23. Hehl S, Stoyanov B, Oehrl W, Schnherr R, Wetzker R, Heinemann SH. 2001. Phosphoinositide 3-kinase-gamma induces Xenopus oocyte maturation via lipid kinase activity. *Biochemical Journal* 360:691--8

24. Goss GG, Jiang L, Vandorpe DH, Kieller D, Chernova MN, et al. 2001. Role of JNK in hypertonic activation of Cl(-)-dependent Na(+)/H(+) exchange in Xenopus oocytes. *American journal of physiology. Cell physiology* 281:C1978--90

25. Kneen M, Farinas J, Li Y, Verkman AS. 1998. Green fluorescent protein as a noninvasive intracellular pH indicator. *Biophysj* 74:1591--9

26. Lourenco EV, Roque-Barreira MC. 2010. Immunoenzymatic quantitative analysis of antigens expressed on the cell surface (cell-ELISA). *Methods Mol Biol* 588:301-9

27. Hwang TC, Nagel G, Nairn AC, Gadsby DC. 1994. Regulation of the gating of cystic fibrosis transmembrane conductance regulator C1 channels by phosphorylation and ATP hydrolysis. *Proceedings of the National Academy of Sciences of the United States of America* 91:4698--702

28. Gadsby DC, Nairn AC. 1999. Control of CFTR channel gating by phosphorylation and nucleotide hydrolysis. *Physiological reviews* 79:S77--S107

29. Picciotto MR, Cohn JA, Bertuzzi G, Greengard P, Nairn AC. 1992. Phosphorylation of the cystic fibrosis transmembrane conductance regulator. *The Journal of biological chemistry* 267:12742--52

30. Baldursson O, Berger HA, Welsh MJ. 2000. Contribution of R domain phosphoserines to the function of CFTR studied in Fischer rat thyroid epithelia. *American journal of physiology. Lung cellular and molecular physiology* 279:L835--41

31. Csandy L, Seto-Young D, Chan KW, Cenciarelli C, Angel BB, et al. 2005. Preferential phosphorylation of R-domain Serine 768 dampens activation of CFTR channels by PKA. *The Journal of General Physiology* 125:171--86

32. Hegeds T, Aleksandrov A, Mengos A, Cui L, Jensen TJ, Riordan JR. 2009. Role of individual R domain phosphorylation sites in CFTR regulation by protein kinase A. *BBA - Biomembranes* 1788:1341--9

33. Wilkinson DJ, Strong TV, Mansoura MK, Wood DL, Smith SS, et al. 1997. CFTR activation: additive effects of stimulatory and inhibitory phosphorylation sites in the R domain. *The American journal of physiology* 273:L127--33

34. Wang W, Roessler BC, Kirk KL. 2014. An electrostatic interaction at the tetrahelix bundle promotes phosphorylation-dependent cystic fibrosis transmembrane conductance regulator (CFTR) channel opening. *Journal of Biological Chemistry* 289:30364--78

35. Carson MR, Travis SM, Welsh MJ. 1995. The two nucleotide-binding domains of cystic fibrosis transmembrane conductance regulator (CFTR) have distinct functions in controlling channel activity. *The Journal of biological chemistry* 270:1711--7

36. Gunderson KL, Kopito RR. 1995. Conformational states of CFTR associated with channel gating: the role ATP binding and hydrolysis. *Cell* 82:231--9

37. Csanady L, Chan KW, Seto-Young D, Kopsco DC, Nairn AC, Gadsby DC. 2000. Severed channels probe regulation of gating of cystic fibrosis transmembrane conductance regulator by its cytoplasmic domains. *The Journal of General Physiology* 116:477--500

38. Van Goor F, Hadida S, Grootenhuis PDJ, Burton B, Cao D, et al. 2009. Rescue of CF airway epithelial cell function in vitro by a CFTR potentiator, VX-770. *Proceedings of the National Academy of Sciences* 106:18825--30

39. Jih K-Y, Hwang T-C. 2013. Vx-770 potentiates CFTR function by promoting decoupling between the gating cycle and ATP hydrolysis cycle. *Proceedings of the National Academy of Sciences* 110:4404--9

40. Yu Y-C, Sohma Y, Hwang T-C. 2016. On the mechanism of gating defects caused by the R117H mutation in CFTR. *The Journal of Physiology*:n/a--n/a

41. Hammerle MM, Aleksandrov AA, Riordan JR. 2001. Disease-associated mutations in the extracytoplasmic loops of cystic fibrosis transmembrane conductance regulator do not impede biosynthetic processing but impair chloride channel stability. *The Journal of biological chemistry* 276:14848--54

42. Cui G, Rahman KS, Infield DT, Kuang C, Prince CZ, McCarty NA. 2014. Three charged amino acids in extracellular loop 1 are involved in maintaining the outer pore architecture of CFTR. *The Journal of General Physiology* 144:159--79

43. Cotten JF, Welsh MJ. 1999. Cystic fibrosis-associated mutations at arginine 347 alter the pore architecture of CFTR. Evidence for disruption of a salt bridge. *The Journal of biological chemistry* 274:5429--35

44. Cui L. 2006. The role of cystic fibrosis transmembrane conductance regulator phenylalanine 508 side chain in ion channel gating. *The Journal of Physiology* 572:347--58

45. Laufer J, Boehmer C, Jeyaraj S, Knuwer M, Klaus F, et al. 2009. The C-terminal PDZ-binding motif in the Kv1.5 potassium channel governs its modulation by the Na+/H+ exchanger regulatory factor 2. *Cellular physiology and biochemistry : international journal of experimental cellular physiology, biochemistry, and pharmacology* 23:25--36

46. Cheng J, Wang H, Guggino WB. 2004. Modulation of mature cystic fibrosis transmembrane regulator protein by the PDZ domain protein CAL. *The Journal of biological chemistry* 279:1892--8

47. Guggino WB. 2004. The cystic fibrosis transmembrane regulator forms macromolecular complexes with PDZ domain scaffold proteins. *Proceedings of the American Thoracic Society* 1:28--32

48. Haggie PM, Kim JK, Lukacs GL, Verkman AS. 2006. Tracking of quantum dot-labeled CFTR shows near immobilization by C-terminal PDZ interactions. *Molecular biology of the cell* 17:4937--45

49. Sun F, Hug MJ, Bradbury NA, Frizzell RA. 2000. Protein kinase A associates with cystic fibrosis transmembrane conductance regulator via an interaction with ezrin. *The Journal of biological chemistry* 275:14360--6

50. Saslowsky DE, Tanaka N, Reddy KP, Lencer WI. 2009. Ceramide activates JNK to inhibit a cAMP-gated K+ conductance and Cl- secretion in intestinal epithelia. *The FASEB Journal* 23:259--70

51. Denning GM, Anderson MP, Amara JF, Marshall J, Smith AE, Welsh MJ. 1992. Processing of mutant cystic fibrosis transmembrane conductance regulator is temperature-sensitive. *Nature* 358:761--4

52. Van Goor F, Hadida S, Grootenhuis PDJ, Burton B, Stack JH, et al. 2011. Correction of the F508del-CFTR protein processing defect in vitro by the investigational drug VX-809. *Proceedings of the National Academy of Sciences* 108:18843--8

53. van Meer G, Stelzer EH, Wijnaendts-van-Resandt RW, Simons K. 1987. Sorting of sphingolipids in epithelial (Madin-Darby canine kidney) cells. *The Journal of Cell Biology* 105:1623--35

54. Makino A, Abe M, Murate M, Inaba T, Yilmaz N, et al. 2015. Visualization of the heterogeneous membrane distribution of sphingomyelin associated with cytokinesis, cell polarity, and sphingolipidosis. *The FASEB Journal* 29:477--93

55. Xu Y, Ramu Y, Lu Z. 2008. Removal of phospho-head groups of membrane lipids immobilizes voltage sensors of K+ channels. *Nature* 451:826--9

56. Caohuy H, Yang Q, Eudy Y, Ha TA, Xu AE, et al. 2014. Activation of 3-Phosphoinositide Dependent Kinase 1 (PDK1) and Serum-and Glucocorticoid-Induced Protein Kinase 1 (SGK1) by Short-Chain Sphingolipid C4-Ceramide Rescues the Trafficking Defect of F508 Cystic Fibrosis Transmembrane Conductance Regulator (CFTR). *Journal of Biological Chemistry*

57. Petcoff DW, Holland WL, Stith BJ. 2008. Lipid levels in sperm, eggs, and during fertilization in Xenopus laevis. *Journal of lipid research* 49:2365--78

58. Hannun YA, Obeid LM. 2011. Many ceramides. *Journal of Biological Chemistry* 286:27855--62

59. Hamai H, Keyserman F, Quittell LM, Worgall TS. 2009. Defective CFTR increases synthesis and mass of sphingolipids that modulate membrane composition and lipid signaling. *Journal of lipid research* 50:1101--8

60. Itokazu Y, Pagano RE, Schroeder AS, O'Grady SM, Limper AH, Marks DL. 2014. Reduced GM1 ganglioside in CFTR-deficient human airway cells results in decreased β1-integrin signaling and delayed wound repair. *AJP: Cell Physiology* 306:C819--30

61. Teichgrber V, Ulrich M, Endlich N, Riethmller J, Wilker B, et al. 2008. Ceramide accumulation mediates inflammation, cell death and infection susceptibility in cystic fibrosis. *Nature medicine* 14:382--91

62. Boujaoude LC, Bradshaw-Wilder C, Mao C, Cohn J, Ogretmen B, et al. 2001. Cystic fibrosis transmembrane regulator regulates uptake of sphingoid base phosphates and lysophosphatidic acid: modulation of cellular activity of sphingosine 1-phosphate. *The Journal of biological chemistry* 276:35258--64

63. Peter BF, Lidington D, Harada A, Bolz HJ, Vogel L, et al. 2008. Role of sphingosine-1-phosphate phosphohydrolase 1 in the regulation of resistance artery tone. *Circulation research* 103:315--24

64. Meissner A, Yang J, Kroetsch JT, Sauve M, Dax H, et al. 2012. Tumor Necrosis Factor- -Mediated Downregulation of the Cystic Fibrosis Transmembrane

Conductance Regulator Drives Pathological Sphingosine-1-Phosphate Signaling in a Mouse Model of Heart Failure. *Circulation* 125:2739--50

65. Molina SA, Stauffer B, Moriarty HK, Kim AH, McCarty NA, Koval M. 2015. Junctional abnormalities in human airway epithelial cells expressing F508del CFTR. *AJP: Lung Cellular and Molecular Physiology* 309:L475--L87

66. Grassm. 2001. CD95 signaling via ceramide-rich membrane rafts. *The Journal of biological chemistry* 276:20589--96

67. Chaffin DO, Taylor D, Skerrett SJ, Rubens CE. 2012. Changes in the Staphylococcus aureus transcriptome during early adaptation to the lung. *PLoS ONE* 7:e41329

68. Coleman D, Knights J, Russell R, Shanley D, Birkbeck TH, et al. 1991. Insertional inactivation of the Staphylococcus aureus beta-toxin by bacteriophage phi 13 occurs by site- and orientation-specific integration of the phi 13 genome. *Molecular microbiology* 5:933--9

69. Goerke C, Matias y Papenberg S, Dasbach S, Dietz K, Ziebach R, et al. 2004. Increased frequency of genomic alterations in Staphylococcus aureus during chronic infection is in part due to phage mobilization. *The Journal of infectious diseases* 189:724--34

70. Goerke C, Wirtz C, Flckiger U, Wolz C. 2006. Extensive phage dynamics in Staphylococcus aureus contributes to adaptation to the human host during infection. *Molecular microbiology* 61:1673--85

71. Hayashida A, Bartlett AH, Foster TJ, Park PW. 2010. Staphylococcus aureus Beta-Toxin Induces Lung Injury through Syndecan-1. *The American journal of pathology* 174:509--18

72. Oda M, Hashimoto M, Takahashi M, Ohmae Y, Seike S, et al. 2012. Role of sphingomyelinase in infectious diseases caused by Bacillus cereus. *PLoS ONE* 7:e38054

73. Martinez-Pulgarin S, Dominguez-Bernal G, Orden JA, de la Fuente R. 2009. Simultaneous lack of catalase and beta-toxin in Staphylococcus aureus leads to increased intracellular survival in macrophages and epithelial cells and to attenuated virulence in murine and ovine models. *Microbiology* 155:1505--15

74. Wargo MJ, Gross MJ, Rajamani S, Allard JL, Lundblad LKA, et al. 2011. Hemolytic phospholipase C inhibition protects lung function during Pseudomonas aeruginosa infection. *American Journal of Respiratory and Critical Care Medicine* 184:345--54

75. Stonehouse MJ, Cota-Gomez A, Parker SK, Martin WE, Hankin JA, et al. 2002. A novel class of microbial phosphocholine-specific phospholipases C. *Molecular microbiology* 46:661--76

76. Frizzell RA, Hanrahan JW. 2012. Physiology of Epithelial Chloride and Fluid Secretion. *Cold Spring Harbor Perspectives in Medicine* 2:a009563--a

77. Tarran R, Loewen ME, Paradiso AM, Olsen JC, Gray MA, et al. 2002. Regulation of Murine Airway Surface Liquid Volume by CFTR and Ca 2+-activated Cl −Conductances. *The Journal of General Physiology* 120:407--18

78. Pier GB, Grout M, Zaidi TS, Goldberg JB. 1996. How mutant CFTR may contribute to Pseudomonas aeruginosa infection in cystic fibrosis. *American Journal of Respiratory and Critical Care Medicine* 154:S175--82

79. Pezzulo AA, Tang XX, Hoegger MJ, Abou Alaiwa MH, Ramachandran S, et al. 2012. Reduced airway surface pH impairs bacterial killing in the porcine cystic fibrosis lung. *Nature* 487:109--13

4.2) *Collaborative Research Project - Phosphorylation Dependence of CFTR Potentiation*

4.2.1 *Introduction*

As discussed in Section 1.2, Cystic fibrosis results from loss-of-function mutations in the CFTR chloride channel and presents with dysfunction in multiple organ systems. Historically, treatment has focused on alleviating symptoms but a significant breakthrough occurred in 2012 when the FDA approved the first small molecule to directly potentiate CFTR channel function: VX-770 (Ivacaftor, Kalydeco[TM]). VX-770, which was developed by Vertex Pharmaceuticals in collaboration with the CF Foundation, was initially approved for the treatment of the Class 3 mutation G551D but has now been shown effective for in the treatment of numerous gating mutants (1-3). In addition, it is now included in combination with small molecule correctors that improve the trafficking of Class 2 mutations like F508del, and it has been suggested that VX-770 may be useful to counter the downregulation of CFTR activity commonly observed in COPD (4; 5). Ultimately, the current trend suggests that the prescription of small molecule potentiators like VX-770 will continue to grow. However, important details regarding the mechanism of action of these compounds have yet to be uncovered. For example, consensus is lacking regarding whether VX-770, or other CFTR potentiators, can increase the activity of wildtype CFTR (WT-CFTR) in a wide variety of experimental systems. Furthermore, the activity of potentiators on various disease-associated mutants of CFTR varies between labs studying these compounds (3; 6; 7). It seems possible that this discord may result from differences in how CFTR is controlled in these potentiator studies. Clarification of how experimental conditions influence the efficacy of VX-770 (and potentiators in general) may have great impact on the assays used by industry to identify new CFTR-targeted therapeutics.

CFTR channel activity is controlled by the phosphorylation of its cytosolic R-domain (8; 9). In total, human CFTR contains 11 PKA consensus sites that are serially phosphorylated and have distinct effects on channel gating. For example, phosphorylation of sites such as S700, S795, and S813 increase channel activity while phosphorylation of S737 and S768 decrease channel activity (10; 11). These non-redundant effects lead to the activation of CFTR channels in a graded manner relative to the magnitude of kinase activity. Graded phosphorylation modulates the channels' open probability (the fraction of time that the channel spends in the open state) but does not change the channel conductance (the rate of chloride ion flux)(12; 13) (14; 15). The second requirement for CFTR activity is binding of ATP to the cytosolic nucleotide binding domains (NBDs) and their subsequent dimerization (16; 17). Following dimerization, intrinsic ATPase activity of the NBDs hydrolyzes one of the bound ATP molecules and time is required for the products of hydrolysis to be replaced to enable reopening. Therefore, channel function is finite: there is a limit to how much current a single CFTR protein can pass in time. Given these constraints, it seems likely that the ability of pharmacological modulators to enhance CFTR activity might depend upon the degree to which CFTR is phosphorylated prior to application of the modulator. If applied to channels already maximally activated by phosphorylation, the potentiator may appear to be without effect. This phenomenon is referred to as a "ceiling effect" in pharmacological terms (18). Some experimental data suggest that potentiation of WT CFTR by NPPB follows this pattern(19; 20) but it has never been systematically studied for VX-770, nor has it been tested for CF-associated mutants. If this effect is a feature common to multiple CFTR potentiators or is common to multiple forms of CFTR studied it would have significant impact on designing drug screens for new CFTR potentiators. Such an observation would be consistent with the notion that both phosphorylation-dependent

stimulation of CFTR activity and potentiator-mediated enhancement of CFTR activity reflect allosteric modulation, and that these two processes might be interdependent and therefore limited by the ceiling effect. Based on this line of thinking, we hypothesized that VX-770 efficacy is inversely proportional to the initial level of channel activity.

In this study, we sought to determine whether the efficacy of VX-770-mediated potentiation of CFTR is dependent upon CFTR phosphorylation state. Consistent with this, we found that VX-770-mediated potentiation of CFTR current was inversely proportional to the level of cellular kinase activity. This ceiling effect occurred in multiple heterologous cell systems, from the highly reductionist *Xenopus* oocyte to stably transfected Fisher Rat Thyroid (FRT) cells, which currently serve as the primary system for screening CFTR potentiators. Importantly, the effect was also observed in primary bronchial epithelial cells endogenously expressing CFTR. Finally, post hoc analysis suggests that this inverse relationship between channel activity level and its ability to be potentiated by VX-770 might contribute to the variability in potentiation of CFTR point mutants that was published by Vertex. Ultimately, these data provide insight into the relationship between CFTR activity and potentiators like VX-770, and inform the design of high throughput screening methods for future drug development.

4.2.2) *Results*

Graded activation of CFTR currents in multiple cell systems:

      We first sought to characterize the activation curves of CFTR in the relevant cell systems. This was shown for *Xenopus* oocytes with increasing concentrations of IBMX in Section 4.1 and stepwise activation of CFTR primary epithelial cells was shown in Figure 4.14. Figure 4.19 shows that this relationship also exists in two immortalized cell lines, one endogenously expressing CFTR (Calu-3, Fig. 4.19a, b) and one heterologously expressing WT-CFTR (FRT, Fig. 4.19c). The FRT cell line was chosen because it is commonly used to screen for new CFTR potentiators in pharmaceutical and academic laboratories. These examples, coupled with data presented in Section 4.1, show that graded activation of the CFTR channel was observed in all systems tested and reaffirm the conclusion that it is an inherent characteristic of the channel.

Figure 4.19) Graded activation of CFTR in Calu-3 and FRT cells
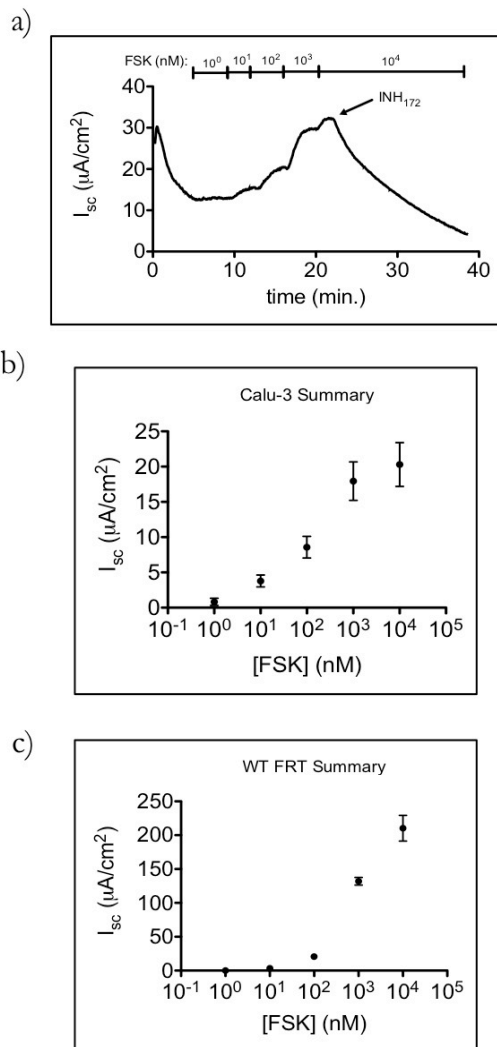
Calu-3 cells:

Figure 4.19) Graded activation of CFTR in Calu-3 and FRT cells: (a) An example trace showing that transepithelial currents in polarized Calu-3 epithelial cells can be activated in a graded fashion similar to that seen in primary NHBEs. (b) Summary data showing a dose-response curve for FSK on Calu-3 cells, n=4. (c) Summary data showing a similar dose-response relationship for in FRT cells expressing WT-CFTR, n=4.

Potentiation of WT CFTR by VX-770 depends on activity level in multiple cell systems

We next asked whether activation level affects potentiation efficacy in the FRT cells expressing WT-CFTR. When WT-CFTR was fully activated by 10 μM forskolin, subsequent exposure to 1 μM VX-770 (~EC$_{90}$) led to a 0.32 ±0.33-fold increase in transepithelial current, shown to be attributable to CFTR by its sensitivity to the CFTR inhibitor INH$_{172}$ (21)(Fig. 4.20a). However, when CFTR in the same cell type was activated submaximally by exposure to lower concentrations of forskolin, the same concentration of VX-770 had much greater effect. At 10 nM forskolin, 1 μM VX-770 potentiated WT-CFTR by approximately 5-fold (Fig. 4.20b). This inverse relationship was observed over the entire 10^5-fold range of FSK concentrations (Fig. 4.20c). To ensure that this effect was not specific to the FRT expression system, we next tested CFTR expressed in *Xenopus* oocytes. In these experiments, we recorded currents from CFTR channels expressed in excised inside-out Macropatches and controlled CFTR activity levels by changing the concentration of PKA perfused onto the cytosolic face of the patch (22). Like in the FRT cells, we observed greater potentiation when channels were submaximally activated with 6.4 units/mL of PKA as opposed to when channels were activated with 127.6 units/mL of PKA (Fig. 4.20d-f).

All systems tested to this point heterologously expressed CFTR so we next asked whether this relationship occurred in primary NHBE cells that endogenously express CFTR. After blocking ENaC currents with amiloride, we activated CFTR currents using either 10 nM or 10 μM FSK. Figure 4.21 shows that, like in the FRT cells, CFTR current amplitude was proportional to the concentration of FSK used to activate the channels. Additionally, the magnitude of potentiation by 1 μM VX-770 was inversely proportional to the FSK concentration. In the presence of 10 nM FSK, 1 μM VX-770 led to a 5.7-fold potentiation of current whereas the potentiation ratio in the presence of 10 μM FSK was 0.18 (Fig. 4.21c).

Figure 4.20) Potentiation of heterologously expressed WT-CFTR by VX-770 is inversely proportional to PKA activity
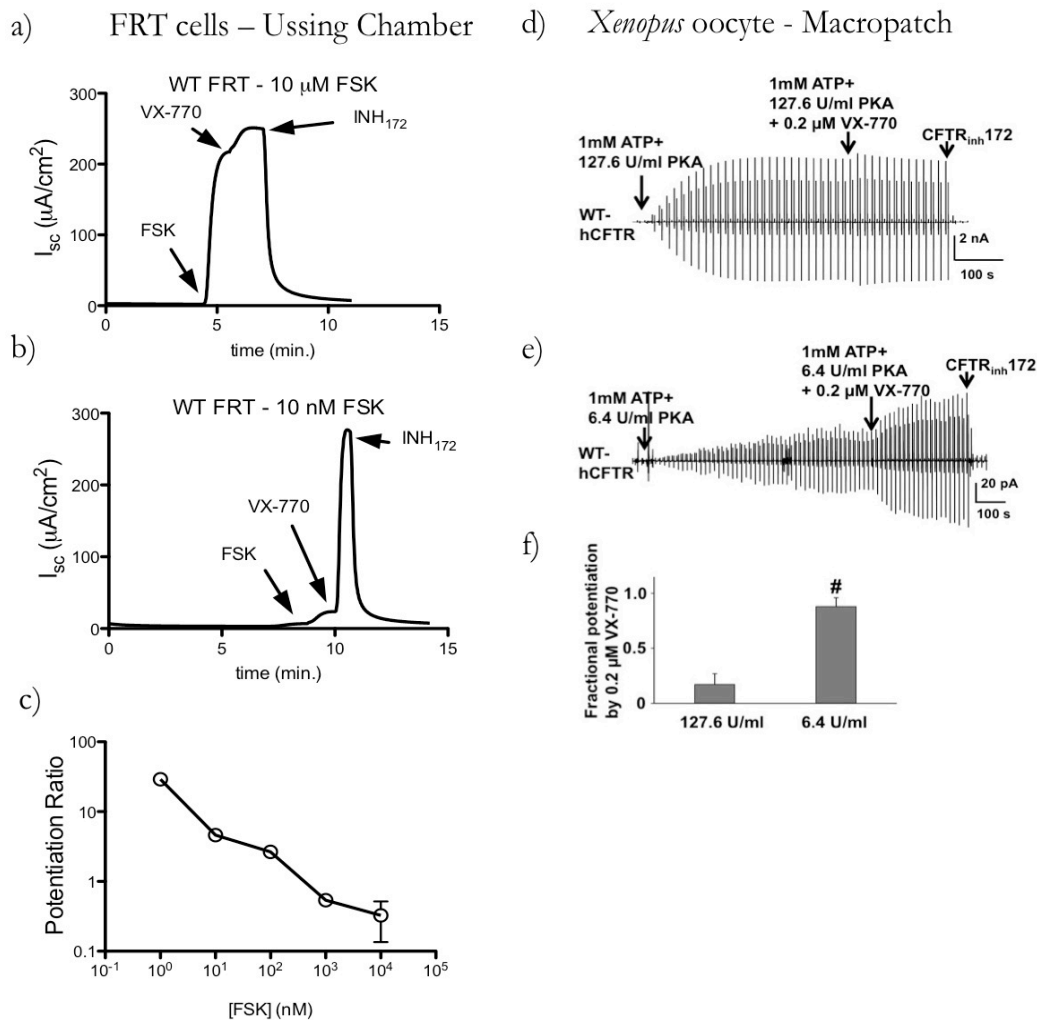
a) FRT cells – Ussing Chamber

d) *Xenopus* oocyte - Macropatch

b)

e)

c)

f)

Figure 4.21) Potentiation of endogenously expressed WT-CFTR by VX-770 is inversely proportional to PKA activity
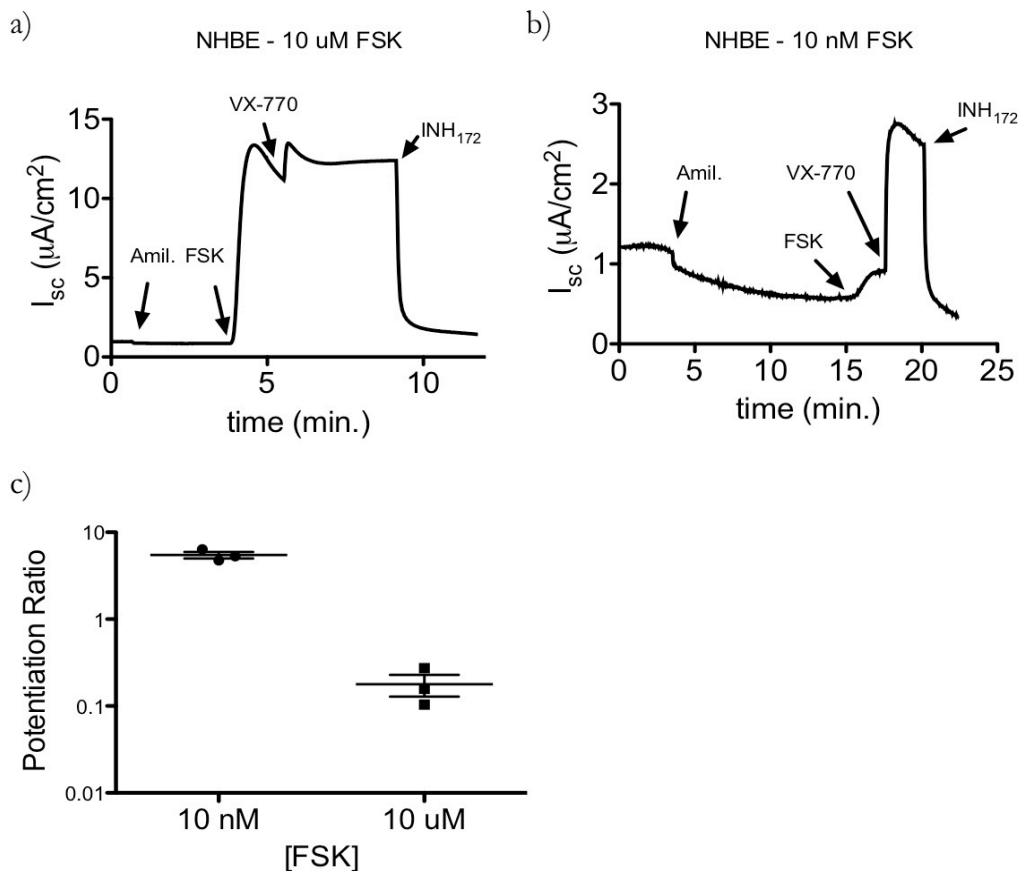
a)

b)

c)

Figure 4.21) Potentiation of endogenously expressed WT-CFTR by VX-770 is inversely proportional to PKA activity: a,b) When NHBE cells expressing WT-CFTR were activated using 10 μM FSK, the VX-770 potentiation ratio was 0.18±0.50 but increased to 5.5±0.47 when 10 nM FSK was used. (c) The inverse relationship was true over the entire range of FSK tested

Potentiation of CF disease-associated mutants

Most CF-associated disease mutants show a similar graded activation with increasing kinase activity (23) so we hypothesized that disease mutants would show the same FSK-dependence of potentiation. The most interest for VX-770 is in its ability to potentiate mutant CFTR channels and most drug screens use a CF-associated CFTR mutant as a target, so such a relationship would be of interest to companies that currently screen for CFTR potentiators. For these experiments, we returned to the heterologous FRT system because they are the most common cell line used in drug screens. We tested 3 CFTR mutants: the most commonly occurring mutation, F508del; P67L, which was tested by Vertex but for which VX-770 was not approved due to low efficacy; and G551D, for which VX-770 was approved and therefore represents a threshold for FDA-approval. The summary data in Figure 4.22c shows that the concentration of FSK used to activate CFTR currents influenced the level of potentiation of F508del-CFTR and P67L-CFTR by VX-770. This relationship closely resembles that seen in cells expressing WT-CFTR. Importantly, when 10 nM FSK was used, VX-770 potentiated P67L- and F508del-CFTR to a similar level as G551D-CFTR (~10-fold). This suggests that with submaximal activation of P67L-CFTR, VX-770 is efficacious enough to satisfy the approval precedent set by the FDA with G551D-CFTR. The FSK-dependence of potentiation curve for FRT cells expressing G551D-CFTR was shallower than the rest with no significant difference between the cells treated with 10 nM FSK and 10 μM FSK. Potential reasons for this difference will be examined in the

Figure 4.22) Multiple disease mutants display the same FSK-dependent phenotype as WT-CFTR
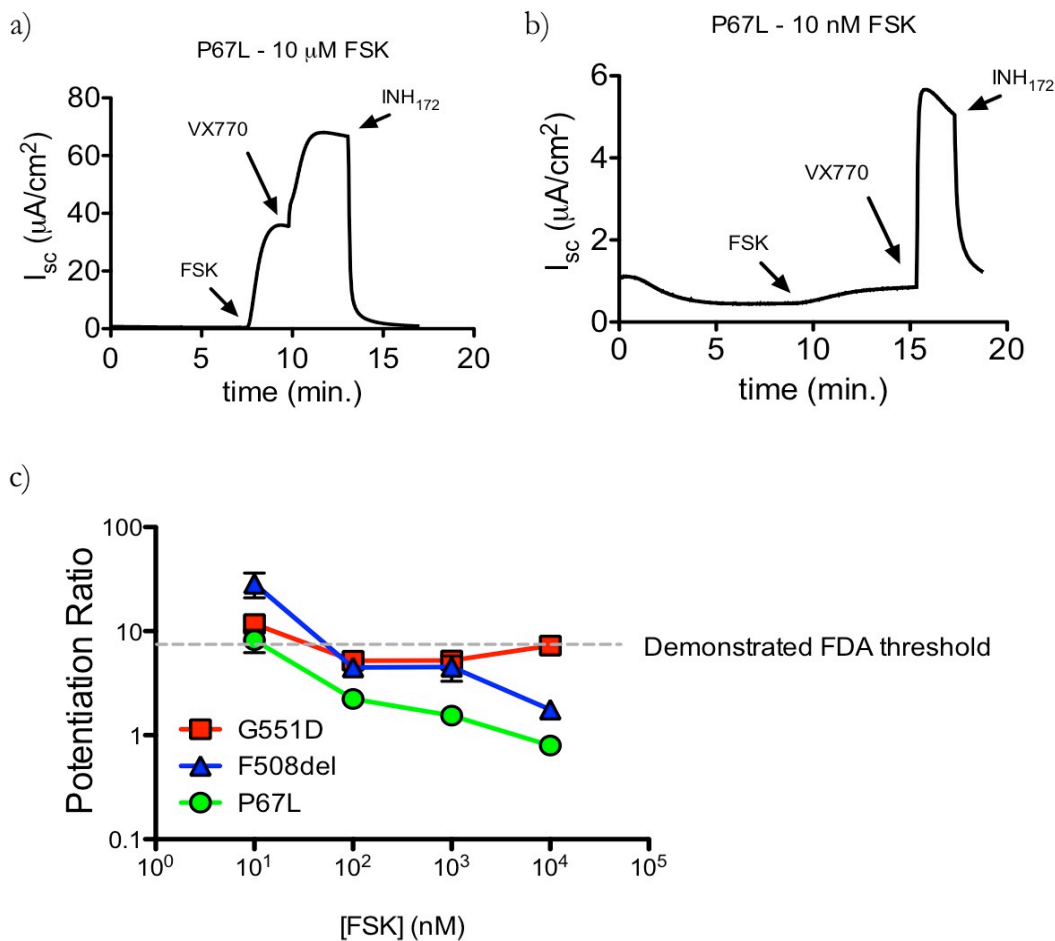
Figure 4.22) Multiple disease mutants display the same FSK-dependent phenotype as WT-CFTR: a, b) When FRT cells expressing P67L-CFTR were activated using 10 μM FSK, the VX-770 potentiation ratio was 1.78 ± 0.05 but increased to 9.2 ± 2.0 when 10 nM FSK was used. (c) The inverse relationship was true over the entire range of FSK tested and was also seen in cells expressing F508del-CFTR. G551D-CFTR showed a more shallow relationship. Of note, decreasing the FSK concentration to 10 nM increased the response of P67L-CFTR and F508del CFTR to levels similar to G551D-CFTR when it was activated with 10 μM FSK. This level of response in FRT cells was integral to FDA approval of VX-770 in patients harboring the G551D mutation.

The efficacy of VX-770 varies greatly between mutants and the reason for this is not clear. The drug has been approved for treatment of patients with mutations that lie across multiple domains of the protein (Green spheres in Fig. 4.23a) so it is unlikely that efficacy is related to proximity of the mutation to the VX-770 binding pocket. Given this, we speculated that some of the variability might result from differences in the ability of 10 μM FSK to activate different disease mutants because Vertex consistently tests their compounds in the presence of 10 μM. We hypothesized that mutants with low activity in the presence of 10 μM FSK would be strongly potentiated by VX-770, whereas channels that showed relatively high levels of activity would be more poorly potentiated. To test this hypothesis, we performed a post hoc analysis of data describing the response of all mutants tested by Vertex. We found that there was a clear relationship between the fold potentiation of VX-770 and the initial activity of the mutant relative to WT-CFTR (Fig. 4.23b). Consistent with this, we found that 9 out of 10 mutations for which VX-770 has already been approved (Green names) all showed very low initial activity and cluster together at the left side of the curve. Given the dramatic shift in efficacy that we observed with P67L- and F508del-CFTR when we decreased the FSK concentration, we would predict that if all mutants shown in red and black were retested at a lower FSK concentration there would be a general increased in the fold potentiation of current elicited by VX-770.

Figure 4.23) Variation in response to VX-770 seen in all mutants tested by Vertex pharmaceuticals correlates with initial channel activity: (a) Ribbon representation of human CFTR shows in green spheres the the location of mutation loci for which VX-770 has been approved. Note that these mutations are note localized to a single location. (b) A plot of initial activity vs. fold potentiation shows an inverse relationship. Variant names in green have been approved for treatment with VX-770; Variant names in black have not been proposed; VX-770 was originally denied for variant names in red; black dots fit inverse function well; red dots cluster in a relatively "non responsive" group that seem to deviate from pure inverse relationship. Data for panel B were assembled by Danny Infield.
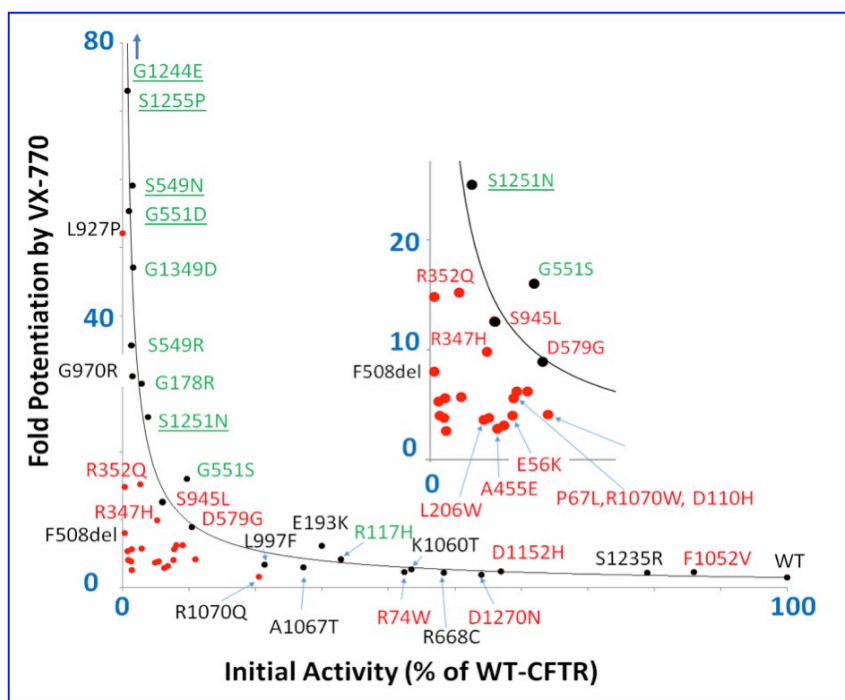
Figure 4.23) Variation in response to VX-770 seen in mutants tested by Vertex pharmaceuticals correlates with initial channel activity

a)
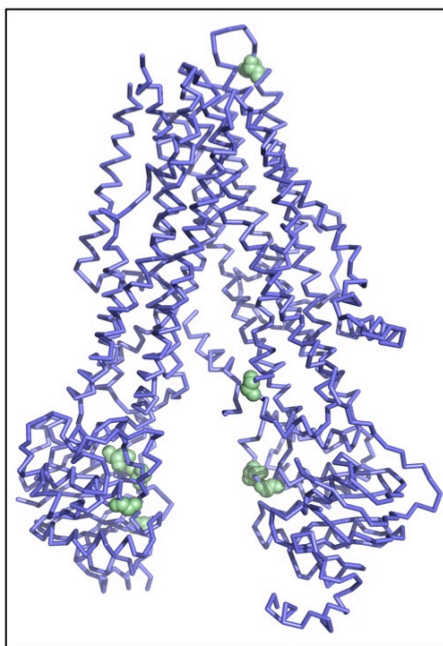
b)

4.2.3) *Discussion*

The discovery of VX-770 has revolutionized CF care for individuals with 10 different Class 3 mutations. Numerous pharmaceutical and academic laboratories have expanded to screen for novel potentiators of CFTR. Despite this massive influx of time and capital, relatively little is known about how potentiators, and specifically VX-770, work. In this study we present evidence that the ability of VX-770 to increase CFTR activity is inversely related to the channel's initial activity level (i.e., when the drug is applied). This effect, classically known as the "ceiling effect," limits the ability of the potentiator to increase channel activity and reflects the physical limit for how much current a single gating CFTR can pass in time.

This interaction between phosphorylation level and VX-770 efficacy is conserved in cells that express both endogenous and heterologous WT-CFTR. In FRT cells, the proverbial "workhorse" cell line in CF drug screening, the relative change in current upon addition of 1 μM VX-770 as compared to the initial current level (the potentiation ratio) changed by a factor of nearly 100 depending on the concentration of FSK. In cells activated with 1 nM FSK, the current increased by ~29-fold, while it increased by only 30% when the channels were activated by 10 μM FSK. We saw a similar difference in primary NHBE cells. After activation with 10 nM FSK, we observed a 5.5-fold increase in current with the application of VX-770 and the potentiation ratio decreased to 0.17 when 10 μM FSK was used to activate channels. The effect was also qualitatively similar in macropatches that were pulled from *Xenopus* oocytes expressing WT CFTR.

Our observation that two disease-associated mutant variants of CFTR also show this activity dependence is the most important finding in this study because it has practical implications. As highlighted in panel c of Figure 4.22, when P67L- and F508del-CFTR are

activated with submaximal FSK, their response to VX-770 can approach the level of efficacy achieved with G551D cells. There are not enough patients with the P67L-CFTR genotype to run a full-scale clinical trial (238 patients total are currently in the CFTR2.org database) so the *in vitro* data will be a large consideration in determining whether VX-770 gets approved. We would predict that if all mutants were screened with a lower concentration of FSK and plotted as in Figure 4.23b, there would be a general upward shift of all mutants labeled in black and red.

Our data also show that G551D-CFTR is significantly more sensitive to potentiation by VX-770 under the standard screening conditions and does not seem to follow the same trend. This was likely the reason that it was the preliminary focus of clinical trials and, in hindsight, it is fortuitous G551D-CFTR responded so well because otherwise VX-770 may have never moved out of preclinical testing. Two possible explanations might account for this distinct sensitivity. The first is that G551D-CFTR has very low activity in the presence of PKA and ATP due to a decreased affinity for ATP, so it resides exclusively on the far left side of the curve regardless of the PKA activity in the cell. Indeed we saw, relatively small currents in the G551D cells with 10 nM FSK eliciting 0.23 ± 0.21 µA/cm2 of current while 10 µM FSK elicited 24.1 ± 5.7 µA/cm2 of current. If this were the case, the shallow FSK-dependence would be completely explained by the inverse relationship described by our study. Our modeling efforts raised a second possibility, however. And that is that when the G551 residue is mutated to D it may form a salt bridge with K1250 (on the opposite NBD) because they are modeled to come within ~4 Å of one another. This is shown in Figure 4.24 using our open state model. If this salt bridge formed during gating it would be expected to greatly increase the stability of the NBD dimer and potentially lock the NBDs together.

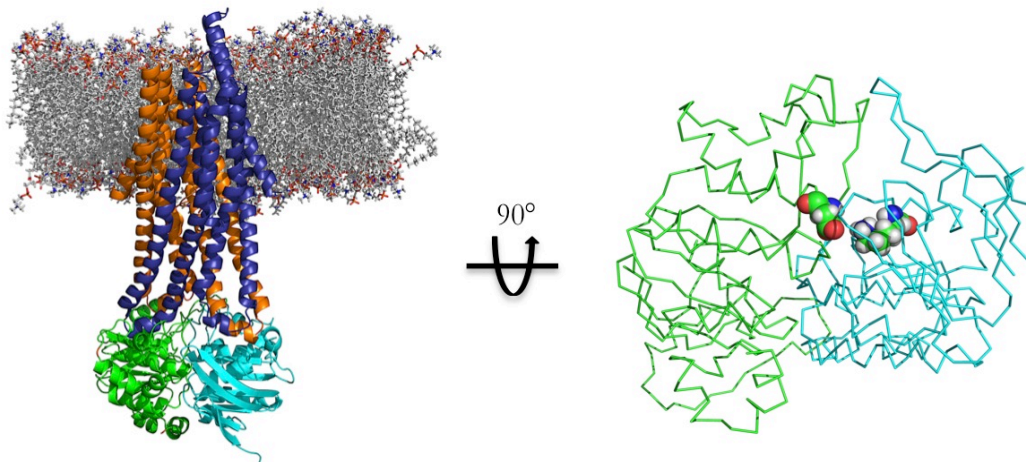Figure 4.24) Potential salt bridge may stabilize G551D NBD dimer

Figure 4.24) Potential salt bridge may stabilize G551D NBD Dimer: *Left* - Homology model of open CFTR is shown for orientation. *Right* – view of the NBD dimer in the G551D *in silico* mutant shows close proximity between D551 in NBD1 (green) and K1250 in NBD2 (cyan). D551 and K1250 are shown as spheres and colored by atom.

Thus, VX-770 could simply increase the opening rate and the salt-bridge would stabilize the open state. Future experiments using point mutations will explore this possibility.

How does this finding translate to CFTR expressed in patients? CFTR activity in tissues is likely tuned in a temporal manner. For example, it is expected that pulmonary CFTR activity would increase during time of high sympathetic input and β2AR activation. Two pieces of evidence suggest that phosphorylation levels are such that CFTR activity *in vivo* normally sits far below its maximum. The first observation is that in the GI tract, the long-term activation that follows cholera poisoning leads to levels of water loss that far exceed normal physiological levels (24). The second observation comes from the clinical lab, in which physicians can monitor CFTR activity by measuring nasal potential differences, or NPDs. An example NPD trace is shown in Figure 4.25 and this measured potential is directly related to ion channel function in the epithelium(25). In a healthy individual, apical perfusion with a zero Cl⁻ solution enables the measurement of resting CFTR activity. However, subsequent perfusion with isoproterenol leads to an increase in channel activity providing clear evidence that CFTR activity is not at maximum under basal conditions. While it is impossible to accurately quantify the basal activity relative to its maximum in this system, it suggests that screening drugs against submaximally activated CFTR is more physiologically relevant. Additionally, our data using P67L-FRT cells suggests that using a lower concentration of forskolin might enable the discovery of more potentiators by increasing the available dynamic range and lead to an expansion of mutations for which VX-770 is approved.

Figure 4.25) An example nasal potential difference (NPD) measurement shows the response in healthy individual and an individual with CF
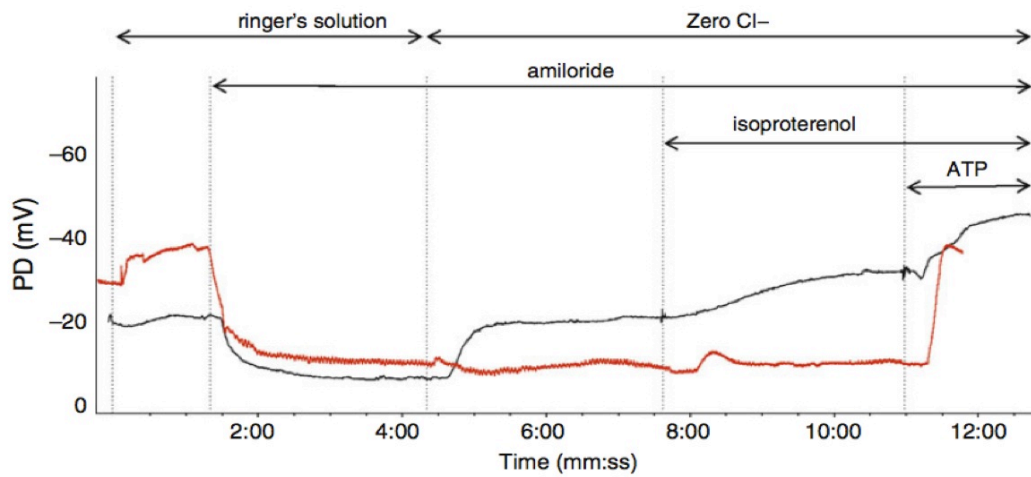
Figure 4.25) An example nasal potential difference (NPD) measurement shows the response in a healthy individual and an individual with CF: Adapted from Rowe et al (24). Amiloride is used to block the ENaC channels and isolate chloride permeability. Changing to a solution with zero chloride facilitates chloride currents through open CFTR channels and is characterized by the first upward deflection. Note that the nasal epithelium of the CF subject does not show a change. Subsequent addition of isoproterenol further activates CFTR ion channel activity in the non-CF individual.

Works Cited:

1. Van Goor F, Hadida S, Grootenhuis PDJ, Burton B, Cao D, et al. 2009. Rescue of CF airway epithelial cell function in vitro by a CFTR potentiator, VX-770. *Proceedings of the National Academy of Sciences* 106:18825--30
2. Accurso FJ, Rowe SM, Clancy JP, Boyle MP, Dunitz JM, et al. 2010. Effect of VX-770 in persons with cystic fibrosis and the G551D-CFTR mutation. *The New England journal of medicine* 363:1991--2003
3. Yu H, Burton B, Huang C-J, Worley J, Cao D, et al. 2012. Ivacaftor potentiation of multiple CFTR channels with gating mutations. *Journal of cystic fibrosis : official journal of the European Cystic Fibrosis Society* 11:237--45
4. Kopeikin Z, Yuksek Z, Yang HY, Bompadre SG. 2014. Combined effects of VX-770 and VX-809 on several functional abnormalities of F508del-CFTR channels. *J Cyst Fibros* 13:508-14
5. 2016. Lumacaftor/ivacaftor (Orkambi) for cystic fibrosis. *Med Lett Drugs Ther* 58:41-2
6. Cui G, Khazanov N, stauffer b, Infield DT, Imhoff BR, et al. 2016. Potentiators exert distinct effects on human, murine, and Xenopus CFTR. *AJP: Lung Cellular and Molecular Physiology*:ajplung.00056.2016
7. Jih K-Y, Hwang T-C. 2013. Vx-770 potentiates CFTR function by promoting decoupling between the gating cycle and ATP hydrolysis cycle. *Proceedings of the National Academy of Sciences* 110:4404--9
8. Gadsby DC, Nairn AC. 1999. Control of CFTR channel gating by phosphorylation and nucleotide hydrolysis. *Physiological reviews* 79:S77--S107
9. Hwang TC, Nagel G, Nairn AC, Gadsby DC. 1994. Regulation of the gating of cystic fibrosis transmembrane conductance regulator C1 channels by phosphorylation and ATP hydrolysis. *Proceedings of the National Academy of Sciences of the United States of America* 91:4698--702
10. Csandy L, Seto-Young D, Chan KW, Cenciarelli C, Angel BB, et al. 2005. Preferential phosphorylation of R-domain Serine 768 dampens activation of CFTR channels by PKA. *The Journal of General Physiology* 125:171--86
11. Moran O. 2016. The gating of the CFTR channel. *Cellular and Molecular Life Sciences*:1--8
12. Baldursson O, Berger HA, Welsh MJ. 2000. Contribution of R domain phosphoserines to the function of CFTR studied in Fischer rat thyroid epithelia. *American journal of physiology. Lung cellular and molecular physiology* 279:L835--41
13. Bozoky Z, Krzeminski M, Muhandiram R, Birtley JR, Al-Zahrani A, et al. 2013. Regulatory R region of the CFTR chloride channel is a dynamic integrator of phospho-dependent intra- and intermolecular interactions. *Proceedings of the National Academy of Sciences*
14. Picciotto MR, Cohn JA, Bertuzzi G, Greengard P, Nairn AC. 1992. Phosphorylation of the cystic fibrosis transmembrane conductance regulator. *The Journal of biological chemistry* 267:12742--52

15. Hegeds T, Aleksandrov A, Mengos A, Cui L, Jensen TJ, Riordan JR. 2009. Role of individual R domain phosphorylation sites in CFTR regulation by protein kinase A. *BBA - Biomembranes* 1788:1341--9

16. Vergani P, Basso C, Mense M, Nairn AC, Gadsby DC. 2005. Control of the CFTR channel's gates. *Biochemical Society Transactions* 33:1003

17. Mense M, Vergani P, White DM, Altberg G, Nairn AC, Gadsby DC. 2006. In vivo phosphorylation of CFTR promotes formation of a nucleotide-binding domain heterodimer. *The EMBO Journal* 25:4728--39

18. Stannard J. 1940. An analysis of the effect of carbon monoxide on the respiration of frog skeletal muscle. *Am J Physiol* 129

19. Wang W, Li G, Clancy JP, Kirk KL. 2005. Activating cystic fibrosis transmembrane conductance regulator channels with pore blocker analogs. *The Journal of biological chemistry* 280:23622--30

20. Csandy L, Trcsik B. 2014. Catalyst-like modulation of transition states for CFTR channel opening and closing: new stimulation strategy exploits nonequilibrium gating. *The Journal of General Physiology* 143:269--87

21. Ma T. 2002. Thiazolidinone CFTR inhibitor identified by high-throughput screening blocks cholera toxin-induced intestinal fluid secretion. *Journal of Clinical Investigation* 110:1651--8

22. Wang W, Roessler BC, Kirk KL. 2014. An electrostatic interaction at the tetrahelix bundle promotes phosphorylation-dependent cystic fibrosis transmembrane conductance regulator (CFTR) channel opening. *Journal of Biological Chemistry* 289:30364--78

23. Drumm ML, Wilkinson DJ, Smit LS, Worrell RT, Strong TV, et al. 1991. Chloride conductance expressed by delta F508 and other mutant CFTRs in Xenopus oocytes. *Science* 254:1797--9

24. Md JBH, Md RCL, PhD FQ, Md PETR, Md PSBC. 2012. Cholera. *The Lancet* 379:2466--76

25. Rowe SM, Clancy JP, Wilschanski M. 2011. Nasal potential difference measurements to assess CFTR ion channel activity. *Methods in molecular biology (Clifton, N.J.)* 741:69--86

5) General Discussion and Future Directions

CFTR is a unique protein and its chloride channel function is crucial to physiologic homeostasis in numerous organ systems. This is evidenced by the myriad pathologies associated with loss-of-function mutations that lead to Cystic Fibrosis. CFTR activity is implicated in multiple other pathologies as well. For example, a progressive loss of CFTR protein expression and activity has been reported in the acquired lung dysfunction that is associated with COPD. Conversely, overactivation of WT CFTR underlies the potentially fatal dehydration that is associated with cholera toxicity. Thus, knowledge related to the regulation of CFTR and the ability to tune its chloride channel activity could help lead to the development of novel treatments for these diseases. In this dissertation I have discussed two different modulators of CFTR ion channel activity, one indirect inhibitor (SMase) and one potentiator (VX-770). The experiments described shed some light on how each one affects CFTR function. Ultimately, understanding how each modulator works may help elucidate the mechanism by which CFTR transitions through its gating cycle.

As discussed in the background section, CFTR evolved from an ancient class of transporters that utilize the energy of ATP binding and hydrolysis to move substrates. This means that CFTR represents a unique union of ATPase and ion channel and as a consequence it undergoes a unique set of conformational changes during its gating cycle. Many ion channels, such as ligand-gated ion channels, are modeled by a process called equilibrium gating. The general idea behind equilibrium gating is that the ligand-gated channels reversibly transition between two states, the unbound closed state and the ligand-bound open state (1). The free energy input that is associated with the transitions originate in the binding and unbinding of ligand. In addition to the ligand-bound open and unbound

closed states, there are brief periods of time in which the protein can be found in the

"transition states" that are associated with gating, but their high free energy makes them

relatively unstable.   For example, channels exist in a ligand-bound closed state before the

energy of binding is transferred to the pore domains through the interconnected protein

structure. In a sense, CFTR is like a ligand gated channel in that the binding of ATP leads to

conformational change that opens the chloride permeant pore. However, where CFTR

differs is that its "ligand" ATP is hydrolyzed to ADP and P_i. This input of free energy leads

to an additional conformation change that leads to closure of the pore. Given that the

closed state immediately preceding transition to the open state (in which the NBDs have two

bound ATPs) is distinct from the closed state immediately following pore closure (in which

there is 1 bound ATP, one bound ADP, and one bound P_i) means that CFTR undergoes

"nonequilibrium gating" (2-5). One of the practical implications of nonequilibrium gating is

that CFTR has multiple closed states that can be affected by small molecules or PTMs.

5.1) *On the inhibition of CFTR channel activity by SMase*

Most inhibitors block channel function by stabilizing a closed state and our

data with mutant CFTR channels suggests that SMase works in a similar way. Determining

which closed state is stabilized would provide clues about the mechanism by which SMase

works. Figure 5.1 shows the simplified gating scheme of CFTR that was first presented in

Figure 1.3 with the addition of arrows that indicate the effects of the R117H and D110R

mutations. As discussed, the R117H mutation stabilizes two states, annotated the C_1 and C_2

states while D110R is thought to stabilize only the C_2 state. We found that the R117H

mutation increased the rate of inhibition by SMase while the D110R mutation had no effect.

These data suggest that SMase affects the C_1 closed state to elicit its effect. It is also possible

that SMase targets the C_0 closed, but distinguishing between C_0 and C_1 experimentally is difficult. We have not ruled out the possibility that SMase affects the C_3 state but that conformation is though to be very brief and given that excised-patch experiments can not (yet) be used to study this effect, it will be very difficult to determine.

What type of event could stabilize these closed states? One possibility is that the formation of ceramide leads to a post-translational modification of CFTR that prevents either the transition from C_0 to C_1, C_1 to C_2, or C_2 to O_f. As mentioned in the Results section, ceramide, and an immediate metabolic product ceramide 1-phosphate, have been shown to activate multiple signaling cascades including JNK, PI3K, MEK/ERK, PP2A, PKCζ, KSR, and CAPK (6-11). Modifications in the region of ATP binding sites might prevent binding of the ATP that facilitates redimerization of the NBDs. Similarly, modifications at the NBD interface could also prevent proper transition to the C_1 or C_2 states by sterically hindering complete dimerization. One approach to test the involvement of these enzymes is to systematically test the effect of inhibitors on SMase-mediated inhibition. We have started testing inhibitors and the preliminary results are shown in Figure 4.4**.** An alternative approach is to look for PTMs on CFTR from SMase-treated oocytes via mass spectrometry. These experiments would offer a site- and pathway-agnostic approach to answer this question and we have established a collaboration with Dr. Ronghu Wu at Georgia Tech to explore this possibility.

Functional roles for PTMs in CFTR that lie outside of the R-domain have not been thoroughly shown. There is one well-accepted example of a PTM site in the NBDs, a widely recognized kinase site at residue S422 in a region known as the "regulatory insert (RI)." The right panel of Figure 5.1b shows the sequence flanking the RI in red on the zebrafish cryo-EM structure (the RI itself could not be modeled based on the cryo-EM density map or the

x-ray crystal structures of mouse NBD1 that were used as a guide, PDB 1Q3H). There is currently no evidence of a role for S422 in normal gating of WT CFTR (12) with loss of the phosphorylation site by either a point mutation (S422A) or deletion of the entire RI (AA 415-433) failing to affect channel activation by PKA and ATP. Evidence suggests that it limits trafficking (13) and, interestingly, deletion of the RI in the F508del protein backbone increases its maturation and stability (14). At this point in time, we have not directly tested this residue for a role in SMase-mediated inhibition.

An alternative possibility is that SMase affects transition of the TMDs from the C_1 closed state to the full open state (O_f). This could potentially be achieved in two ways. The first is to disrupt an interaction between the NBDs and the ICLs of the TMDs. This could effectively uncouple dimerization of the NBDs from the TMDs and prevent the conformational change associated with opening of the pore. CF-associated mutations in the fourth ICL are thought to cause this type of disruption (15) but PTMs in this region have never been found to occur in a reversible fashion on WT CFTR. A mass spec study examining PTMs of CFTR did not find any modifications on the serine and threonine residues of ICL 1, 2, or 3, (S169 - ICL1, fully conserved between human, mouse, Xenopus, and zebrafish), S271 (ICL2, fully conserved), T966 (ICL3, K in mouse)(16). The residue T1064 (ICL4, fully conserved) was not covered in this study. These residues are shown in pink in Figure 5.1b.

Another possibility is that SMase leads to the formation of a new lipid (something downstream of ceramide) that affects the conformational freedom of the TMDs. The lipid dependence of CFTR channel function has not been systematically tested but there is some evidence that lipids can influence CFTR. Specifically, Hildebrandt and colleagues showed that purified CFTR is stabilized by the presence of POPS, but not POPC or POPE, and that

the lipid increases CFTR's ATPase activity when it is included in the proteoliposomes (17). While measuring ATPase activity is not a direct measure of TMD function, it is likely indicative of an interaction between POPS and the pore domain. As discussed, in ABC-Ts the NBDs are allosterically coupled to the TMDs to promote gating. That coupling is likely bidirectional as evidenced by studies of ABC-Ts that transport lipophilic molecules. In many of those proteins, addition of the substrate leads to a dramatic increase in the ATP turnover rate (18). Christine Bear's group showed this TMD-to-NBD coupling for CFTR by demonstrating that mutations at R347, which is in TM6, diminished ATPase activity of purified protein (19). They observed a similar decrease upon incubation with specific pore blockers as well, suggesting that this did not result from a generalized structural perturbation caused by the mutation. The ideal approach to determining the lipid dependence of CFTR channel function, however, would be to record the activity of pure protein in planar lipid bilayers while systematically changing the lipid make up of the bilayer. The MacKinnon group has used this approach in the past to elucidate the role of the lipid headgroup in voltage-gated K^+ channel gating (20). To date, all planar bilayer recording of CFTR has used a similar mixture of PE, PS, and, less often, PC in the bilayer (14; 21-23).

It is tempting to speculate that lipids may be an integral part of the TMD domains of CFTR and, therefore, may be in a prime position to modulate TMD dynamics. Recent developments in mass spectrometry have enabled the detection of lipids associated with the ABC transporter macB, a noncannonical bacterial ABC exporter (24). A similar approach was applied to probe the lipid specificity of murine PgP (a.k.a. Multidrug Resistance Protein 1, MDR1, ABCB1)(25), an exporter that was used as a structural template for homology models of CFTR in the closed state (26; 27). Interestingly, the recent cryo-EM structure of zebrafish CFTR may support a high affinity interaction between lipids and the TMDs of

CFTR (28). Specifically, the electron density map shows two aliphatic chains, assigned as decane, bound in hydrophobic grooves (shown in pale yellow in Figure 5.1b). One is interacting relatively superficially with TMD1 while the second is buried in a pocket of TMD2 made up of TMs 9,10, 11, and 12 (Fig. 5.1b,c). Interestingly, this groove includes a motif previously characterized as a sphingolipid binding motif (Fig. 5.1c, red residues). This groove is also featured in the unpublished human CFTR structure from the same group, though in that structure it does not contain a bound aliphatic chain. It is difficult to predict whether this hydrophobic groove undergoes structural changes with gating and it will be interesting to see whether it is maintained in the open conformation of the channel once that structure becomes available.

Whether SMase-mediated inhibition of CFTR occurs *in vivo* remains to be seen. Data obtained with primary HBEs showed an activity-dependent inhibition of FSK-stimulated currents suggesting that a similar effect may be occurring in both the *Xenopus* oocyte and mammalian cells. As discussed previously, transepithelial currents result from the coordinated activity of multiple channels and this increased complexity means that other effects may influence the Ussing chamber results. For example, Saslowski and colleagues showed that ceramide-mediated activation of JNK inhibits basolateral voltage-gated K^+ channels in the T-84 colon epithelial cell line (29). Inhibition of these K_v channels would be expected to limit the maximal current and likely do not explain the high level of inhibition we observed at low FSK levels; however, this effect may be contributing to the ~20% inhibition that we observe with high concentrations of FSK. This effect on K_v channels has not previously been reported in pulmonary epithelial cells. Future studies that characterize the pharmacological profile of the SMase effect in each system and the use of a membrane permeabilizing agents in the Ussing chamber will offer insights into this question.

Multiple cell types in the lung could secrete SMase to elicit this effect. Interest in this project was based on the hypothesis that SMase of bacterial origin, which has been implicated in the pathogenicity of numerous species, might be eliciting this effect. In general, CF-associated infections are thought to reside in the lumen of the lung so we would expect that most of the bacterial SMase resides on the apical side of the epithelial cells. We saw no effect of apical SMase on epithelial ion channel function, so this may limit the influence of bacterial SMase on ion channel function *in vivo*. Another intriguing possibility is that transmigrating immune cells could elicit this effect as they move from the interstitial space, through the epithelial cells, and into the lumen because some lymphcytes have been shown to traffic acid SMase to the plasma membrane upon activation (30). A high number of transmigrating neutrophils is a well accepted CF phenotype (31) so it would be interesting to determine whether CF neutrophils contain measurable levels of SMase on their surface or in their released ectosomes. If so, we would predict that incubating activated neutrophils on the basolateral side of a model epithelium would recapitulate the reduction in current and the change in sphingomyelin distribution that we observed following exposure to purified SMase.

5.2) *On the potentiation of CFTR by VX-770*

The discovery of VX-770 has revolutionized the treatment of patients with a subset of CF-associated CFTR genotypes. After demonstrations of safety and efficacy in patients with the Class 3 gating mutation G551D (32), it was quickly adopted by CF-physicians and continued to show positive results in adults in phase 4 trials(33). Since its initial success in adults with G551D-CFTR, it has since been utilized in children between the ages of 2 and 5(34; 35) and in patients harboring other mutations, for example R117H (36). It is also

being tested in small patient populations off label, such as an individual with the P67L

mutation (37). Despite its overwhelming clinical success, relatively little is known about how

VX-770 works to increase channel activity and how best to screen for this relatively novel

class of drugs. In the last 4-5 years basic science labs began performing mechanistic studies

to frame its activity in terms a binding site and modulation of the gating scheme discussed

earlier.

It is fairly well established that VX-770 works by directly binding to CFTR. The first

evidence was provided by Eckford and colleagues who demonstrated that VX-770

effectively potentiated purified CFTR in bilayers(38). This is not absolute proof of a direct

interaction because it is possible, though unlikely, that VX-770 may work through an

unidentified, copurified protein. However, this offered relatively strong evidence that VX-

770 acts via a direct interaction with CFTR. Consistent with a direct interaction, Lui and

Dawson showed that VX-770 also increases the thermal stability of G551D-CFTR, a mutant

whose activity is diminished upon heating to 37°C (39).

The next basic question is, where on CFTR does VX-770 bind to elicit its effect?

Multiple groups are actively attempting to answer this question and studies using domain-

deletion mutants have provided insight. First, our group and others have observed

potentiation of split-ΔR-CFTR by VX-770. This observation clearly demonstrates that VX-

770 does not act via an interaction with the R-domain (40). Multiple groups have also

shown potentiation of a CFTR construct that lacks the entire NBD2 (ΔNBD2-CFTR) (41;

42). This channel has a very low resting P_o and its channel activity is thought to represent

equilibrium gating of the TMDs (40; 42). These data strongly suggest that VX-770 works by

interacting with the TMDs and/or NBD1. Additionally, it suggests that the free energy of

VX-770 binding must be at least equal to that of 2 ATPs binding to the NBDs, an

observation that may be useful in exploratory docking studies. Our group has shown that VX-770 exhibits differential effects on various orthologs of CFTR (43; 44). It is not clear whether this is the result of changes in affinity or efficacy, but it suggests that either the VX-770 binding site or the interaction network utilized by VX-770 differs between species. These differential effects also make possible the use of chimeric CFTR proteins to help elucidate the binding site and/or intraprotein signaling network.

Some groups have provided evidence that VX-770 can facilitate channel function in the absence of ATP binding. This was first proposed by Eckford and colleagues who, again recording currents from purified CFTR in planar lipid bilayers, found that the inclusion of VX770 in the recording chamber lead to clear opening events in the absence of ATP (38). It is worth noting that the channels required phosphorylation before currents were seen. This means that channels were preincubated with ATP and PKA while conjugated to the purification resin before incorporation into proteoliposomes. It is possible that a small amount of ATP may have remained bound to the channels during this step and was later incorporated, and the authors did not include hexokinase and glucose to ensure that their recording chamber was devoid of ATP. The ATP-free hypothesis is supported, however, by the observation the VX-770 can open ΔNBD2-CFTR because this mutant clearly lacks the ability to undergo the NBD dimerization that is classically thought to be how ATP binding influences CFTR channel function (41; 42). Some groups suggest that the residual channel activity that can be seen seconds after fast washout of ATP is indicative of ATP-independent activity and this activity has been shown to increase with pretreatment of VX-770 (40); however, data from our group suggests that some ATP may still be present during this time because VX-770 treatment many minutes after washout of ATP does not lead to activation. Other groups have suggested that VX-770 can open channels with only a single ATP bound

in the nonhydrolytic sight (40; 45). While unconventional, it may be consistent with our results in that the longer washout enables unbinding of ATP from the nonhydrolytic sight. This unique behavior of the drug is of interest to many and will certainly be studied more extensively.

Coadministration experiments using VX-770 have provided additional information and it was recently shown that VX-770 could work synergistically with other potentiators to increase CFTR channel function. Kirk and colleagues demonstrated that sequential application of VX-770 and curcumin led to stepwise increases in current in both W1282X-CFTR (a truncated protein that lacks most of NBD2) and ΔNBD2-CFTR(42). The combination ultimately led to channels that appeared to be locked open in single channel recordings. Similarly, Lin and colleagues showed that sequential application of VX-770 and NPPB synergistically increased G551D-CFTR currents (45). These data suggest that VX-770 works by binding to a site that is not bound by curcumin and NPPB and also facilitates channel opening by a mechanism unlike the other two potentiators. Clinically, these data suggest that in patients harboring mutants that are less responsive to VX-770, a combination therapy may be beneficial.

Where in the gating scheme does VX-770 influence CFTR? Most ion channels are potentiated by molecules that stabilize the open state; however, due to the nonequilibrium gating of CFTR, molecules that stabilize a C_2 to O_f transition state can also potentiate CFTR currents. This concept was termed "catalyst-like" modulation and was elegantly shown by Csanady and Torocsik in 2014 using NPPB, a relatively well-established pore blocker of CFTR that also potentiates CFTR current at positive membrane potentials (3) (46). As expected with a potentiator, perfusion of NPPB onto gating WT channels at positive potentials leads to a net increase in current. However, Csanady and Toroscik found that it

also increased the rate of closure in the nonhydrolytic K1250A mutant of CFTR following washout of ATP. Due to the fact that this channel does not hydrolyze ATP, its gating is similar to that of an equilibrium gating scheme and these data suggest that NPPB effectively decreases the energy barrier between the C_2 and O_f states. Unlike other equilibrium-gated channels, these data demonstrate that the macroscopic currents of CFTR can be increased by either stabilizing a transition state or stabilizing the open state. Lin and colleagues applied this approach to VX-770 in 2016 (45) and found that, unlike NPPB, VX-770 pretreatment slowed the closure of K1250A-CFTR following washout of ATP. This suggests that at least part of the mechanism by which VX-770 works involves stabilizing the open state of CFTR. Consistent with this, single channel traces have shown that VX-770 increases the mean burst duration of the channel (40).

Our data with VX-770 provide insight into the best way to screen for novel CFTR potentiators. Consistent with the idea that VX-770 increases both opening rate and burst duration, we observe a steep, nonlinear relationship between the initial P_o of CFTR and the level of potentiation with VX-770. This relationship was also observed in post hoc analysis of data published by Vertex Pharmaceuticals. The fact that VX-770 does not lock channels open suggests that it does not work by simply preventing catalysis of ATP by the NBDs. Consistent with this, we do not see maximal transepithelial currents elicited by VX-770 in epithelial cells. Instead, its efficacy is a function of channel activity and regulated by physiologic input (i.e., phosphorylation) suggesting that is works allosterically to facilitate channel gating.

6) Concluding Remarks:

The data included in this dissertation provide insight into the regulation of the CFTR channel activity by two different modulators, one inhibitor and one potentiator. Our studies of SMase demonstrated that sphingomyelin catabolism is linked to CFTR channel activity and modulates its channel function via a novel, state-dependent mechanism. This crosstalk may be conserved in polarized human bronchial epithelial cells and this interaction may be a significant influence in pulmonary epithelial function, particularly in obstructive pulmonary diseases. The second part of our study showed that CFTR is subject to the ceiling effect and that VX-770 is more efficacious when channels are submaximally activated. This observation provides valuable insight into the optimal design of drug screens with the goal of discovering novel CFTR potentiators. While their effects are quite different, the action of both of these modulators depends upon the initial activity of channel. This suggests that a general consideration of channel activity and dwell times should always be taken into account when assessing the function of CFTR gating modifiers.

Works Cited:

1. Auerbach A. 2013. The Energy and Work of a Ligand-Gated Ion Channel. *Journal of Molecular Biology* 425:1461--75

2. Csandy L, Nairn AC, Gadsby DC. 2006. Thermodynamics of CFTR channel gating: a spreading conformational change initiates an irreversible gating cycle. *The Journal of General Physiology* 128:523--33

3. Csandy L, Trcsik B. 2014. Catalyst-like modulation of transition states for CFTR channel opening and closing: new stimulation strategy exploits nonequilibrium gating. *The Journal of General Physiology* 143:269--87

4. Zhou Z, Wang X, Li M, Sohma Y, Zou X, Hwang T-C. 2005. High affinity ATP/ADP analogues as new tools for studying CFTR gating. *The Journal of Physiology* 569:447--57

5. Jih K-Y, Hwang T-C. 2012. Nonequilibrium gating of CFTR on an equilibrium theme. *Physiology (Bethesda, Md.)* 27:351--61

6. Mller G, Ayoub M, Storz P, Rennecke J, Fabbro D, Pfizenmaier K. 1995. PKC zeta is a molecular switch in signal transduction of TNF-alpha, bifunctionally regulated by ceramide and arachidonic acid. *The EMBO Journal* 14:1961--9

7. Bourbon NA, Sandirasegarane L, Kester M. 2002. Ceramide-induced Inhibition of Akt Is Mediated through Protein Kinase C : IMPLICATIONS FOR GROWTH ARREST. *Journal of Biological Chemistry* 277:3286--92

8. Chalfant CE. 2003. The structural requirements for ceramide activation of serine-threonine protein phosphatases. *Journal of lipid research* 45:496--506

9. Bao HF, Zhang ZR, Liang YY, Ma JJ, Eaton DC, Ma HP. 2007. Ceramide mediates inhibition of the renal epithelial sodium channel by tumor necrosis factor- through protein kinase C. *AJP: Renal Physiology* 293:F1178--F86

10. Heinrich M, Neumeyer J, Jakob M, Hallas C, Tchikov V, et al. 2004. Cathepsin D links TNF-induced acid sphingomyelinase to Bid-mediated caspase-9 and -3 activation. *Cell Death and Differentiation* 11:550--63

11. Stancevic B, Kolesnick R. 2010. Ceramide-rich platforms in transmembrane signaling. *FEBS Letters* 584:1728--40

12. Csanady L. 2004. Functional Roles of Nonconserved Structural Segments in CFTR's NH2-terminal Nucleotide Binding Domain. *The Journal of General Physiology* 125:43--55

13. Luz S, Kongsuphol P, Mendes AI, Romeiras F, Sousa M, et al. 2011. Contribution of casein kinase 2 and spleen tyrosine kinase to CFTR trafficking and protein kinase A-induced activity. *Molecular and cellular biology* 31:4392--404

14. Aleksandrov AA, Kota P, Aleksandrov LA, He L, Jensen T, et al. 2010. Regulatory Insertion Removal Restores Maturation, Stability and Function of ΔF508 CFTR. *Journal of Molecular Biology* 401:194--210

15. Cotten JF, Ostedgaard LS, Carson MR, Welsh MJ. 1996. Effect of cystic fibrosis-associated mutations in the fourth intracellular loop of cystic fibrosis transmembrane conductance regulator. *The Journal of biological chemistry* 271:21279--84

16. McClure M, DeLucas LJ, Wilson L, Ray M, Rowe SM, et al. 2011. Purification of CFTR for mass spectrometry analysis: identification of palmitoylation and other post-translational modifications. *Protein Engineering Design and Selection* 25:7--14

17. Hildebrandt E, Khazanov N, Kappes JC, Dai Q, Senderowitz H, Urbatsch IL. 2017. Specific stabilization of CFTR by phosphatidylserine. *BBA - Biomembranes* 1859:289--93

18. Ambudkar SV, Lelong IH, Zhang J, Cardarelli CO, Gottesman MM, Pastan I. 1992. Partial purification and reconstitution of the human multidrug-resistance pump: characterization of the drug-stimulatable ATP hydrolysis. *Proceedings of the National Academy of Sciences of the United States of America* 89:8472--6

19. Kogan I, Ramjeesingh M, Huan LJ, Wang Y, Bear CE. 2001. Perturbation of the pore of the cystic fibrosis transmembrane conductance regulator (CFTR) inhibits its ATPase activity. *The Journal of biological chemistry* 276:11575--81

20. Schmidt D, Jiang Q-X, MacKinnon R. 2006. Phospholipids and the origin of cationic gating charges in voltage sensors. *Nature* 444:775--9

21. Bear CE, Li CH, Kartner N, Bridges RJ, Jensen TJ, et al. 1992. Purification and functional reconstitution of the cystic fibrosis transmembrane conductance regulator (CFTR). *Cell* 68:809--18

22. Tilly BC, Winter MC, Ostedgaard LS, O'Riordan C, Smith AE, Welsh MJ. 1992. Cyclic AMP-dependent protein kinase activation of cystic fibrosis transmembrane conductance regulator chloride channels in planar lipid bilayers. *The Journal of biological chemistry* 267:9470--3

23. Gunderson KL, Kopito RR. 1994. Effects of pyrophosphate and nucleotide analogs suggest a role for ATP hydrolysis in cystic fibrosis transmembrane regulator channel gating. *The Journal of biological chemistry* 269:19349--53

24. Barrera NP, Isaacson SC, Zhou M, Bavro VN, Welch A, et al. 2009. Mass spectrometry of membrane transporters reveals subunit stoichiometry and interactions. *Nature Methods* 6:585--7

25. Marcoux J, Wang SC, Politis A, Reading E, Ma J, et al. 2013. Mass spectrometry reveals synergistic effects of nucleotides, lipids, and drugs binding to a multidrug resistance efflux pump. *Proceedings of the National Academy of Sciences* 110:9704--9

26. Aller SG, Yu J, Ward A, Weng Y, Chittaboina S, et al. 2009. Structure of P-Glycoprotein Reveals a Molecular Basis for Poly-Specific Drug Binding. *Science* 323:1718--22

27. Rahman KS, Cui G, Harvey SC, McCarty NA. 2013. Modeling the conformational changes underlying channel opening in CFTR. *PLoS ONE* 8:e74574

28. Zhang Z, Chen J. 2016. Atomic Structure of the Cystic Fibrosis Transmembrane Conductance Regulator.1--22

29. Saslowsky DE, Tanaka N, Reddy KP, Lencer WI. 2009. Ceramide activates JNK to inhibit a cAMP-gated K+ conductance and Cl- secretion in intestinal epithelia. *The FASEB Journal* 23:259--70

30.   Grassm. 2001. CD95 signaling via ceramide-rich membrane rafts. *The Journal of biological chemistry* 276:20589--96

31.   Elborn JS. 2016. Cystic fibrosis. *Lancet*

32.   Md DEFM, Md PDB, Md PD, Md PMG, Md PMWK, et al. 2014. Long-term safety and efficacy of ivacaftor in patients with cystic fibrosis who have the Gly551Asp-CFTR mutation: a phase 3, open-label extension study (PERSIST). *The Lancet Respiratory* 2:902--10

33.   Quittner A, Suthoff E, Rendas-Baum R, Bayliss MS, Sermet-Gaudelus I, et al. 2015. Effect of ivacaftor treatment in patients with cystic fibrosis and the G551D-CFTR mutation: patient-reported outcomes in the STRIVE randomized, controlled trial. *Health and quality of life outcomes* 13:93

34.   Davies JC, Wainwright CE, Canny GJ, Chilvers MA, Howenstine MS, et al. 2013. Efficacy and Safety of Ivacaftor in Patients Aged 6 to 11 Years with Cystic Fibrosis with a G551DMutation. *American Journal of Respiratory and Critical Care Medicine* 187:1219--25

35.   Md PJCD, MbchB SC, Md WTH, Md AL, Md WER, et al. 2016. Safety, pharmacokinetics, and pharmacodynamics of ivacaftor in patients aged 2 to 5 years with cystic fibrosis and a CFTR gating mutation (KIWI): an open-label, single-arm study. *The Lancet Respiratory* 4:107--15

36.   Md PDRBM, Md PPAF, Md PJSE, Msc JC, Md SMR, et al. 2015. Efficacy and safety of ivacaftor in patients with cystic fibrosis who have an Arg117His-CFTR mutation: a double-blind, randomised controlled trial. *The Lancet Respiratory* 3:524--33

37.   Md SY, Md GMS, Md AB, Steven M Rowe Md M, Md AAC. 2015. Improved Clinical and Radiographic Outcomes After Treatment With Ivacaftor in a Young Adult With Cystic Fibrosis With theP67LCFTR Mutation. *Chest* 147:e79--e82

38.   Eckford PDW, Li C, Ramjeesingh M, Bear CE. 2012. Cystic fibrosis transmembrane conductance regulator (CFTR) potentiator VX-770 (ivacaftor) opens the defective channel gate of mutant CFTR in a phosphorylation-dependent but ATP-independent manner. *Journal of Biological Chemistry* 287:36639--49

39.   Liu X, Dawson DC. 2014. Cystic fibrosis transmembrane conductance regulator (CFTR) potentiators protect G551D but not ΔF508 CFTR from thermal instability. *Biochemistry* 53:5613--8

40.   Jih K-Y, Hwang T-C. 2013. Vx-770 potentiates CFTR function by promoting decoupling between the gating cycle and ATP hydrolysis cycle. *Proceedings of the National Academy of Sciences* 110:4404--9

41.   Yeh H-I, Yeh J-T, Hwang T-C. 2015. Modulation of CFTR gating by permeant ions. *The Journal of General Physiology* 145:47--60

42.   Wang W, Hong JS, Rab A, Sorscher EJ, Kirk KL. 2016. Robust Stimulation of W1282X-CFTR Channel Activity by a Combination of Allosteric Modulators. *PLoS ONE* 11:e0152232

43.   Cui G, McCarty NA. 2015. Murine and human CFTR exhibit different sensitivities to CFTR potentiators. *AJP: Lung Cellular and Molecular Physiology* 309:L687--L99

44.   Cui G, Khazanov N, Stauffer B, Infield DT, Imhoff BR, et al. 2016. Potentiators exert distinct effects on human, murine, and Xenopus CFTR. *AJP: Lung Cellular and Molecular Physiology*:ajplung.00056.2016

45.   Lin WY, Sohma Y, Hwang TC. 2016. Synergistic Potentiation of Cystic Fibrosis Transmembrane Conductance Regulator Gating by Two Chemically Distinct Potentiators, Ivacaftor (VX-770) and 5-Nitro-2-(3-Phenylpropylamino) Benzoate. *Molecular Pharmacology* 90:275--85

46.   Wang W, Li G, Clancy JP, Kirk KL. 2005. Activating cystic fibrosis transmembrane conductance regulator channels with pore blocker analogs. *The Journal of biological chemistry* 280:23622--30

7) Appendices

This section is will provide brief summaries of additional studies in which I participated.

7.1)   *Potentiators exert distinct effects on human, murine, and Xenopus CFTR.* Cui G, Khazanov N, Stauffer BB, Infield DT, Imhoff BR, Senderowitz H, McCarty NA. AJP: Lung Cellular and Molecular Physiology 2016 June:311(2):L192-207

The discovery of VX-770 has served as a proof of principle that small molecule potentiators can be effective in the clinic and thus has catalyzed a search for new potentiators that work on additional disease-associated mutations and do not interfere with the efficacy of small molecule correctors (1; 2). Currently, VX-770 is the only potentiator that has been approved by the FDA for use in CF patients but its development has spurred continuing research. Specifically, it is currently unknown where VX-770 binds to the protein and how binding elicits the increase in opening rate and mean burst duration that has been observed.

In the first part of this study, we compared the efficacy of small molecule modulators on multiple homologs of CFTR, specifically on human-, murine-, and *Xenopus*-CFTR, expressed in *Xenopus* oocytes. We tested VX-770, NPPB, Gly-H, P1, P2, and P3, and found that they all exhibited ortholog specific behavior. For example, 5 μM VX-770 potentiated *Xenopus* and murine CFTR by ~100% and 30%, respectively, while it potentiated human CFTR by ~10% when applied at in the presence of the β2 agonist isoproterenol. *Xenopus* CFTR has a similar activity level as human so this difference is not the result of lower starting activity (3). Thus, these data suggest that the homologs vary in either the structure of the VX-770 binding site or in the structural network utilized by VX-770 to elicit

its effect. These differences also suggest that a chimera-based approach may be useful in future studies to elucidate the VX-770 binding site(s). The idea is that if the domain containing the high-efficacy site from *Xenopus*-CFTR is introduced into the human protein, it might lead to increased potentiation in the chimeric protein versus the human WT protein. Based in the data presented in Results section 2, such experiments need to be carefully controlled for activation level to avoid false positives.

In the second part of the study, we utilized a pharmacophore modeling approach to search for new potentiators in currently available libraries. By overlaying known CFTR potentiators, our collaborators identified patterns in the spatial organization of common motifs such as an aromatic ring, a negative ionizable moiety, and a H-bond donor. By comparing these structural characteristics with 7.37 million compounds in the ZINC database, we identified 3 new compounds that effectively potentiated CFTR currents in *Xenopus* oocytes, specifically, IOWH-032, OSSK-2, and OSSK-3. These compounds showed both inhibitory and stimulatory effects on CFTR currents so they cannot be utilized clinically themselves; however, they provide a starting point for future structure-activity relationship studies and rational drug design.

This manuscript provided some initial characterization of multiple CFTR modulators on 3 different homologs of CFTR. We observed ortholog specific differences for all molecules tested with various patterns of effect, and this information provides the necessary groundwork for future chimera studies with these compounds. Additionally, we successfully utilized the pharmacophore modeling approach to discover 3 new potentiators of CFTR in the ZINC database of drug-like compounds.

7.2)   *Junctional Abnormalities In Human Airway Epithelial Cells Expressing F508del CFTR.*

Molina SA, Stauffer BB, Moriarty HK, Kim AH, McCarty NA, Koval M. AJP: Lung

Cellular and Molecular Physiology 2015 Sep.;309(5):L475-L487.

Cell lines that reliably model healthy and CF pulmonary epithelia are limited. The

gold standard is to use primary bronchial epithelial cells from healthy and CF donors but

these cells are often difficult to obtain and expand. Most of the immortalized cell lines used

are either derived from cancerous tumors (e.g., Calu-3) or epithelial cells that have been

virally transduced to over express WT or mutant CFTR protein (e.g, CFBE41σ-), but both

of these approaches can obscure normal cellular functions associated with healthy epithelial

cell physiology. Therefore, new, well-characterized epithelial cell lines that do not rely on

malignant or viral alterations are useful. In this study we characterized the NuLi-1 and CuFi-

5 pulmonary epithelial cell lines to better understand their utility in studies of airway

physiology and CF.

The NuLi and CuFi cell lines are telomerase-immortalized human airway epithelial

cells that represent a system with features such as genomic stability and known age, sex, and

donor genotype(4). NuLi and CuFi cells are particularly advantageous because they are

realtively easy to propagate in culture and have the ability to polarize and differentiate when

cultured at an air-liquid interface (ALI). These cells also appear to exhibit near-physiological

levels of CFTR mRNA and protein (4), making them particularly well suited to CF research.

Despite what is known about NuLi and CuFi cells, only a handful of studies have utilized

these human airway cell models. Moreover, comparison between these studies is difficult

because of varying maturation conditions. Several studies have used NuLi and CuFi cells

differentiated on Transwell permeable supports at ALI for 4 – 6 weeks (5-7), although cells

at ALI for 2–3 weeks have also been used (4; 8; 9), as have cells on collagen-coated tissue culture plastic (10; 11).

Given that maturation time and culture conditions can have a significant effect on cell function, we phenotypically profiled the NuLi-1 (CFTR$^{WT/WT}$) and CuFi-5 (CFTR$^{F508del/F508del}$) cell lines at weeks *3, 5*, and *7* of ALI culture. We then focused on the utility of these cells for studying tight junctions and gap junctions. The electrophysiological profile and CFTR expression were also assessed at different times following ALI culture. Since primary cells are known to take weeks-to-months to fully differentiate, we compared the transcriptional and phenotypic changes that occurred with time in ALI culture in NuLi-1 and CuFi-5 cells with changes in primary patient-derived HBE cells from non-CF lungs (NHBE cells) and CF lungs homozygous for F508del CFTR (CFHBE cells). We found that NuLi-1 and CuFi-5 cells continue to differentiate in ALI culture and require 6–7 weeks to fully stabilize, which has implications for their composition in culture and their proper optimization for use in airway research. We also found that NuLi-1 and CuFi-5 cells represent pseudostratified epithelia for serous columnar cells. This finding has considerable utility since recent research has shown that CF disease impairs diverse airway cells, such as goblet cells, wherein mutant CFTR channels impair detachment of mucus. Additionally, we demonstrated that expression of F508del CFTR in these cell lines impairs gap junction function by altering connexin-43 trafficking.

Ultimately this publication provided basic characterizations of the NuLi-1 and Cufi-5 cell lines and demonstrated that they offer some advantages for the study of nonciliated cell types found in the airway. Additionally, we provided evidence of their utility in studying the gap-junction dysfunction that is associated with CFTR mutation.

7.3) *Inflammation and ER stress downregulate BDH2 expression and dysregulate intracellular iron in*

macrophages. Zughaier SM, Stauffer BB, McCarty NA. J Immunol Res

2014;2014(11):1-16.

Iron is an essential nutrient that is required for numerous cell functions but free iron

can be toxic to mammalian cells and speed up growth of infectious bacteria. Therefore, iron

homeostasis is tightly controlled (12). One mechanism by which interstitial iron is taken up

is via endocytosis by macrophages. Once engulfed, the free iron is immobilized by complex

to siderophores, or iron chelating molecules(12). The molecule 2,5-dihydroxybenzoic acid

(2,5 DHBA) often acts as the iron binding motif in siderophore proteins. The enzyme that

catalyzes the synthesis of 2,5 DHBA is called 3-hydroxybutyrate dehydrogenase type 2

(BDH2) (13), thus BDH2 is a key regulator of iron homeostasis.

Intracellular iron homeostasis in macrophages is disrupted by ER stress, which often

develops upon expression of mutant CFTR (14). ER-stress induced cellular changes are

mediated by the unfolded protein response, which is required for cellular survival (15). One

of the mechanisms by which ER stress affects iron homeostasis is through the induction of

hepcidin, a protein that decreases iron sequestration through binding to and inactivation of

the iron transporting protein ferroportin (16), but it was unknown whether ER stress also

affects the expression of BDH2. Therefore, the goal of this study was to investigate whether

ER stress and inflammation modulate BDH2 expression in macrophages.

In this study, we showed that LPS-induced inflammation combined with chemically

induced ER stress led to BDH2 downregulation, increased the expression of ER stress

markers including CHOP, upregulated hepcidin expression, downregulated ferroportin

expression, caused iron retention in macrophages, and dysregulated cytokine release from macrophages. We also show that vitamin D treatment prior to LPS restored BDH2 expression. This is the first report to show that ER stress and inflammation downregulate the expression of BDH2 in human THP-1 macrophages and the results suggest that BDH2 plays an important role in modulating iron-limiting innate immune defenses.

Works Cited:

1. Veit G, Avramescu RG, Perdomo D, Phuan PW, Bagdany M, et al. 2014. Some gating potentiators, including VX-770, diminish F508-CFTR functional expression. *Science translational medicine* 6:246ra97--ra97

2. Cholon DM, Quinney NL, Fulcher ML, Esther CR, Das J, et al. 2014. Potentiator ivacaftor abrogates pharmacological correction of F508 CFTR in cystic fibrosis. *Science translational medicine* 6:246ra96--ra96

3. Price MP, Ishihara H, Sheppard DN, Welsh MJ. 1996. Function of Xenopus cystic fibrosis transmembrane conductance regulator (CFTR) Cl channels and use of human-Xenopus chimeras to investigate the pore properties of CFTR. *The Journal of biological chemistry* 271:25184--91

4. Zabner J, Karp P, Seiler M, Phillips SL, Mitchell CJ, et al. 2003. Development of cystic fibrosis and noncystic fibrosis airway cell lines. *Am J Physiol Lung Cell Mol Physiol* 284:L844-54

5. Al-Alawi M, Buchanan P, Verriere V, Higgins G, McCabe O, et al. 2014. Physiological levels of lipoxin A4 inhibit ENaC and restore airway surface liquid height in cystic fibrosis bronchial epithelium. *Physiol Rep* 2

6. Higgins G, Buchanan P, Perriere M, Al-Alawi M, Costello RW, et al. 2014. Activation of P2RY11 and ATP release by lipoxin A4 restores the airway surface liquid layer and epithelial repair in cystic fibrosis. *Am J Respir Cell Mol Biol* 51:178-90

7. Klein H, Garneau L, Trinh NT, Prive A, Dionne F, et al. 2009. Inhibition of the KCa3.1 channels by AMP-activated protein kinase in human airway epithelial cells. *Am J Physiol Cell Physiol* 296:C285-95

8. Buchanan PJ, McNally P, Harvey BJ, Urbach V. 2013. Lipoxin A(4)-mediated KATP potassium channel activation results in cystic fibrosis airway epithelial repair. *Am J Physiol Lung Cell Mol Physiol* 305:L193-201

9. Voisin G, Bouvet GF, Legendre P, Dagenais A, Masse C, Berthiaume Y. 2014. Oxidative stress modulates the expression of genes involved in cell survival in DeltaF508 cystic fibrosis airway epithelial cells. *Physiol Genomics* 46:634-46

10. Dannhoffer L, Billet A, Jollivet M, Melin-Heschel P, Faveau C, Becq F. 2011. Stimulation of Wild-Type, F508del- and G551D-CFTR Chloride Channels by Non-Toxic Modified pyrrolo[2,3-b]pyrazine Derivatives. *Front Pharmacol* 2:48

11. Mayer ML, Sheridan JA, Blohmke CJ, Turvey SE, Hancock RE. 2011. The Pseudomonas aeruginosa autoinducer 3O-C12 homoserine lactone provokes hyperinflammatory responses from cystic fibrosis airway epithelial cells. *PLoS One* 6:e16246

12. Wang J, Pantopoulos K. 2011. Regulation of cellular iron metabolism. *Biochem J* 434:365-81

13. Devireddy LR, Hart DO, Goetz DH, Green MR. 2010. A mammalian siderophore synthesized by an enzyme with a bacterial homolog involved in enterobactin production. *Cell* 141:1006-17

14. de Sousa DL, de Sousa RB, Pinto DN, Neto JJ, de Carvalho CB, de Almeida PC. 2011. Antibacterial effects of chemomechanical instrumentation and calcium hydroxide in primary teeth with pulp necrosis. *Pediatr Dent* 33:307-11

15. Suh DH, Kim MK, Kim HS, Chung HH, Song YS. 2012. Unfolded protein response to autophagy as a promising druggable target for anticancer therapy. *Ann N Y Acad Sci* 1271:20-32

16. Vecchi C, Montosi G, Zhang K, Lamberti I, Duncan SA, et al. 2009. ER stress controls iron metabolism through induction of hepcidin. *Science* 325:877-80